CHARLES UNIVERSITY

Faculty of Science

Department of Physical and Macromolecular Chemistry

STRUCTURAL STUDIES OF SELECTED PROTEIN COMPLEXES INVOLVED IN SIGNAL TRANSDUCTION

Strukturní studie vybraných proteinových komplexů účastnících se přenosu signálu v buňce

Mgr. Karolína Honzejková

Doctoral thesis

of study program Physical Chemistry

Supervisor: prof. RNDr. Tomáš Obšil, Ph.D.

Consultant: RNDr. Veronika Obšilová, Ph.D.

Prague 2024

Declaration

I declare that I wrote this thesis independently and that I cited all the information sources and literature used. This work, or any substantial part of it, has not been submitted for the award of any other or the same academic degree.

In Prague, 15 January 2024. Karolína Honzejková

Acknowledgement (in Czech)

Tomáši, děkuji Vám za Vaše vedení, podporu a porozumění. Za to, že jste si na mě vždy udělal čas, i když jste byl zrovna zavalený spoustou dalších povinností. Za to, že jste mi umožnil zúčastnit se mnoha konferencí a kurzů. Že nepřikrášlujete realitu vědy, ale zároveň se dokážete nadchnout pro maličkosti.

Veru, děkuji za Tvou podporu, pomoc, lidský přístup a vlídné slovo.

Dalibore, jsem moc ráda, že jsi přišel k nám do laborky. Získala jsem tak někoho, s kým jsem mohla podrobně diskutovat věci kolem ASK1 a kdo byl do věci podobně zapálený jako já. Děkuju Ti za všechno, co jsi se mě snažil naučit o kryo-EM, za všechny naše rozhovory o vědě i dalších věcech a za skvělé připomínky při připravování prezentací.

Děkuji všem současným i minulým členům celé laborky. Gábi, děkuji Ti, že se neustále snažíš, aby nám nic nechybělo a skvěle nás podporuješ. Danko, děkuju Ti, že si vždycky najdeš čas, když máme problém s molekulárkou. Olí a Niki, děkuju Vám za všechno, bez Vás by žádná CaMKK publikace nebyla. Pavle, díky za Tvoje nadšení a všechny naše kávičkové debaty. Klári, děkuji Ti za to, že jsi mě celou dobu motivovala a sdílela se mnou útrapy PhD. Maša, thank you for being so kind and down-to-earth and for all our conversations. Jayshri, thank you for being such a wonderful student. Raju, thank you for being my friend in the lab. Děkuju i Vám všem ostatním, kteří vytváříte příjemnou atmosféru, díky které je chodit do práce radost.

Páji a Petře, děkuji Vám za pomoc s HDX měřením, za všechna vysvětlování a za ochotu, kterou jste projevovali, ať už se jednalo o první nebo n-tý pokus.

Bente, I am grateful for the opportunity to contribute a tiny bit to you ERα paper. It was a refreshing experience and I thank you for being such a great collaborator.

Jirko, děkuji Ti za asistenci se screeningem mřížek a za trénink na mikroskopu. Matyáši, děkuji Ti za kolekci dat a veškeré rady.

Mami, tati, Toníku, děkuju Vám za všechnu Vaši podporu a pomoc, za to, že mě vždycky vyslechnete, když mám něco na srdci anebo si chci jen tak popovídat. Děkuju Vám, že jste tu vždycky pro mě.

Maťo, děkuju Ti, že jsi to celé absolvoval se mnou.

Abstract

Protein-protein interactions are critical for most physiological and pathophysiological processes. Detailed characterization of these interactions is therefore essential not only to understand the nature of these events, but also to design strategies to target these interactions. This work focuses on the study of the structure and interactions of several proteins and their complexes. Apoptosis signal-regulating kinase 1 (ASK1) is a mitogen-activated protein kinase kinase kinase (MAP3K) that activates the p38/JNK protein kinase pathways, thereby directing cells toward an inflammatory response or apoptosis. ASK1 interacts with thioredoxin (TRX), a small dithiol oxidoreductase, which inhibits ASK1, but the mechanism of this inhibition has not been clarified. CaMKK1 and CaMKK2 are Ca^{2+}/calmodulin (CaM)-dependent protein kinases that regulate cellular energy balance, memory, and inflammation, among others. Both are inhibited by 14-3-3 proteins, but despite their domain and sequence similarities, the extent of 14-3-3 protein-mediated inhibition is different. Estrogen receptor alpha (ERα) is a nuclear receptor involved in breast cancer. Tamoxifen, an ERα antagonist, is used to treat this disease, but resistance often develops. 14-3-3 proteins interact with ERα and inhibit its transcriptional activity, but the nature of this interaction remains unclear. To better understand these protein-protein interactions, the proteins and their complexes were biophysically and structurally characterized. The cryo-EM structure of ASK1, together with analysis by analytical ultracentrifugation, shows that ASK1 forms a compact dimer with large intra- and inter-chain interactions that stabilize the active conformation of the kinase domain. Hydrogen-deuterium exchange coupled to mass spectrometry shows that TRX binding affects not only the TRX-binding domain, but also all other domains, the activation segment in the kinase domain included. Models of the pCaMKK1:14-3-3γ and pCaMKK2:14-3-3γ complexes obtained from the analysis of small angle X-ray scattering data suggest pCaMKK1 interacts with 14-3-3γ directly through its N-lobe and active site region, whereas pCaMKK2 forms minimal contacts with 14-3-3γ. Biophysical analysis of the ERα/14-3-3ζ complex shows that this complex forms with a stoichiometry of 2:2 and that neither the ERα-Y537S mutation nor ligand binding disrupts or prevents the formation of the complex. These results explain some aspects of the regulation of selected protein complexes and suggest possible ways to intervene in case of their dysregulation.

Abstrakt

Protein-proteinové interakce jsou klíčové pro většinu fyziologických i patofyziologických dějů. Detailní charakterizace těchto interakcí je proto nezbytná nejen k porozumění podstaty těchto dějů, ale i pro návrh strategií, jak tyto interakce cíleně ovlivňovat. Tato práce se zaměřuje na studium struktury a interakcí několika proteinů a jejich komplexů. ASK1 (z anglického „apoptosis signal-regulating kinase 1“) je mitogeny aktivovaná proteinkinasa kinasa kinasa (MAP3K), která aktivuje dráhy proteinkinas p38/JNK, čímž směruje buňky k zánětlivé reakci nebo apoptóze. ASK1 interaguje s thioredoxinem (TRX), malou dithioloxidoreduktasou, která inhibuje ASK1, nicméně mechanismus této inhibice je nejasný. CaMKK1 a CaMKK2 jsou Ca^{2+}/kalmodulin (CaM)-dependentní proteinkinasy, které regulují např. energetickou rovnováhu buňky, paměť či zánět. Obě jsou inhibovány proteiny 14-3-3, ale navzdory svým doménovým a sekvenčním podobnostem je rozsah inhibice zprostředkovaný proteiny 14-3-3 odlišný. Estrogenový receptor alfa (ERα) je jaderný receptor, který se podílí na vzniku rakoviny prsu. Pro léčbu tohoto onemocnění se používá tamoxifen, antagonista ERα, který však často způsobuje vznik rezistence. Proteiny 14-3-3 interagují s ERα a inhibují jeho transkripční aktivitu, povaha této interakce je však stále nejasná. Pro lepší pochopení těchto protein-proteinových interakcí jsme provedli biofyzikální a strukturní charakterizaci příslušných proteinů a jejich komplexů. Kryo-EM struktura ASK1 spolu s analýzou pomocí analytické ultracentrifugace ukazují, že ASK1 tvoří kompaktní dimer s rozsáhlým interakčním rozhraním jak mezi doménami v rámci jednoho řetězce, tak mezi řetězci navzájem. Tyto interakce stabilizují aktivní konformaci kinázové domény. Z vodík-deuteriové výměny spojené s hmotnostní spektrometrií je patrné, že vazba TRX ovlivňuje nejen TRX-vazebnou doménu, ale také centrální regulační oblast a aktivační segment v kinasové doméně. Modely komplexů pCaMKK1:14-3-3γ a pCaMKK2:14-3-3γ založené na analýze maloúhlového rozptylu rentgenového záření ukazují, že pCaMKK1 interaguje s 14-3-3γ přímo prostřednictvím svého N-lóbu a oblasti aktivního místa, zatímco pCaMKK2 tvoří s 14-3-3γ minimum kontaktů. Biofyzikální analýza komplexu ERα/14-3-3ζ ukazuje, že tento komplex vzniká se stechiometrií 2:2 a že ani mutace ERα-Y537S, ani vazba ligandu komplex nenarušují, případně nebrání v jeho vzniku. Získané výsledky vysvětlují některé aspekty regulace vybraných proteinových komplexů a naznačují možné způsoby zásahu v případě jejich dysregulace.

Table of contents

List of publications

Honzejkova, K., Kosek, D., Obsilova, V., Obsil, T. (2024). The cryo-EM structure of ASK1 reveals an asymmetric architecture allosterically modulated by TRX1. Under review in *eLife*.

> **Contribution:** I expressed and purified all proteins. I prepared the samples, performed the SV AUC experiments, and analyzed the data. I prepared the samples and partially analyzed the HDX-MS data. I prepared the samples and partially processed the cryo-EM data. I prepared the figures and participated in the writing of the manuscript.

Petrvalska, O., **Honzejkova, K.**, Koupilova, N., Herman, P., Obsilova, V., Obsil, T. (2023). 14-3-3 protein inhibits CaMKK1 by blocking the kinase active site with its last two C-terminal helices. *Protein Science*, 32(11), e4805. DOI: 10.1002/pro.4805

> **Contribution:** I expressed and purified proteins. I prepared the samples, performed SV AUC measurements and analyzed the data. I prepared the samples and analyzed SAXS data. I prepared the figures.

Somsen, B. A., Sijbesma, E., Leysen, S., **Honzejkova, K**., Visser, E. J., Cossar, P. J., Obšil, T., Brunsveld, L., Ottmann, C. (2023). Molecular basis and dual ligand regulation of tetrameric estrogen receptor α/14-3-3ζ protein complex. *The Journal of Biological Chemistry*, 299(7), 104855. DOI: 10.1016/j.jbc.2023.104855

> **Contribution:** I performed SV AUC measurements and analyzed the data.

Other publications:

Obsilova, V., Honzejkova, K., Obsil, T. (2021). Structural Insights Support Targeting ASK1 Kinase for Therapeutic Interventions. *International Journal of Molecular Sciences*, 22(24), 13395. DOI: 10.3390/ijms222413395

Abbreviations

4-OHT	4-hydroxytamoxifen
AID	autoinhibitory domain
AMP	adenosine monophosphate
ASK1	apoptosis signal-regulating kinase 1
ASK1-CC	coiled-coil domain of ASK1
ASK1-CRR	central regulatory region of ASK1
ASK1-KD	kinase domain of ASK1
ASK1-PH	pleckstrin homology domain of ASK1
ASK1-SAM	sterile alpha motif domain of ASK1
ASK1-TBD	thioredoxin binding domain of ASK1
ASK1-TPR	tetratricopeptide repeats domain of ASK1
ATP	adenosine triphosphate
β-ME	beta-mercaptoethanol
***c*(*s*)**	distribution of sedimentation coefficients
CaM	calmodulin
CaMK	calcium/calmodulin-dependent protein kinase
CaMKK	calcium/calmodulin-dependent protein kinase kinase
CBD	calmodulin-binding domain
Cdc25	cell division cycle 25
CHAPSO	3-[(3-cholamidopropyl)dimethylammonio]-2-hydroxy-1-propanesulfonate
Cryo-EM	cryogenic electron microscopy
CTD	C-terminal domain
D_{max}	maximum particle dimension
DBD	DNA-binding domain
DSF	differential scanning fluorimetry
DTT	dithiothreitol
E2	estradiol
EPK	eukaryotic protein kinase
ER	endoplasmic reticulum

ERK1	extracellular signal-regulated kinase 1
ER*α*	estrogen receptor alpha
FC-A	fusicoccin A
FOXO	forkhead box O
GB1	B1 domain of *Streptococcal* protein G
GSFSC	gold standard Fourier shell correlation
HDX-MS	hydrogen-deuterium exchange coupled to mass spectrometry
IKK	inhibitor of kappa B kinase
IMAC	immobilized metal affinity chromatography
IPTG	isopropyl β-D-1-thiogalactopyranoside
JNK	c-Jun amino-terminal kinase
K_D	dissociation constant
LBD	ligand-binding domain
MAP2K	mitogen-activated protein kinase kinase
MAP3K	mitogen-activated protein kinase kinase kinase
MAP4K	mitogen-activated protein kinase kinase kinase kinase
MAPK	mitogen-activated protein kinase
MKK6	mitogen-activated protein kinase kinase 6
MLCK	myosin light chain kinase
MPK38	murine ser/thr protein kinase 38
NCC	N-terminal coiled-coil domain
NLS	nuclear localization sequence
NMR	nuclear magnetic resonance
NR	nuclear receptor
NTD	N-terminal domain
***P*(*r*)**	distance distribution function
PKB	protein kinase B
PMSF	phenylmethylsulfonyl fluoride
PP1	protein phosphatase 1
PP2A	protein phosphatase 2A

PP2Cε	protein phosphatase 2C isoform epsilon
PP5	protein phosphatase 5
PTPN5	protein tyrosine phosphatase non-receptor type 5
PPEF2	protein phosphatase with EF-hand domain 2
PPI	protein-protein interaction
PRMT	protein arginine methyl transferase
PTM	post-translational modification
R_g	radius of gyration
RING	really interesting new gene domain
RNS	reactive nitrogen species
ROS	reactive oxygen species
RP	arginine-proline rich
SAXS	small-angle X-ray scattering
SDS-PAGE	sodium dodecyl sulfate–polyacrylamide gel electrophoresis
SEC	size-exclusion chromatography
SPA	single particle analysis
$s_{w(20,w)}$	sedimentation coefficient corrected for the density and viscosity of water and 20 °C
TCEP	tris(2-carboxyethyl)phosphine
TEV	tobacco etch virus
TRAF	tumor necrosis factor receptor-associated factor
TRX	thioredoxin
TXNIP	thioredoxin-interacting protein
UPS	ubiquitin-proteasome system
V_C	volume-of-correlation
V_P	Porod volume

1 Literature review

1.1 Protein-protein interactions

Proteins are indispensable for life as we know it. They provide living organisms with key functions ranging from reaction catalysis and DNA replication through molecular transport and maintaining cellular architecture to organismal defense and signal transduction (Alberts et al., 2002; Nelson et al., 2017).

Proteins always exist within an environment composed of a vast number of molecules – both non-protein such as sugars, nucleic acids, lipids, small organic molecules and ions, and other proteins (Gonzalez & Kann, 2012). Of course, these molecules inevitably affect the protein and can also regulate its biological function. Out of all the possible interactions proteins may be part of, this thesis focuses mainly on the interactions of proteins with other proteins (be it the same or different one).

Protein-protein interactions (PPIs) in cell assemble into a very complex system of mutually linked proteins called an interactome (Vidal, 2005). It is believed there is a characteristic interactome for any healthy cell type and organism and that any disruption of homeostasis within an organism may result in disturbance of the healthy pattern of PPIs. Some of the disruptions may be only correlative with a disease with no actual impact, others may be causative with significant roles in disease appearance and further progression (Kuzmanov & Emili, 2013). Either way, mapping PPIs is potentially interesting from both diagnostic and therapeutic point of view. This idea was acknowledged by many research teams and there are different viral, bacterial, and eukaryotic interactomes available now, including that of humans (Cherkasov et al., 2011; Hagen et al., 2014; Luck et al., 2020; Vo et al., 2016). An example of the interactome of human ASK1 is shown in Fig. 1.1 on page 13.

PPIs, however, were for long considered undruggable and are viewed as challenging biological targets even now. The reason behind that is the nature of the binding interface, which is large (usually reaches 1500 – 3000 Å), hydrophobic and shallow with few distinct pockets or grooves (Alzyoud et al., 2022). Fortunately, it was later found out via point mutation studies that despite the large binding interface, there are usually only a few residues critical for the interaction. These residues are called hot-spots and their emergence made coming up with interaction modulators much easier (Bogan & Thorn, 1998). In fact,

there are not only modulators interfering with the binding interface, so called orthosteric modulators, but also those interacting at allosteric sites – allosteric modulators. They act by either stabilizing or inhibiting the PPI and belong to one of three groups – small molecules, antibodies or peptides. Multiple modulators of PPIs have been already approved, others are in different phases of clinical trials (Lu et al., 2020). Overall, the study of PPIs can bring us not only a better understanding of the very principles of biochemistry of life, but also solutions to various problems we are currently facing.

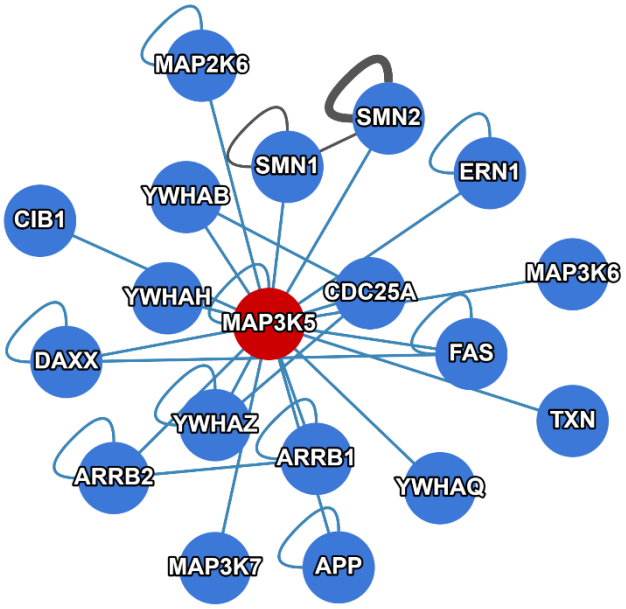

Figure 1.1 Interactome of human ASK1 (MAP3K5)
Human ASK1 is labeled in red. Interacting partners of ASK1 are shown in blue. Lines indicate interactions of proteins with each other or with themselves (Luck et al., 2020).

The subject of this thesis is the study of several PPIs. All the studies have one common denominator, 14-3-3 proteins, which play a central role in our group´s research. For this reason, I start the literature review with a brief overview of 14-3-3 proteins.

1.2 14-3-3 proteins

The name of 14-3-3 proteins comes from the way they were discovered – more precisely, it refers to a specific fraction on diethylaminoethyl cellulose column chromatography and a position on the starch gel electrophoresis, which were performed on the soluble extract from bovine brain (B. E. Moore & Perez, 1967). Seven 14-3-3 isoforms denoted by Greek letters β, γ, η, ε, σ, τ and ζ were identified in humans, all

of them with a molecular weight around 30 kDa and a pI value between 4.6 and 5.2 (Ichimura et al., 1988). All 14-3-3 isoforms were shown to form tight dimers, as was also confirmed by the first crystal structures of 14-3-3 isoforms τ and ζ (D. Liu et al., 1995; Xiao et al., 1995). The 14-3-3 dimer can consist of both, two monomers of the same isoform (a 14-3-3 homodimer) and two monomers each of a different isoform (a 14-3-3 heterodimer). There is only one exception, 14-3-3σ, which was shown to form solely homodimers (Verdoodt et al., 2006).

The monomer is formed by nine α-helices (H1 - H9) arranged in an antiparallel manner with the N-terminal α-helices mediating the dimerization between protomers. The dimer is cup-shaped, contains a central channel composed of α-helices H3, H5, H7 and H9 and two ligand-binding grooves – one per protomer (Fig. 1.2). One part of the binding groove comprising α-helices H3 and H5 contains mainly polar and charged residues, the other part comprising α-helices H7 and H9 contains mostly hydrophobic residues, together forming an amphipathic groove. The surface residues of the inner side of the groove are highly conserved among 14-3-3 isoforms. Residues in the binding groove shown to be especially important for ligand binding form a basic patch and include residues K49, R56 and R127 (Fu et al., 2000; Obsilova & Obsil, 2022).

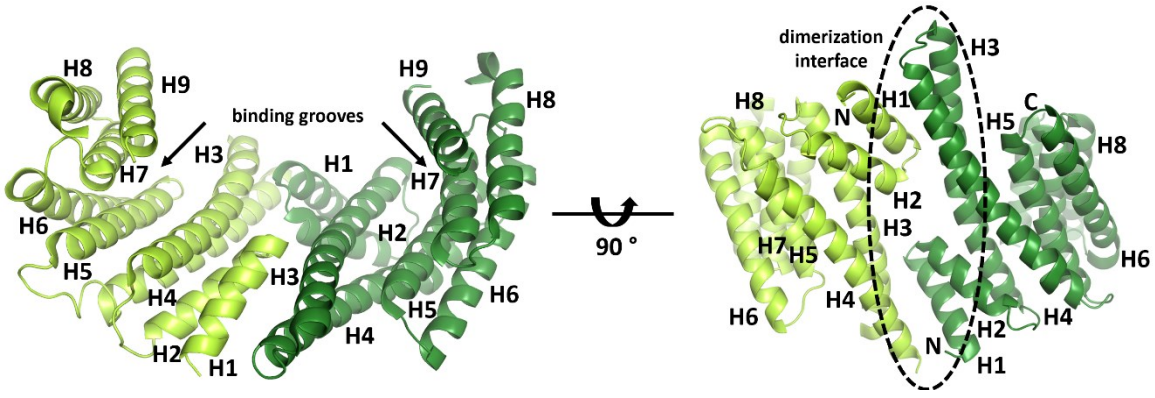

Figure 1.2 Crystal structure of 14-3-3γΔC
14-3-3γ ΔC homodimer with protomers distinguished by color. PDB ID:6FEL (Psenakova et al., 2018). The dimerization interface is indicated by the black ellipse.

Although 14-3-3 proteins sometimes bind ligands in a phosphorylation-independent fashion, it is much more common for them to bind phosphorylated motifs (Muslin et al., 1996; Ottmann et al., 2007). Three canonical motifs have been identified. Motifs I and II are formed by the sequences R[S/Φ][+](pS/pT)XP and RX[Φ/S][+](pS/pT)XP, where Φ stands for an aromatic residue, pS/pT stands for phosphoserine or phosphothreonine,

+ represents a basic residue and X can be anything, but usually is leucine, glutamate, alanine or methionine (Rittinger et al., 1999; Yaffe et al., 1997). Motif III was discovered a bit later and is characterized by the sequence pS/pT(X1-2)-COOH (Ganguly et al., 2005). Some of the targets that are bound by 14-3-3 proteins phosphorylation-independently include Exoenzyme S cytotoxin, an ADP-ribosyltransferase (Masters et al., 1999), human telomerase hTERT (Seimiya et al., 2000) or R18 peptide shown to bind the same site as phosphorylated targets and to be able to compete with them, thus suggested as a potential 14-3-3 antagonist (B. Wang et al., 1999).

The 14-3-3 proteins are called "hub proteins" because they interact with a large number of protein partners (recently estimated to be more than 1,200), including signaling proteins, transcription factors, metabolic enzymes, cytoskeletal components, apoptotic proteins, or cell cycle proteins, which implies that they are involved in the regulation of every conceivable process (Sluchanko & Bustos, 2019). Examples of 14-3-3 protein partners are the apoptotic proteins Bad, caspase-2 or Bim, whose interaction with 14-3-3 leads to their inhibition and therefore cell survival promotion. It has also been shown that 14-3-3 binding to p53 and its negative regulator MDMX promotes p53 activity. The interaction of 14-3-3 with the phosphorylated transcription factor forkhead box O (FOXO) prevents FOXO from translocating to the nucleus and as such blocks the upregulation of many genes, e.g. the pro-apoptotic proteins TRAIL, Puma or Bim (Pennington et al., 2018). The protein kinases apoptosis signal-regulating kinase 1 (ASK1), Ca^{2+}/calmodulin-dependent protein kinase kinase 1 and 2 (CaMKK1 and CaMKK2) as well as the nuclear receptor estrogen receptor alpha (ERα) are among the many targets of 14-3-3 proteins and it is these proteins that I will focus on in the following chapters.

1.3 Protein kinases

Protein phosphorylation is the most widespread post-translational modification in signal transduction and significantly affects virtually all cellular processes, e.g. differentiation, growth, metabolism, immunity and others (Manning, Plowman, et al., 2002). By covalently attaching the phosphate group to the target site, protein kinases introduce a charged and hydrophilic group to their substrate which leads to conformational changes and reorganization of the bonding networks. That results in the activation, deactivation or generally change of function of the target protein (Johnson & Barford, 1993). Phosphorylation can be reversed by the process of dephosphorylation, which

is carried out by protein phosphatases (Fig. 1.3). Together, these two opposing processes can be viewed as a molecular switch (Smoly et al., 2017).

Given the importance of protein kinases, it is no surprise that protein kinase-coding genes represent one of the largest gene families in eukaryotes constituting approximately 2 % of the genome. The human kinome includes nearly 540 protein kinases which were, based on their sequence similarity, classified into eight typical (AGC, CAMK, CK1, CMGC, STE, TK, TKL, Other) and 13 atypical families (Fig 1.4 on page 18) (Eid et al., 2017; Manning, Whyte, et al., 2002).

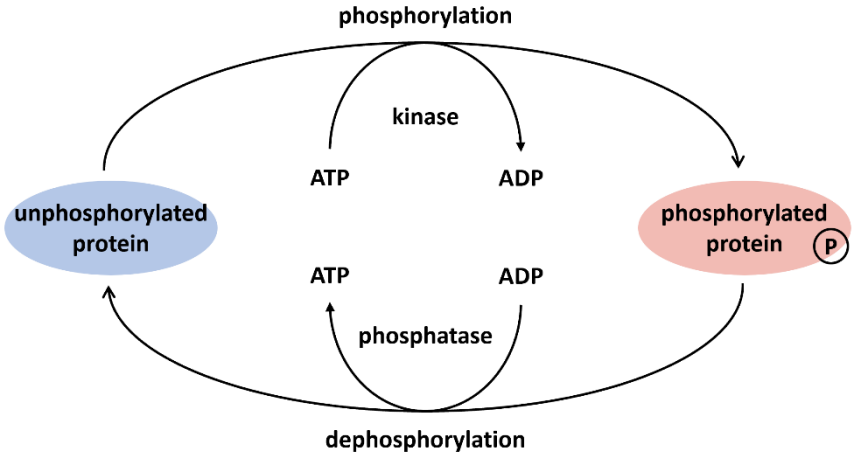

Figure 1.3 Reversible phosphorylation of a protein substrate
The transfer of the phosphate group, whose donor is usually an ATP molecule, is catalyzed by protein kinases. This is counteracted by protein phosphatases, which in turn remove the phosphate group.

Protein kinases are also sortable by specificity. The most common are serine/threonine protein kinases, but there are also tyrosine kinases and so-called dual specificity protein kinases which can act as both serine/threonine and tyrosine kinases (Lin et al., 1995). It is estimated that about half to two-thirds of human proteins are regulated by phosphorylation, and some proteins may contain dozens of phosphorylation sites. With several thousand proteins in total, this means that there could be up to several hundred thousand phosphorylation sites (Vlastaridis et al., 2017).

With only about 540 known protein kinases, it had long been a mystery how a given protein kinase chooses the right one from among so many potential phosphorylation sites. The specificity is ensured thanks to the combination of several mechanisms. Tyrosine protein kinases, compared to serine/threonine kinases, have a deeper catalytic cleft as the tyrosine residues are bigger and can bridge a greater distance between the protein

backbone and γ-phosphate of adenosine triphosphate (ATP). The amino acid sequence in the catalytic site of the kinase is just as important as the sequence surrounding the phosphorylation site within the substrate – there are known consensus phosphorylation sites for many protein kinases. Besides the local interactions in the proximity to the catalytic site, the specificity is also achieved thanks to other domains in addition to the catalytic one, which may bind to docking motifs on the substrate and hence increase the affinity. An important parameter affecting specificity is the localization of the kinase – sequestration into subcellular organelles may both increase the local concentration of the kinase as well as restrict the number of substrates available. Another layer of regulation is performed by scaffold proteins which may function as the docking platform for both the kinase and the substrate and by changing their conformation, they enable or block the phosphorylation. Additional mechanisms include the competition between several substrates, need for sequential multiple site phosphorylation and finally the existence of protein phosphatases, which can reset the effect of protein kinases (Ubersax & Ferrell, 2007).

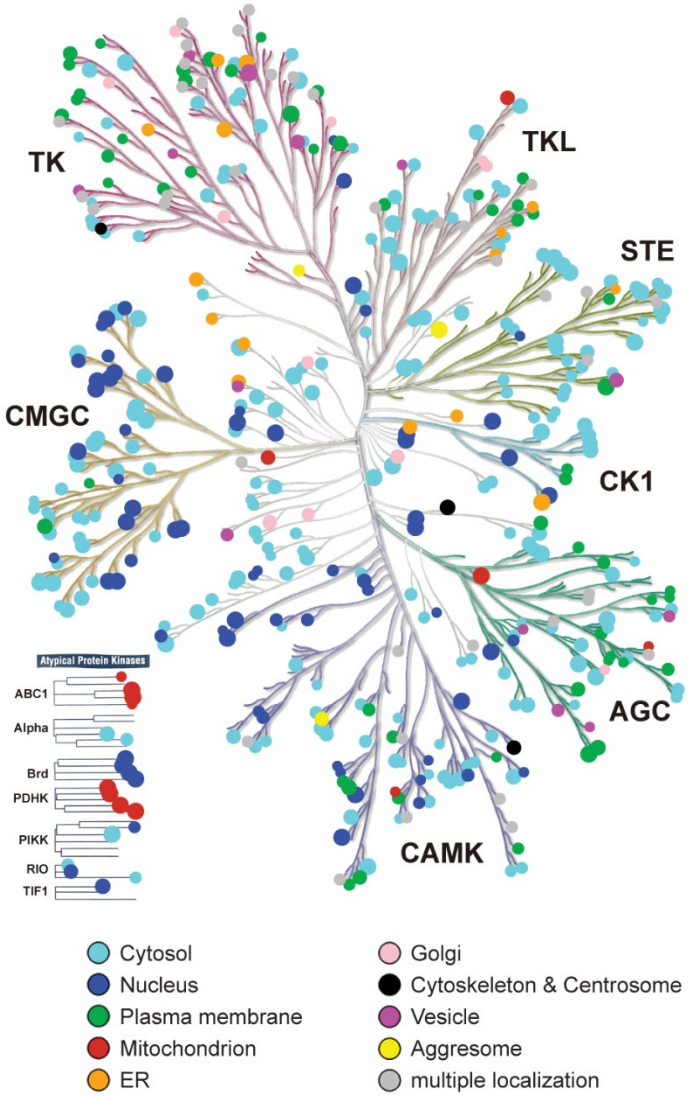

Figure 1.4 Phylogenetic tree showing the sequence similarity of the catalytic domains of human protein kinases.
Seven major groups of protein kinases are shown - AGC (protein kinase families A, G and C), CAMK (Ca^{2+}/calmodulin-dependent kinases), CK1 (casein kinase 1), CMGC (initial letters of some of the kinases, including MAPK growth and stress kinases and cyclin-dependent kinases), STE (homologs of the yeast kinases Sterile 7/11/20), TK (tyrosine kinases), and TKL (tyrosine kinase-like). The localization of each kinase is color-coded. Dot size is a measure of localization score. Adapted from Zhang et al., 2021.

Eukaryotic protein kinases (EPK) are defined by a conserved kinase core formed by about 250-300 residues, which are necessary for catalysis and scaffolding. Besides, EPKs contain variable number of additional domains, linkers and other regulatory sites. The kinase core is divided into two distinct parts, N-terminal lobe formed largely by an antiparallel β-sheet and mostly α-helical C-terminal lobe. They are connected through a hinge region creating a catalytic cleft where the adenine ring of ATP binds thereby

positioning the γ-phosphate at the outer side of the cleft (Hanks & Hunter, 1995; Taylor et al., 2012). The first protein kinase structure solved in 1991 was that of the catalytic subunit of cAMP-dependent protein kinase or protein kinase A (PKA), which later became the representative for all members of protein kinase family as it turned out they all share the same kinase fold (Knighton et al., 1991).

The N-lobe is formed by a five-stranded β-sheet composed of β-strands 1 to 5. β1 is linked to β2 by a glycine-rich loop, which lines the ATP from the top side and ensures that the γ-phosphate is positioned correctly for the subsequent transfer. In active conformation, a very important lysine residue (K72 in PKA) from β3 interacts with a glutamate (E91 in PKA) from the only conserved α-helix present in N-lobe, the αC-helix, located between β3 and β4 (some kinases, PKA included, also have a short αB-helix). The C-lobe is predominantly α-helical, but it also contains a four-stranded β-sheet ´sitting´ on the helical part. The β-sheet lines the bottom side of the catalytic cleft and contains important catalytic residues. These are residues H/YRDXKXXN from the conserved catalytic loop between β6 and β7 which play a key role in the transfer of γ-phosphate of ATP to the kinase substrate. β8 is connected to β9 via a magnesium positioning loop. This loop contains the DFG motif from which the conserved aspartate (D184 in PKA) is necessary for binding of the catalytic Mg^{2+} ion (Bossemeyer, 1995; Taylor et al., 2012). The DFG motif represents the beginning of an activation segment, the length of which is variable and in case of PKA extends to E208. It is a crucial part of the kinase responsible for the precise switch between the ´on´ and ´off´ state, the regulation of which is complex and special to each kinase. The rest of the C-lobe comprises helices named αD to αI forming an extremely stable structure important for substrate binding (Taylor & Kornev, 2011). Structure of the kinase domain of PKA with functional elements highlighted is shown in Fig 1.5 on page 20.

Due to the involvement of protein kinases in virtually all important processes in the body, their dysregulation plays a major role in the development of many diseases - especially malignancies, but also inflammatory or neurodegenerative diseases. This fact makes protein kinases the second most common drug target (Cohen, 2002; Knapp, 2018). As of the end of 2022, a total of 72 therapeutic agents targeting just over 20 different protein kinases have been approved by the FDA (Roskoski, 2023). Most currently approved drugs target the ATP-binding site, which is associated with many adverse events. For this reason, efforts are now being made to develop molecules that bind outside the active site (allosteric

inhibitors), using information about the regulation of specific protein kinases. However, to design such inhibitors, a detailed understanding of how a particular kinase is regulated is imperative (Bhullar et al., 2018).

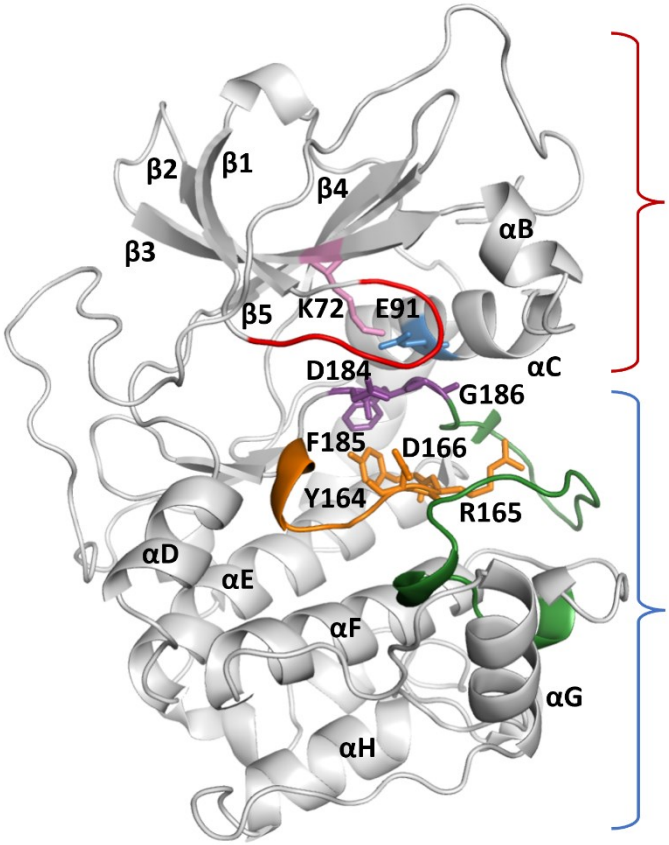

Figure 1.5 Crystal structure of the kinase domain of PKA.
The structure of the kinase domain of PKA consists of the N-lobe and C-lobe marked in red and blue, respectively. The N-lobe is mainly composed of β-strands β1-5 and helix αB and αC, while the C-lobe is predominantly helical, consisting of helices αD-J. In the active conformation, K72 (pink) and E91 (blue) interact. The glycine-rich loop is shown in red, the catalytic loop in orange, the Mg^{2+} positioning loop in purple, and the activation segment in green. PDB ID: 2CPK (Knighton et al., 1991).

1.4 MAPK signaling

Mitogen-activated protein kinase (MAPK) cascades are evolutionarily conserved in all eukaryotes (Widmann et al., 1999). They are essential for the transmission of a large number of signals from the extracellular environment to the nucleus to ensure an appropriate cellular response to a specific situation (Seger & Krebs, 1995). The first member of this family to be discovered is extracellular signal-regulated kinase 1 (ERK1),

a serine/threonine kinase that is activated in response to growth factors. It is because other members of this family have been also shown to be activated in response to growth factors that the protein family was given the name ´mitogen-activated´ protein kinases (Sturgill et al., 1988). The list of stimuli besides growth factors activating MAPK pathways includes for example cytokines, G-protein coupled receptor ligands, hormones, and environmental stresses such as ionizing radiation, osmotic shock, temperature, or ischemic injury (Kyriakis & Avruch, 2001; Pearson et al., 2001), and this activation can lead to responses including apoptosis, cell division, gene expression, differentiation, regulation of motility and metabolism, and more (Cargnello & Roux, 2011; Schaeffer & Weber, 1999).

MAPK signaling pathways share a common architecture characterized by three levels of protein kinases that transduce signals through sequential phosphorylation. MAPK kinase kinases (MAP3Ks) are the topmost and once activated, they pass the signal through phosphorylation to their substrates, the intermediate MAPK kinases (MAP2Ks), which then phosphorylate and activate the downstream MAPKs in the same manner (Cargnello & Roux, 2011; Ferrell, 1996). There are four conventional MAPK modules named after the downstream MAPKs – ERK1/2, ERK5, c-Jun amino-terminal kinases 1 to 3 (JNK1/2/3) and p38 kinases (p38α/β/γ/δ) (Cargnello & Roux, 2011). The MAPKs are serine/threonine protein kinases. In contrast, MAP2Ks are dual-specificity kinases that phosphorylate threonine and tyrosine residues of the tripeptide motif Thr-X-Tyr in the activation loop of their fellow MAPKs, and there are seven of them in mammals. The MAP3Ks are serine/threonine kinases. They are the most abundant group with a total of 24 members (Kassouf & Sumara, 2020; Manning, Whyte, et al., 2002; A. F. Peterson et al., 2022). They are activated either by an upstream kinase, the MAP3K kinase (MAP4K), or by other mechanisms involving oligomerization, subcellular localization, and interactions with other proteins (I. W. Leung & Lassam, 1998; Luo et al., 1996; Widmann et al., 1999). The architecture and composition of the MAPK signaling pathways is summarized in Fig. 1.6 on page 22.

There are numerous mechanisms regulating MAPK pathways to ensure an appropriate response to a specific stimulus. Dephosphorylation via phosphatases, including serine/threonine protein phosphatases 2A and Cε (PP2A and PP2Cε), protein tyrosine phosphatases like protein-tyrosine phosphatase non-receptor type 5 (PTPN5), and/or dual specificity phosphatases can prevent the generation and transmission of the signal by phosphorylation (Alessi et al., 1995; Keyse, 2000). The extent and duration

of kinase activation are affected by dephosphorylation (Krishna & Narang, 2008). Adaptor proteins are also involved in regulation, facilitating the interaction between proteins of a given pathway, affecting their cellular location, or maintaining them in inhibited state, for instance (Obsilova & Obsil, 2020). Another regulatory mechanism is related to cellular localization. Translocation to the nucleus only occurs in JNK and p38 kinases after they are activated (H. L. Cheng & Feldman, 1998). In ERK5, the association between the protein´s termini is disrupted after the activating phosphorylation by the upstream MEK5, which, in turn, blocks the nuclear export of ERK5 and leads to its import into the nucleus (Kondoh et al., 2006). Additionally, the MAPK cascade is modulated through crosstalk with other signaling pathways, such as the communication between the MAPK pathway and the cAMP-dependent pathway (Takahashi et al., 2004; Yehia et al., 2001). Regulation also occurs through post-translational modifications (PTMs), such as ubiquitination followed by proteasomal degradation (Mathien et al., 2021).

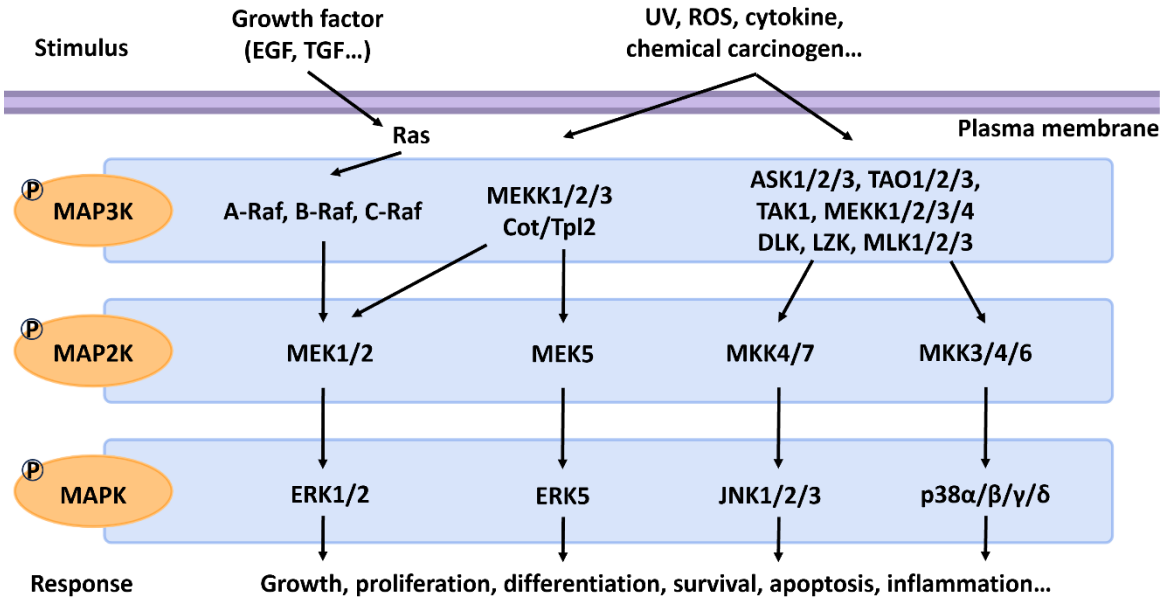

Figure 1.6 The architecture of MAPK cascade.
Various stimuli activate MAP3Ks, which then phosphorylate MAP2Ks, which then phosphorylate MAPKs. MAPKs then phosphorylate other targets to ensure a specific cellular response to the initial stimulus. Adapted from Kamiyama et al., 2015.

1.4.1 Apoptosis signal-regulating kinase 1 (ASK1)

ASK1 is a member of MAP3K family. It was discovered as the protein responsible for the activation of p38 and JNK signaling pathway through MAP2Ks MKK3/MKK6

and MKK4/MKK7, respectively, as shown in Fig 1.7 (Ichijo et al., 1997). ASK1 further belongs to the ASK protein family encompassing two more members – ASK2 and ASK3. All three proteins are similar in length and share similar features, especially within their kinase domains (KD) (Nishida et al., 2017). While ASK2 was discovered a year after ASK1 as its interaction partner, ASK3 waited more than a decade to be discovered (Kaji et al., 2010; X. S. Wang et al., 1998). The expression of ASK3 is the highest in kidney. It was shown to react to osmotic stress and affect blood pressure via WNK1-SPAK/OSR1 signaling (Naguro et al., 2012). Nevertheless, ASK2 and ASK3 remain understudied when compared to ASK1.

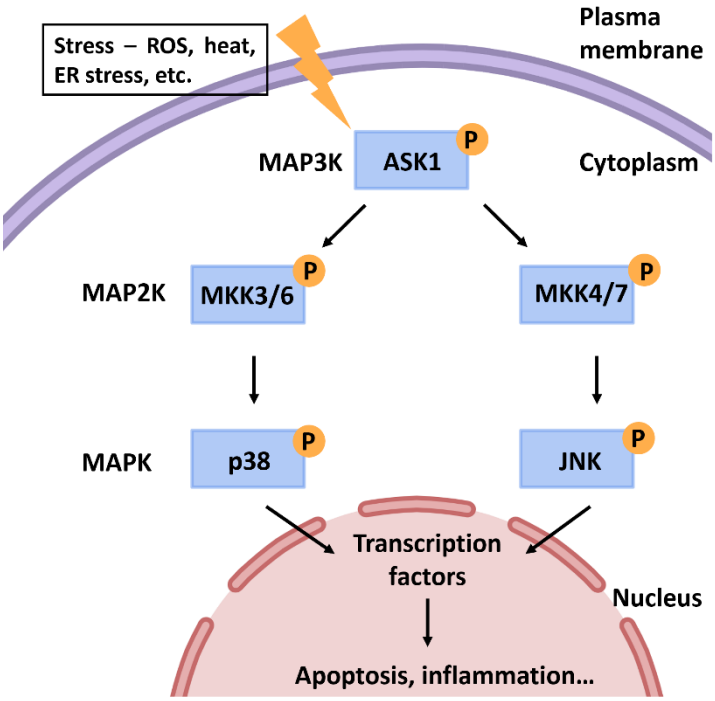

Figure 1.7 ASK1-p38/JNK pathway.
When ASK1 is activated by cellular stress, p38/JNK pathways can be activated. Activation of p38 occurs when ASK1 phosphorylates and thereby activates MKK3/6 substrates, which in turn phosphorylate p38. JNK activation occurs as a result of phosphorylation of MKK4/7, which provide JNK phosphorylation. Activated p38 and JNK then phosphorylate e.g. transcription factors and can ultimately lead to cell death or inflammation. Adapted from Obsilova et al., 2021.

Various stimuli promote ASK1 activation, the most potent one being oxidative stress (Saitoh et al., 1998; Tobiume et al., 2001). Besides that, ASK1 is also activated in response to other stimuli such as tumor necrosis factor α (TNF- α) (Gotoh & Cooper, 1998; Ichijo et al., 1997), calcium influx (Takeda et al., 2004), lipopolysaccharides (Matsuzawa et al., 2005), or endoplasmic reticulum (ER) stress (Nishitoh et al., 2002). The overexpression

and activation of ASK1 leads to inflammation and cell death (Ichijo et al., 1997; Iriyama et al., 2009; Takeda et al., 2003; Yoshikawa et al., 2020).

ASK1 has been implicated in a plethora of diseases, spanning from neurodegenerative, inflammatory, and autoimmune diseases to kidney and liver diseases, cardiovascular diseases, and cancer. Many neurodegenerative diseases are characterized by the accumulation of structurally abnormal proteins that form insoluble aggregates. For example, in Alzheimer's disease, amyloid-β forms these aggregates; in Parkinson's disease, α-synuclein does; and in Huntington's disease, polyQ fragments do. The buildup of these aggregates induces ER-stress and generates reactive oxygen species (ROS). These, in turn, activate ASK1-p38/ASK1-JNK pathways that result in neuronal cell death (Araki et al., 2019; Hsu et al., 2007; Kadowaki et al., 2005; Sekine et al., 2006). ASK1 was shown to be involved in signaling relevant to rheumatoid arthritis, an inflammatory disease characteristic by gradual bone and cartilage degradation as well as synovial hyperplasia. In response to inflammatory cytokines, ASK1 is upregulated and as such plays a role in the advancement of the disease (Mnich et al., 2010; Nygaard et al., 2018). Another study suggested targeting ASK1 in autoimmune demyelinating disorders, possibly including multiple sclerosis, as ASK1 knockout mice demonstrated reduced neuroinflammation in experimental autoimmune encephalomyelitis (Guo et al., 2010). Activation of ASK1 is linked to increased lipid accumulation in the liver, elevated blood glucose levels, and increased inflammation both in the liver and systemically (Schuster & Feldstein, 2017). A Phase III clinical trial showed that selonsertib, an ASK1 inhibitor, did not reduce fibrosis in patients with non-alcoholic steatohepatitis (Harrison et al., 2020). Inhibition of the ASK1-p38 pathway in the heart in response to ROS has also been found to protect the heart and prevent hypertension-induced cardiac remodeling, suggesting that targeting this pathway could potentially be used to treat hypertensive heart disease (Meijles et al., 2020). ASK1 is critical in tumorigenesis and has been shown to have a dual effect. In certain scenarios, it displays anti-tumor properties while promoting tumor growth in others. Lung cancer cell proliferation and migration are inhibited by ASK1 overexpression. This is achieved by having ASK1 interact with transcriptional co-activator with PDZ-binding motif (TAZ), which ASK1 inactivates. (Han et al., 2020). Conversely, ASK1 within bone marrow-derived cells appears to facilitate the metastasis of lung tumor (Kamiyama et al., 2017). Correspondingly, high levels of ASK1 have been identified in pancreatic cancer cell

lines, wherein ASK1 induces proliferation and promotes carcinogenic potential of pancreatic cancer cells (Luo et al., 2016).

As can be seen from the above, upregulation of the JNK and p38 pathways, with ASK1 as their upstream activator, is involved in the development of many serious diseases. There have been efforts to develop p38 and JNK inhibitors, but these have been either ineffective or associated with side effects (Obsilova et al., 2021; Ogier et al., 2020). It is for this reason that ASK1 is now being considered as a target for therapeutic intervention instead.

1.4.1.1 Domain structure

Human ASK1 comprises 1374 amino acid residues, which together form several domains (Ichijo et al., 1997). The kinase domain (ASK1-KD), the core of the enzyme, is located approximately in the center (Bunkoczi et al., 2007; Ichijo et al., 1997). It is flanked at the N-terminus by the thioredoxin-binding domain (ASK1-TBD) (Saitoh et al., 1998) and the central regulatory region (ASK1-CRR), which is further subdivided into the tetratricopeptide repeat domain (ASK1-TPR) and the pleckstrin homology domain (ASK1-PH) (H. Liu et al., 2000; Weijman et al., 2017). C-terminal to the KD is a disordered region containing a 14-3-3 binding motif (L. Zhang et al., 1999), a predicted coiled-coil domain (ASK1-CC) (Tobiume et al., 2002) and the last discovered sterile alpha motif domain (ASK1-SAM) (Trevelyan et al., 2020). The domain architecture and the structure of individual domains is illustrated in Fig 1.8 on page 26. ASK2 and ASK3 are 1288 and 1313 amino- acid-long and their KDs share 82% and 88% amino acid identity with that of ASK1 (Kaji et al., 2010; X. S. Wang et al., 1998).

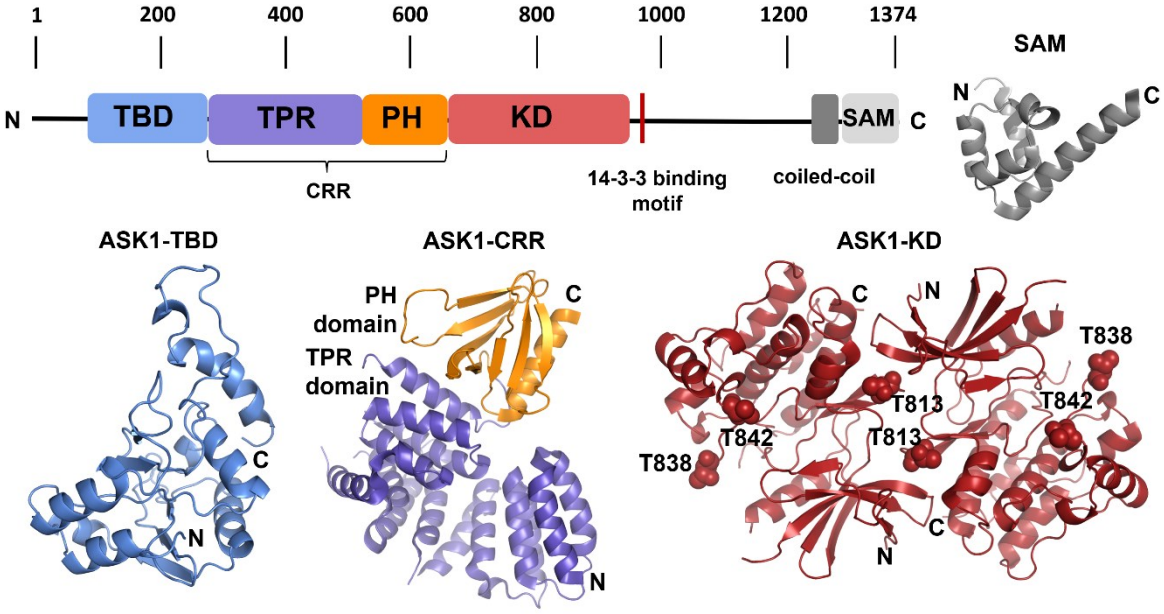

Figure 1.8 Domain architecture of ASK1 and the structure of individual domains. The individual color-coded domains of ASK1 are shown schematically at the top of the figure. The currently available structures of each domain are shown below. The NMR-based model for ASK1-TBD is shown in blue (Psenakova et al., 2020), ASK1-TPR is shown in purple, and ASK1PH is shown in orange. These two are part of the crystal structure of ASK1-CRR (PDB ID:5ULM) (Weijman et al., 2020). The crystal structure of the ASK1-KD dimer (PDB ID:2CLQ) is shown in red, with the three autophosphorylation sites T813, T838 and T842 represented by spheres (Bunkoczi et al., 2007). The crystal structure of ASK3-SAM (PDB ID:6V0M is shown in grey (Trevelyan et al., 2020). Adapted from Obsilova et al., 2021.

1.4.1.2 Thioredoxin-binding domain

As the name suggests, ASK1-TBD was originally discovered as the region responsible for interacting with the thioredoxin (TRX) protein. The binding of TRX to ASK1 is redox-dependent and inhibits ASK1 activity, in part by inducing ubiquitination and subsequent degradation. When TRX is oxidized, its interaction with ASK1 is blocked (Y. Liu & Min, 2002; Saitoh et al., 1998). Using truncation studies, a region in the range 46-267 containing eight cysteine residues was found to be specifically responsible for TRX binding (Fujino et al., 2007). Biophysical analysis revealed that ASK1-TBD is monomeric and structurally rigid in solution. Interaction studies with TRX revealed that the ASK1-TBD:TRX complex has a 1:1 stoichiometry. Affinity studies of ASK1-TBD and TRX using different mutant forms of both proteins or different redox states confirmed that oxidized TRX forms a weaker complex with ASK1-TBD and its redox inactive variant with cysteines mutated to serines hardly binds. At the same time, the $W^{31}CGPC^{35}$ catalytic

motif of TRX was shown to be essential for the stability of the complex, as well as C250 of ASK1-TBD (Kosek et al., 2014; Kylarova et al., 2016). Formation of intramolecular disulfide bridges upon oxidation of ASK1-TBD affects the domain conformation. C250 near the C-terminus of the domain is essential for preserving the structure of ASK1-TBD (Kylarova et al., 2016; Psenakova et al., 2020). A structural model of the ASK1-TBD based on nuclear magnetic resonance (NMR) data (Fig 1.9A) shows that the domain is structurally similar to the TRX molecule. It consists of a six-stranded beta sheet decorated with six alpha helices and loop regions (Psenakova et al., 2020). Further insight into the structure of this domain is provided by the AlphaFold model (Fig 1.9B), which agrees with the NMR-based model to some extent - the elements of the secondary structure are essentially the same, but the overall shape is different (Jumper et al., 2021; Varadi et al., 2022). An experimental high-resolution structure of ASK1-TBD is still missing.

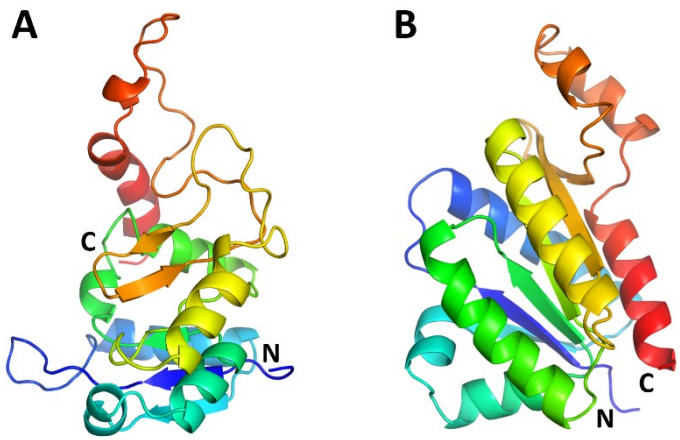

Figure 1.9 Comparison of the ASK1-TBD structural models.
A – NMR-based structural model (Psenakova et al., 2020). B – AlphaFold structural model (Jumper et al., 2021; Varadi et al., 2022). Both models are colored from blue (N-terminal) to red (C-terminal).

1.4.1.3 Central regulatory region

The part of the ASK1 molecule that overlaps with the region now called ASK1-CRR was previously called the TRAF-binding domain. Shortly after its discovery, ASK1 was found to interact with the tumor necrosis factor receptor-associated factor (TRAF) family of proteins, specifically TRAF2, TRAF5, and TRAF6, through their C-terminal TRAF domain. When TRAF proteins were overexpressed, ASK1 was activated. Further experiments showed that ASK1 mediates JNK activation through activation by TRAF

proteins (Nishitoh et al., 1998). Truncation studies showed that TRAF proteins interact with both the N-terminal portion of ASK1 (amino acid range 1-460) and the C-terminal portion (937-1374). Although no interaction of ASK1 with the N-terminal really interesting new gene (RING) domain was detected, this domain is important for ASK1 activation, most likely for promoting its homooligomerization (H. Liu et al., 2000). The interaction between TRAF2 and ASK1 is redox-dependent, and it has been shown that overexpressed TRX can prevent both this interaction and ultimately JNK activation (H. Liu et al., 2000; Noguchi et al., 2005). Another study investigating the interaction between TRAF2/6 and ASK1 identified a binding site for these proteins on ASK1 between residues 384-655. At the same time, the so-called N-terminal coiled-coil domain (NCC), located in the amino acid region 297-324, was mentioned. This region is reported to be required for homooligomerization of the N-terminal portion of ASK1 and subsequent activation. Binding of TRX to the ASK1-TBD is thought to inhibit this oligomerization, whereas overexpression of TRAF2, TRAF6, or treatment with H_2O_2 promotes the homooligomerization (Fujino et al., 2007). Defining ASK1-CRR was only achieved by solving the crystal structure of this domain. It turned out ASK1-CRR can be further subdivided. The first subdomain, ASK1-TPR, consists of 14 α-helices (seven TPR repeats) that are packed together in such a way that even amino acids far apart in sequence are in close contact. The second subdomain, ASK1-PH, is folded on ASK1-TPR and consists of two β-sheets and a C-terminal α-helix. It has been shown in vitro that when ASK1-CRR is added in trans to ASK1-KD, there is an increase in phosphorylation of the substrate MKK6. In addition, it was found that ASK1-CRR is monomeric in solution and that maintaining its architecture is important for maintaining its ability to phosphorylate the substrate (Weijman et al., 2017).

1.4.1.4 Kinase domain

ASK1-KD was identified as the first of all ASK1 domains based on sequence similarity to the kinase domains of other MAP3Ks (Ichijo et al., 1997). Similarly, the crystal structure of ASK1-KD was the first solved domain of ASK1. This structure showed that ASK1-KD has a fold that is typical of most kinases - it consists of two lobes that are connected to each other by a hinge region that lines the ATP-binding site. The smaller N-terminal lobe consists of a five-stranded beta sheet and an alpha-C helix, while the larger C-terminal lobe is predominantly alpha-helical. The structure of ASK1-KD was crystallized in complex with the inhibitor staurosporine, which probably caused an outward shift of the alpha-C helix compared to the classical active conformation

and a reorganization of the interatomic contacts in the region around the active site. The crystallization of ASK1-KD as a dimeric protein was followed by the determination of its dissociation constant in solution, which was found to be about 200 nM. The structure of ASK1-KD contains three autophosphorylation sites, T813, T838 and T842 (Bunkoczi et al., 2007). Phosphorylation of T838 in the activation loop is essential for the activation of ASK1 in response to oxidative stress, and its phosphorylation can occur either by trans-autophosphorylation or possibly by trans-phosphorylation with the help of an upstream kinase (Tobiume et al., 2002). In the related kinases ASK2 and ASK3, the key T838 of ASK1 corresponds to T806 and T808, respectively (Nishida et al., 2017). The upstream kinase partially responsible for ASK1 phosphorylation at T838 is murine protein Ser/Thr kinase 38 (MPK38), which belongs to the AMP-activated protein kinase family. These two kinases interact through their C-terminal regulatory domains, the region 941-1374 in ASK1 and 270-643 in MPK38. Phosphorylation of ASK1 by MPK38 promotes ASK1 activity and thereby signal transduction to p38 and JNK (Jung et al., 2008). C-terminal to the ASK1-KD there is also a binding motif for 14-3-3 proteins, which interacts with the phosphorylated S966 and inhibits the activity of ASK1 *in vivo* and *in vitro* (Petrvalska et al., 2016; L. Zhang et al., 1999). This interaction can be counteracted by oxidative stress-induced dephosphorylation of S966 through the action of PP1 (protein phosphatase 1) or PP2A (protein phosphatase 2A) phosphatases (Goldman et al., 2004). The complex of phosphorylated ASK1-KD and 14-3-3 forms a 1:1 stoichiometry complex (14-3-3 dimer with ASK1 dimer), is extended and relatively flexible. 14-3-3 binds ASK1-KD in the C-lobe region close to both the active site and the activation segment and affects the dynamics of two autophosphorylation sites - crucial T838 and T842 (Petrvalska et al., 2016). 14-3-3 proteins also interact with ASK2, specifically with phosphorylated S964, and there are reports that ASK1 forms a heterodimer with ASK2 and both proteins together form a ternary complex with 14-3-3 proteins (Cockrell et al., 2010; Federspiel et al., 2016).

1.4.1.5 C-terminal regulatory domains

The region C-terminal to the kinase domain is important for ASK1 oligomerization and plays role in ASK1 activity and signaling to p38 and JNK. At the same time, it is the least structurally explored region. Based on the sequence, the presence of the CC motif was predicted in the region of residues 1236-1293 (Lupas et al., 1991; Tobiume et al., 2002). These motifs are formed by multiple helices coiled together and were shown to play a role in the oligomerization of several other kinases (J. Liu et al., 2006; Roe et al.,

1997; Vacratsis & Gallo, 2000). They can be also used as tags to enforce a particular oligomeric state (Deiss et al., 2014). Deletion of the predicted CC motif in the ASK1 C-terminus confirmed its importance for homooligomerization (Tobiume et al., 2002), but the structure remains unknown. Three years ago, a SAM domain, previously undiscovered in ASK proteins, was identified in ASK1, ASK2 and ASK3 (Trevelyan et al., 2020). SAM domains are known to mediate both homotypic and heterotypic interactions (A. J. Peterson et al., 1997). This was also confirmed for proteins of the ASK family, where this domain was discovered at the C-terminal end. Isolated SAM domains from ASK1-3 differ in their oligomeric behavior – while ASK1-SAM itself forms concentration-dependent oligomers and ASK2-SAM is monomeric, ASK3-SAM forms stable oligomers. More interestingly, when ASK1/2-SAMs are in solution together, a stable heterocomplex is formed despite the behavior of each domain separately. The crystal structure of ASK3-SAM revealed that each monomer is composed of five helices, as is typical of the SAM fold. The molecules interact with each other through the so-called mid-loop-end-helix interaction, which was observed in many other proteins containing SAM domains. In both ASK1 and ASK2, five helices have also been predicted in this region, and thus the structure of ASK1-SAM and ASK2-SAM is predicted to be very similar (Trevelyan et al., 2020).

1.4.1.6 Thioredoxin

Under physiological conditions, redox homeostasis is maintained in cells - the ROS and RNS (reactive nitrogen species) production is countered by reactions that eliminate these substances. This is a highly dynamic process that requires systems that can respond rapidly to changes in redox status. Cells have enzymes that can directly eliminate ROS/RNS, such as superoxide dismutase and catalase, which remove the superoxide radical and hydrogen peroxide, respectively. However, when ROS/RNS are present in the cell, oxidation of proteins containing thiol groups also occurs. To ensure the reduction of these oxidized proteins, two major systems are available in the cell, the TRX (Fig. 1.10A on page 31) and glutaredoxin (GRX) systems (Le Gal et al., 2021; Trachootham et al., 2008).

TRX, a small and heat-stable protein, was first isolated from *E. coli* in 1964, along with the enzyme responsible for TRX reduction, TRX reductase (Laurent et al., 1964). TRX is a ubiquitous protein present in all species from bacteria, yeast and plants to humans and has a molecular weight of about 12 kD. Its active center is formed by the sequence

WCGPC, and redox reactions involve reversible oxidation of the two cysteines in the active site (Holmgren, 1985). In human TRX, there are three other cysteines at positions 62, 69, and 73 which are not required for the activity, in addition to the two catalytically active cysteines (Forman-Kay et al., 1992). The structure of TRX consists of a twisted five-stranded beta sheet decorated with four helices as shown in Fig. 1.10B (Weichsel et al., 1996). In addition to cytosolic TRX1, TRX2 is found in human mitochondrial matrix (Tanaka et al., 2002). TRXs regulate many important processes by interacting with other proteins. They can activate or inhibit transcription factors, promote neuronal survival during ischemia, or regulate apoptosis (Arnér & Holmgren, 2000).

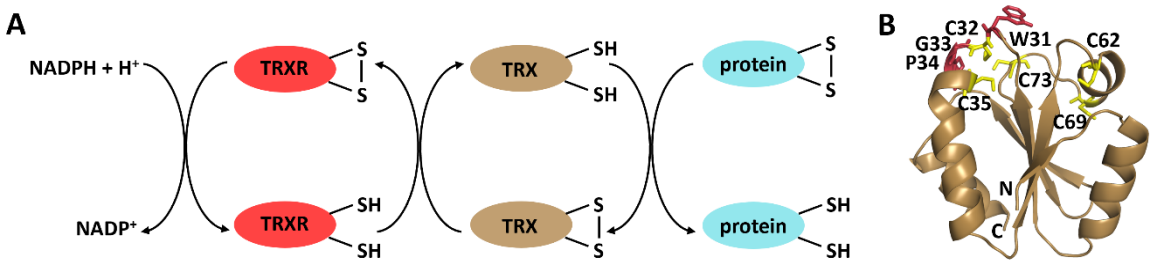

Figure 1.10 TRX as important cellular reductant.
A – Schematic representation of the TRX system in a cell. TRX reduces oxidized proteins and in doing so, oxidizes itself. Its reduction is performed by TRX reductase (TRXR), which is able to perform this function thanks to the presence of reduced NADPH. Adapted from Dunn et al., 2010. B – Crystal structure of reduced TRX. The catalytic region is shown in red sticks, the cysteines (including the catalytic ones) are shown in yellow sticks. PDB ID:1ERT (Weichsel et al., 1996).

1.4.1.7 Regulation of ASK1

ASK1 is an essential MAP3K that plays a prominent role in activating p38 and JNK. Its tight control is essential to prevent the development of the diseases discussed in chapter 1.5. TRX was the first discovered interaction partner of ASK1, acting as a physiological inhibitor of ASK1 (Saitoh et al., 1998). The ASK1-TRX interaction is redox-dependent - oxidized TRX interacts with ASK1 with much lower affinity and dissociates from ASK1 due to the formation of a C32-C35 disulfide bridge in the active site of the enzyme (Kosek et al., 2014; Kylarova et al., 2016; Saitoh et al., 1998). The association of TRX with the ASK1-TBD is thought to prevent homooligomerization of the N-terminal portion of ASK1, which is required for full ASK1 activation, and may also prevent TRAF2/6 from accessing the TRAF binding site (Fujino et al., 2007). The nature of the interaction between TRX and ASK1 has not been completely clarified, with some studies indicating

a non-covalent interaction, while others suggest a possible role for disulfide bonding and a different mechanism of ASK1 inhibition by TRX based on TRX reductase activity alone (Kosek et al., 2014; Kylarova et al., 2016; Nadeau et al., 2007, 2009; Psenakova et al., 2020). There are other proteins involved in the regulation of ASK1 by TRX. These include TRX reductase, which negatively regulates ASK1 activity by reducing TRX, or thioredoxin-interacting protein (TXNIP), which positively regulates ASK1 activity by binding to TRX, thereby preventing it from interacting with ASK1 (Holmgren, 1995; Junn et al., 2000; Nishiyama et al., 1999). In addition to TRX, ASK1 is also negatively regulated by the aforementioned GRX, which interacts with the C-terminus of ASK1 (Song et al., 2002).

Another physiological inhibitor of ASK1 is the 14-3-3 proteins, whose binding close to the C-terminus of the ASK1-KD to a motif containing a phosphorylated S966 negatively regulates ASK1 (L. Zhang et al., 1999). Inhibitor of kappa B kinase (IKK) is responsible for the phosphorylation of S966 (Puckett et al., 2013). The 14-3-3 protein bound to ASK1 probably exerts its inhibitory effect by blocking the active site of ASK1 and by affecting the dynamics of the activation segment, including the two important autophosphorylation sites T838 and T842 (Petrvalska et al., 2016). Phosphatases that counteract IKK activity and dephosphorylate S966 then positively regulate ASK1 activity by disrupting the interaction between ASK1 and 14-3-3 (Goldman et al., 2004).

In contrast, ASK1 is positively regulated by redox-dependent interactions with TRAF2/5/6 (Nishitoh et al., 1998). Overexpression of TRAF proteins causes dissociation of TRX and promotes homooligomerization of ASK1 (Fujino et al., 2007; H. Liu et al., 2000).

Furthermore, ASK1 is regulated by PTMs. Critical for ASK1 activation is the phosphorylation of T838 in the activation loop, which can occur by trans-autophosphorylation or phosphorylation by ASK2 or MPK38 (Jung et al., 2008; Takeda et al., 2007; Tobiume et al., 2002). Thus, negative regulation can occur naturally by phosphatases acting to dephosphorylate this regulatory T838. PP5 (protein phosphatase 5) and PPEF2 (protein phosphatase with EF-hand domain 2) dephosphorylate T838 and inhibit ASK1 under oxidative stress conditions, whereas PP2Cε (protein phosphatase 2C isoform epsilon) dephosphorylates ASK1 and exerts its inhibitory effect under resting conditions (Kutuzov et al., 2010; Morita et al., 2001; Saito et al., 2007). Cdc25 phosphatase (cell division cycle 25) regulates ASK1 activity during the cell cycle in a similar manner

(Y.-C. Cho et al., 2015). In addition to T838, there are other phosphorylation sites in ASK1, which, by contrast, exert an inhibitory effect on ASK1 activity. Protein kinase B (PKB) phosphorylates S83 (Kim et al., 2001) and phosphorylation of T718, S1033, T1109, or T1326 has also been shown (Jin et al., 2013; Nishida et al., 2017; Yu et al., 2009).

PTMs other than phosphorylation can be found in ASK1. For example, it has been shown that S-nitrosylation of C869 under cerebral ischemia-reperfusion conditions and in interferon-gamma-treated L929 cells has a positive and negative effect on ASK1 activity, respectively (D.-H. Liu et al., 2013; Park et al., 2004). Protein arginine methyltransferases (PRMTs) 1 and 5 also negatively affect ASK1 activity through methylation of some amino acids. PRMT1 methylates R78 and R80, thereby inhibiting TRX dissociation and protein association with TRAF2 (J.-H. Cho et al., 2012). PRMT5, by methylating R89, facilitates the interaction of ASK1 with PKB and the subsequent phosphorylation of S83 (Chen et al., 2016).

As a final example of ASK1 regulation, let´s consider regulation via degradation by the ubiquitin-proteasome system (UPS). Proteins that provide regulation of ASK1 in this manner include the E3 ubiquitin ligases Roquin2, β-transducin repeat containing protein (β-TrCP), and cellular inhibitor of apoptosis 1 (cIAP-1) (R. Cheng et al., 2018; Maruyama et al., 2014; Zhao et al., 2007).

The currently accepted model for ASK1 activation in response to oxidative stress is as follows. Inactive ASK1 is thought to oligomerize via the C-terminal CC domain and is maintained inactive by TRX association with the ASK1-TBD and by association with 14-3-3 proteins C-terminal to the kinase domain. However, once too much oxidative stress occurs, the oxidized TRX dissociates and so do the 14-3-3 proteins (Cockrell et al., 2010; Gotoh & Cooper, 1998; Noguchi et al., 2005; Saitoh et al., 1998; Tobiume et al., 2002; L. Zhang et al., 1999). In contrast, TRAF proteins associate with ASK1 in the ASK1-CRR region, leading to homo-oligomerization also in the N-terminal part of ASK1 and subsequent phosphorylation of the activating T838 and overall activation of the enzyme (Fujino et al., 2007; Goldman et al., 2004; H. Liu et al., 2000; Noguchi et al., 2005; Tobiume et al., 2002). This activation model is obviously very simplified, and even in this simplified form the sub-steps of activation are not completely clear, which leaves room for further investigation.

1.5 Calcium signaling

Similarly to the phosphate group, binding of Ca^{2+} ions changes the protein charge and conformation, which makes Ca^{2+} ions a universal tool for signal transduction (Clapham, 2007). The functioning of Ca^{2+} signaling is ensured by strict maintenance of its concentration. Resting cytoplasmic Ca^{2+} concentration is maintained near 100 nM, which is in strong contrast to about 1.1 to 1.4 mM Ca^{2+} in the extracellular environment (Atchison & Beierwaltes, 2013). The low intracellular Ca^{2+} concentration is maintained by the activity of Ca^{2+} ATPases at the plasma membrane or endoplasmic/sarcoplasmic reticulum and by the Na^{+}/Ca^{2+} antiporter, which uses the huge gradient of extracellular Na^{+} concentration to push Ca^{2+} out of the cell. However, as soon as the cell is stimulated, e.g., by mechanical deformation, hormonal activation, or depolarization, the rate of Ca^{2+} efflux is lower than the Ca^{2+} influx from the extracellular environment or internal Ca^{2+} stores mediated by various types of ion channels. This causes an increase in intracellular Ca^{2+} concentration to about 1 μM (locally much more) and the generation of a signal that can be transmitted to an incredible number of targets within the cell to regulate, for example, muscle contraction, cell proliferation or gene transcription (Bootman et al., 2001). Calcium ions can act on their targets either directly or via Ca^{2+} sensing proteins such as troponin C or calmodulin (CaM) (Bootman, 2012; Endo, 2006). An overview of calcium signaling is shown in Fig. 1.11 on page 35.

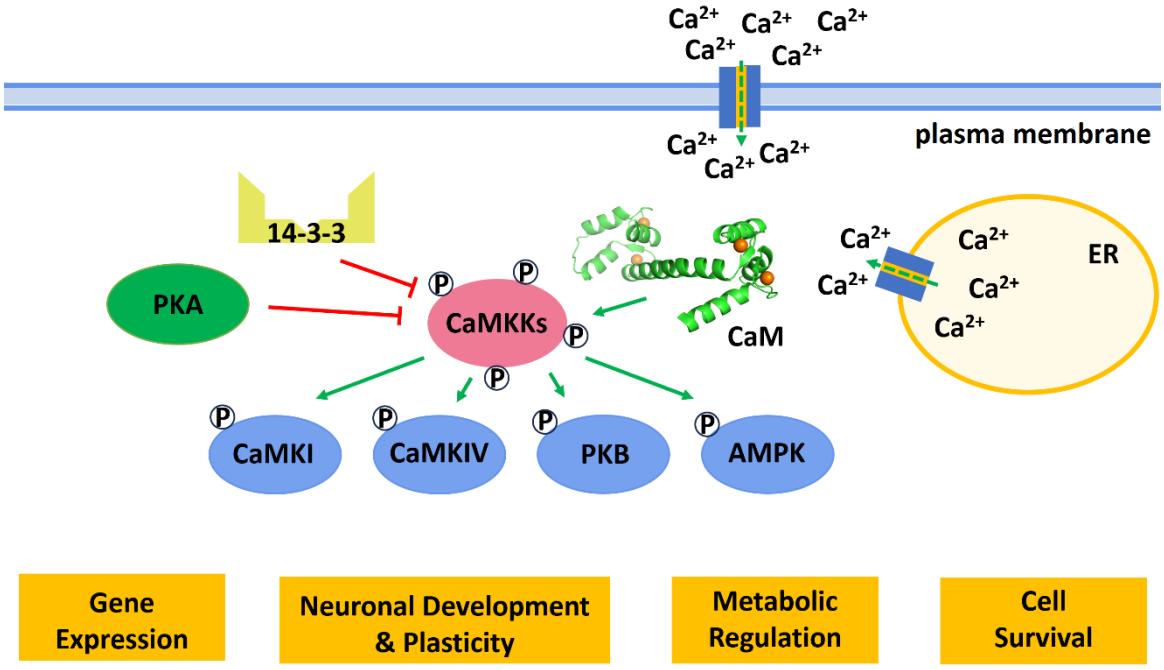

Figure 1.11 Calcium signaling scheme.
When the cellular Ca^{2+} concentration increases, calmodulin undergoes a conformational change due to calcium binding. Calmodulin binds to the calmodulin-binding domains of many proteins, including CaMKKs. Its binding to CaMKKs causes their activation and subsequent phosphorylation of their substrates, which in turn phosphorylate their targets and thus help regulate some of the processes outlined in the orange boxes. In addition to activation by calmodulin, CaMKKs are regulated in other ways, including inhibition by PKA or 14-3-3 proteins. Adapted from Tokumitsu & Sakagami, 2022.

1.5.1 Calmodulin

Calmodulin named for CALcium MODULated proteIN is a highly conserved protein abundant in cells with a molecular weight of about 17 kDa (C.-F. Yang & Tsai, 2022). It belongs to a group of proteins containing the EF-hand motif (Tanaka, 1988), which consists of a conserved sequence of about 30 amino acids and is structurally characterized by two helices E and F (E-helix is N-terminal, F-helix is C-terminal) connected by a loop. The arrangement of the motif resembles a right hand clenched into a fist with the thumb (F-helix) and index finger (E-helix) extended and the rest of the palm representing the connecting loop - hence the name EF-hand (A. K.-W. Leung et al., 2019). Although there are several Ca^{2+}-binding motifs found in proteins, the most common is the EF-hand motif (Rigden & Galperin, 2004), in which a sequence of usually 12 residues from the loop between the helices is specifically responsible for Ca^{2+} binding (Lewit-Bentley & Réty,

2000). Ca^{2+} is usually coordinated by oxygen from the amino acid side chains at positions 1, 3, 5 and 12, by the carbonyl oxygen of the amino acid at position 7 and finally by oxygen from the glutamate side chain at position 9 (Carafoli, 2002).

EF-hand motif proteins can respond to a signal in the form of increased cytoplasmic Ca^{2+} concentration in one of two ways. In the first case, these proteins bind Ca^{2+} without undergoing any significant change and thus serve to transport or buffer Ca^{2+}. In the second case, the proteins undergo a conformational change, which is also the case of calmodulin (Chin & Means, 2000).

Calmodulin is dumbbell-shaped - it consists of two lobes (N-terminal and C-terminal), which are connected by a long flexible helix. Each of the lobes contains two EF-hand motifs, which allows calmodulin to bind four Ca^{2+} ions in total, as shown in Fig 1.12 (Andrews et al., 2020).

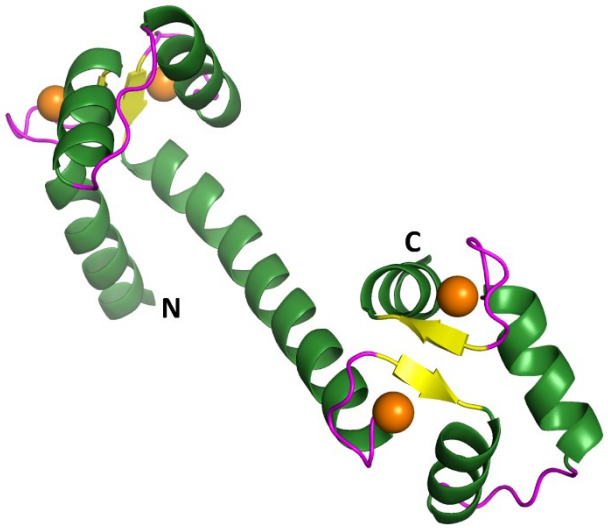

Figure 1.12 Crystal structure of calmodulin.
Calmodulin is composed of two lobes, each of them containing three α-helices (green), three $Ca2^{+}$ binding loops (magenta) and one two-stranded antiparallel β-sheet (yellow). The lobes are connected by a long central helix. The four Ca^{2+} binding regions represent a typical EF-hand fold formed by helix-turn-helix motif. PDB ID: 3CLN (Babu et al., 1988).

At resting Ca^{2+} concentration, the N-lobe is in a closed conformation with helices from both motifs close to each other. The C-lobe is in a semi-open conformation with partially exposed hydrophobic region mediating interaction with target proteins. Once the Ca^{2+} concentration in the cytoplasm increases, all EF-hand motifs bind Ca^{2+}, which leads to a significant conformational change (Chin & Means, 2000). Hydrophobic regions

in both calmodulin domains are exposed and the affinity for protein partners is increased and allows calmodulin binding to them. Such interaction can, for example, abolish autoinhibition, alter the active site or affect the oligomeric state of the target protein (Clapham, 2007; Hoeflich & Ikura, 2002).

1.5.2 Ca^{2+}/CaM-dependent protein kinases (CaMKs)

The family of CaMKs is among the more than 300 proteins that bind to and are activated by calmodulin (Andrews et al., 2020). They are involved in the regulation of various processes, such as cell proliferation, gene expression, neurotransmitter release, or metabolism (Hanson & Schulman, 1992). They are all serine/threonine protein kinases and fall into one of two groups according to their selectivity. The first group comprises multifunctional kinases CaMKI, CaMKII and CaMKIV all capable of phosphorylating several substrates, the second group contains substrate-specific kinases and is represented by myosin light chain kinase (MLCK), phosphorylase kinase, and elongation factor 2 kinase, also known as CaMKIII (Swulius & Waxham, 2008).

All CaMKs (besides CaMKIII) share common domain organization – they are formed by a disordered N-terminal part of varying length, a conserved KD, an autoinhibitory domain (AID) overlapping or immediately followed by calmodulin-binding domain (CBD), and a disordered C-terminus of different length. In case of CaMKII, the disordered C-terminus is replaced by an association domain, which mediates oligomerization (Soderling & Stull, 2001).

Regulation of all CaMKs has a common feature. At resting conditions, the AID interacts with the KD changing its conformation and hindering access to the active site. However, upon Ca^{2+} concentration increase and conformational change of calmodulin, the affinity of CaMKs for calmodulin increases, giving rise to interaction of calmodulin with the CBD of CaMKs. Given the overlap/proximity between the AID and CBD, calmodulin binding causes dissociation of the AID from KD and release of the autoinhibition (Goldberg et al., 1996). To become fully activated, CaMK needs to be phosphorylated at a crucial threonine located in the activation segment. This can occur either through autophosphorylation, such as in the case of CaMKII, or via phosphorylation by an upstream kinase as in CaMKI and CaMKIV (Colbran, 2004; Goldberg et al., 1996; Krebs, 1998).

1.5.3 Ca^{2+}/CaM-dependent protein kinase kinases 1 and 2 (CaMKK1/2)

CaMKK1 and CaMKK2 are both upstream activators of substrate CaMKI and CaMKIV, through which they regulate axon/dendritic outgrowth, aldosterone synthase expression, memory, immune and inflammatory responses, among others (Condon et al., 2002; Racioppi & Means, 2008; Wayman et al., 2004; Wei et al., 2002). On top of that, CaMKK1 also serves as an upstream activator of AMP-activated protein kinase (AMPK) and therefore takes part in maintaining the energy balance (Hawley et al., 1995; Szewczuk et al., 2020). Conversely, CaMKK2 promotes cell survival by activating protein kinase B (PKB) pathway, which results in phosphorylation of pro-apoptotic bcl-2 protein Bad and its sequestration in cytoplasm by 14-3-3 proteins (Yano et al., 1998).

Human CaMKK1 is a protein with a molecular weight of about 56 kDa, human CaMKK2 has a molecular weight of about 65 kDa. They share about 65 % sequence homology; the highest homology is found in their KD. Their domain structure closely resembles that described before for CaMKs, and thus contains KD, AID, CBD and disordered N- and C-termini as shown in Fig. 1.13 on page 39 (Anderson et al., 1998; Green et al., 2011; Tokumitsu et al., 1997). In comparison to other protein kinases, the amino acid sequence of both CaMKK1 and CaMKK2 contains a unique positively charged stretch of ~ 25 amino acid residues within their KD (residues 165-190 in CaMKK1 and 201-226 in CaMKK2) rich in arginines and prolines, so-called RP-insert (Hanks et al., 1988). Deletion and mutagenesis studies in CaMKKs showed that the RP-insert is crucial for the recognition and phosphorylation of the substrates CaMKI and CaMKIV, but not necessary for the same process in case of PKB. Besides that, RP-insert has no effect on the catalytic activity itself – autophosphorylation stays intact (Tokumitsu et al., 1999). It was suggested that targeting the RP-insert might be a promising strategy for designing CaMKKs´ inhibitors, unfortunately no structural information on it is currently available (Kaneshige et al., 2022). The only high-resolution structural information at hand for CaMKK1 and CaMKK2 are the crystal structures of their KDs in complex with inhibitors hesperidin and STO-609, respectively (CaMKK1 – PDB: 6CCF, CaMKK2 – PDB: 2ZV2) (Kukimoto-Niino et al., 2011). The RP-insert is not visible in either of these structures suggesting it is a disordered region.

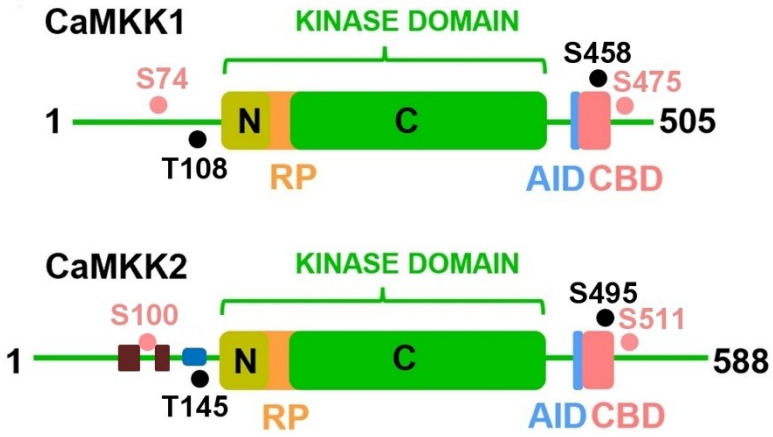

Figure 1.13 Domain scheme of the CaMKK1 and CaMKK2 protein kinases.
The N-lobe of the kinase domain is yellow, the C-lobe green, and the RP insert is shown in orange. The partially overlapping autoinhibitory domain and the calmodulin-binding domain are shown in blue and pink, respectively. PKA phosphorylation sites are indicated by dots. Marked in pink are those that additionally represent 14-3-3 binding motifs. CaMKK2 has an extra N-terminal regulatory stretch in the amino acid region 129-151 indicated in blue and two additional insertions indicated in brown. AID - autoinhibitory domain, CBD - calmodulin binding domain, RP – RP insert. Adapted from Petrvalska et al., 2023.

1.5.3.1 Regulation of CaMKK1 and CaMKK2

Despite having a high degree of sequence homology and similar domain structure, there are notable distinctions in the regulation of the catalytic activities between CaMKK1 and CaMKK2. The activity of CaMKK1 strongly depends on the presence of Ca^{2+}/CaM, whereas that of CaMKK2 is, to some extent, CaM-independent A 23-amino acid segment (residues 129–151) just before the catalytic domain controls this activity. (Tokumitsu et al., 2001).

Both CaMKKs undergo phosphorylation by PKA at multiple sites, including S52, S74, T108, S458, and S475 in CaMKK1, as well as S100, T145, S495, and S511 in CaMKK2 (Langendorf et al., 2020; Matsushita & Nairn, 1999; Takabatake et al., 2019; Wayman et al., 1997). Phosphorylation of the threonine residue preceding the kinase domain (T108 in CaMKK1 and T145 in CaMKK2) by PKA partially inhibits both kinases as does phosphorylation of the serine residue found in the CBD (S458 in CaMKK1 and S495 in CaMKK2). The latter reduces the binding affinity to Ca^{2+}/CaM (Wayman et al., 1997).

Furthermore, PKA-mediated phosphorylation exposes the binding motifs for the scaffolding and adaptor proteins 14-3-3 (Obsilova & Obsil, 2022). 14-3-3 proteins bind both CaMKKs via two phosphorylated motifs, one located N-terminally to the KD (Ser74 in CaMKK1, Ser100 in CaMKK2), the other C-terminally to the regulatory region (Ser475 in CaMKK1, Ser511 in CaMKK2). The C-terminal motif is more likely to play a dominant role in preserving the stability of the complex because it shows higher affinity for 14- 3-3 proteins (Langendorf et al., 2020; Lentini Santo et al., 2020; Yaffe, 2002). The interaction with 14-3-3 proteins additionally regulates the catalytic activity of both CaMKKs.

Association with 14-3-3 proteins inhibits dephosphorylation of phosphorylated serine residues in the CBD of both CaMKKs in *in vitro* and *in vivo* studies. This suggests that 14-3-3 binding sustains CaMKKs in a state of partial inhibition caused by PKA phosphorylation. However, the effect of this interaction on the remaining catalytic activity of CaMKKs varies. CaMKK1 undergoes significant inhibition upon binding with 14-3-3, while the activity of CaMKK2 remains mostly unaltered. The exact mechanism behind this difference has not yet been fully elucidated (Davare et al., 2004; Ichimura et al., 2008; Langendorf et al., 2020; Psenakova et al., 2018).

1.6 Estrogen receptor α

Estrogen receptor α (ERα) is a member of the nuclear receptor (NR) protein family. A total of 48 NRs is encoded in the human genome, divided into seven subgroups (Frigo et al., 2021). NRs are transcription factors that are activated by the binding of a ligand, which is usually a small, lipophilic molecule capable of crossing the plasma membrane - ligands can be, for example, certain steroid hormones such as estrogen, progesterone or testosterone, or other fat-soluble substances such as retinoic acid or thyroid hormones (Sladek, 2011). The ligands of some NRs are not yet known - such receptors are called orphan NRs. Once activated, NRs regulate the transcription of many genes, thereby controlling important processes like development, cell proliferation and reproduction (Escriva et al., 2000). When NRs are not properly regulated, many diseases develop, including cancer, diabetes, and infertility (Dhiman et al., 2018; Sever & Glass, 2013). NRs can function as monomers or homo/heterodimers. They are characterized by their domain structure, which typically includes several conserved domains. At the N-terminus we find the A/B domain, also called the N-terminal domain (NTD), which is internally disordered

and also contains the first of the activation function (AF) transactivation region 1. Adjacent to the NTD is the C domain, also called the DNA-binding domain (DBD), which contains two zinc finger motifs. The D domain represents a short region with a nuclear localization sequence (NLS), followed towards the C-terminus by the E domain or ligand-binding domain (LBD), which can mediate dimerization and where we also find the second AF2. Finally, in some NRs we find a fifth domain called the C-terminal (CTD) domain or simply the F domain. The schematic representation of the domain organization of ERα is illustrated in Fig. 1.14A on page 42. Since NRs are activated by small molecules, they represent a potential target for designing molecules that act either agonistically or antagonistically. Indeed, NRs are among the most frequently targeted proteins. However, in the human body, there are many genes in different tissues that are regulated by a single NR. This is what tends to cause the side effects of such drugs (Frigo et al., 2021; Sever & Glass, 2013).

ERα exists in two subtypes, ERα and ERβ. The former is expressed primarily in the mammary gland, uterus, ovary, bone, and male reproductive organs, while the latter is expressed primarily in the prostate, intestine, adipose tissue, and immune system (Dahlman-Wright et al., 2006; Heldring et al., 2007). ERα is expressed in approximately 70% of breast cancers, and the growth of these tumors is typically dependent on ERα-mediated transcriptional activity. Therefore, agents that block ERα activation are used to treat breast tumors. Typically, either agents that inhibit estrogen biosynthesis or ERα modulators are used (Arnesen et al., 2021; Traphagen et al., 2021). One such modulator is tamoxifen, an ERα antagonist used to treat ERα-positive breast tumors. Fig. 1.14B on page 42 shows how binding of 4-hydroxy tamoxifen (4-OHT) to LBD changes the conformation of helix 12 compared to binding of the agonist estradiol (E2). The problem, however, is that given the prevalence of ERα not only in the breast, tamoxifen also acts where it ideally should not. Another problem is the emergence of resistance (Paterni et al., 2014; Sharma et al., 2018). Mutations in the LBD of ERα, most commonly tyrosine 537 or aspartate 538 mutations, are responsible for the emergence of resistance, resulting in an active conformation even in the absence of ligand (Arnesen et al., 2021). A better understanding of the regulatory mechanisms in specific cell types is desirable for the design of more targeted drugs.

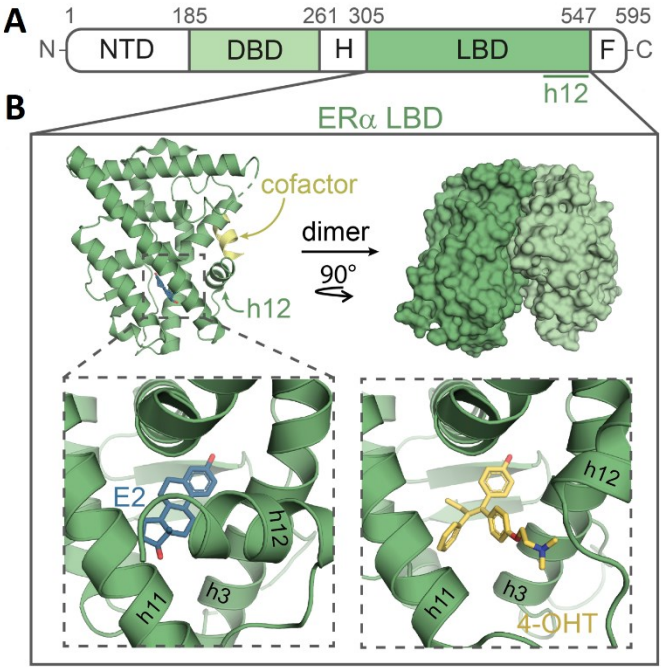

Figure 1.14 Domain structure of ERα.
A – ERα domain scheme. NTD – N-terminal domain, DBD – DNA binding domain, H – hinge region, LBD – ligand binding domain, F – F-domain. B - The structure of the LBD showing a comparison of the conformation of helix 12 upon binding of the E2 agonist and the 4-OHT antagonist. Adapted from Somsen et al., 2023.

The F domain of ERα, specifically the motif around the phosphorylated T594, binds 14-3-3 proteins, whose binding reduces ERα transcriptional activity in response to estradiol agonist binding. The interaction between 14-3-3 and ERα can be regulated by small molecules, and it has been shown that the natural product fussicoccin A can stabilize the 14-3-3:ERα complex and thus reduce ERα-dependent transcriptional activity (De Vries-van Leeuwen et al., 2013). The stabilization of 14-3-3:ERα cane be also further promoted by various other small molecules (Gigante et al., 2020). The study of the mechanisms regulating these interactions opens the way to the design of more targeted drugs, e.g. targeting not only orthosteric sites but also allosteric sites or different aspects of NR regulation such as oligomerization, DNA binding, etc. (Caboni & Lloyd, 2013; Meijer et al., 2019; T. W. Moore et al., 2010).

2 Aims

The goal of this thesis is to provide mechanistic insights into the function and regulation of several protein complexes. This was done using combined biochemical and biophysical methods.

Specific aims:

1. Study of the structure of the N-terminal part of the protein kinase ASK1 and the role of thioredoxin in its regulation.
    - To determine the structure of the N-terminal part of ASK1
    - To compare the oligomerization behavior of different protein constructs covering the N-terminal part of ASK1
    - To investigate the effect of thioredoxin binding on the oligomerization of the N-terminal part of ASK1
    - To examine the impact of thioredoxin binding on the structure/conformation of the N-terminal part of ASK1

2. Study of the differential effect of 14-3-3γ on CaMKK1 and CaMKK2 activity
    - To prepare structural models of the pCaMKK1:14-3-3γ and pCaMKK2:14-3-3γ complexes
    - To compare the structural models of the two complexes and explain the differing influence of 14-3-3γ on the activity of pCaMKK1 and pCaMKK2

3. Study of the interaction between the nuclear receptor ERα and 14-3-3ζ
    - To determine the stoichiometry of the ERα:14-3-3ζ complex
    - To investigate the effect of ligand binding on the complex formation and stability
    - To investigate the effect of Y537S mutation on the complex formation and stability

3 Material and methods

3.1 Material

3.1.1 Biological material and chemicals

1, 4-dithiothreitol (DTT)	Carl Roth GmbH, Germany
1 kBP DNA ladder	Fermetas, Canada
2-mercaptoethanol	Sigma-Aldrich, USA
4-(2-hydroxyethyl)-1 piperazineethanesulfonic acid (HEPES)	Sigma-Aldrich, USA
Acrylamide	Carl Roth GmbH, Germany
Adenosine 5´-triphosphate (ATP)	Sigma-Aldrich, USA
Agarose GTQ	Carl Roth GmbH, Germany
Ammonium persulfate (APS)	Sigma-Aldrich, USA
Ampicillin	Sigma-Aldrich, USA
BamHI	New England Biolabs, USA
Bis-acrylamide	Carl Roth GmbH, Germany
Bromophenol blue	Carl Roth GmbH, Germany
Calcium chloride	PENTA s.r.o., Czech Republic
Chloramphenicol	Sigma-Aldrich, USA
Coomassie Brilliant Blue R 250	LKB Bromma, Sweden
Disodium (EDTA)	Lachema, s.r.o., Czech Republic
DNase	ZellBio GmbH, Germany
DNA polymerase Phusion High-fidelity	New England BioLabs, USA
Electrophoresis Loading-Dye	New England BioLabs, USA
Escherichia coli BL21(DE3) strain	Stratagene, USA
Escherichia coli Rosetta(DE3) strain	Stratagene, USA
Escherichia coli TOP10 strain	Stratagene, USA
Ethanol 96% v/v for UV spectroscopy	PENTA s.r.o., Czech Republic
Ethyl acohol 96% G.R.	Lach:Ner, s.r.o., Czech Republic
GelRed™	New England BioLabs, USA
Glycerol	PENTA s.r.o., Czech Republic
Glycine	Carl Roth GmbH, Germany

Hydrochloric acid	PENTA s.r.o., Czech Republic
Imidazole	Carl Roth GmbH, Germany
Isopropyl β-D-1-thiogalactopyranoside	EMD Biosciences, Inc., Germany
Isopropyl alcohol	Genomed, Germany
Kanamycin	Sigma-Aldrich, USA
Luria-Bertani (LB) agar	Carl Roth GmbH, Germany
Luria-Bertani (LB) medium	Carl Roth GmbH, Germany
Lysozyme	SERVA Electrophoresis GmbH, Germany
Magnesium chloride	PENTA s.r.o., Czech Republic
Manganese chloride tetrahydrate	PENTA s.r.o., Czech Republic
Nickel sulfate hexahydrate	PENTA s.r.o., Czech Republic
NotI	New England Biolabs, USA
Phenylmethylsulfonyl fluoride (PMSF)	Carl Roth GmbH, Germany
Phusion high-fidelity DNA polymerase	New England Biolabs, United Kingdom
cAMP-dependent kinase (PKA)	Prepared in our laboratory
Plasmid pHGT2 (It was prepared by the modification of pRSFDuet-1 plasmid by insertion of GB1)	Gifted by Dr. Evžen Bouřa (IOCB), Czech Republic
Plasmid pST39	Novagen, USA
Precision plus protein standard (dual color)	Bio-Rad Laboratory, USA
Roti marker Tricolor protein marker	Carl Roth GmbH, Germany
Sodium azide	Sigma-Aldrich, USA
Sodium chloride	Lach:Ner, s.r.o., Czech Republic
Sodium dodecyl sulfate (SDS)	Carl Roth GmbH, Germany
Sodium hydroxide	Lach:Ner, s.r.o., Czech Republic
T4 ligase	Thermofisher Scientific, USA
Terrific Broth (TB) medium	Carl Roth GmbH, Germany
Thiamin hydrochloride	Sigma-Aldrich, USA
Tris(2-carboxyethyl)phosphine (TCEP)	Sigma-Aldrich, USA
Tris(hydroxymethyl)aminomethane (Tris)	Carl Roth GmbH, Germany
Tobacco Etch Virus nuclear-inclusion-a endopeptidase (TEV protease)	Prepared in our laboratory
XbaI	New England Biolabs, USA
Zinc chloride	PENTA s.r.o., Czech Republic

3.1.2 Other materials

Analytical ultracentrifugation cuvettes	Beckman Coulter, USA
Analytical ultracentrifugation cuvettes	Nanolytics Instruments GmbH, Germany
Chelating Sepharose Fast Flow	GE Healthcare, USA
Dialysis membrane, type 27/32 (cut off 14000)	Carl Roth GmbH, Germany
DNA isolation kit	Thermofisher Scientific, USA
Gravity chromatography columns	Bio-Rad Laboratories, USA
HiLoad 26/600 Superdex 75 pg column	GE Healthcare, USA
HiLoad 26/600 Superdex 200 pg column	GE Healthcare, USA
LUNA Omega Polar C18 Column	Phenomenex, USA
MonoQ™ 5/50 GL column	GE Healthcare, USA
Quick Change™ Mutagenesis kit	Stratagene, USA
SecurityGuard™ pre-column	Phenomenex, USA
Spartan 13/0.45 RC filter unit	GE Healthcare, USA
Spectra/pro membrane (cut off 6000-8000)	Spectrum, USA
Superdex™ 75 Increase 10/300 GL	GE Healthcare, USA
Syringes	Braun, Germany
UltrAuFoil holey grids (R1.2/1.3)	Quantifoil, Germany
Vivaspin Turbo centrifugal filter device (cut off 5000, 10000 and 30000)	Sartorius, United Kingdom
Whatman™ membrane filters 0.45µm	GE Healthcare, USA

3.1.3 Equipment

3505 pH Meter	Nova Capital Ltd., United Kingdom
Analytical ultracentrifuge ProteomLab™ XL-I	Beckman Coulter, USA
Automatic pipettes	Eppendorf AG, Germany
Centrifuge 5804R	Eppendorf, Germany
Centrifuge Hermle Z323K	Hermle Labortechnik GmbH, Germany
Centrifuge Sigma 8K	Sigma Laborzentrifugen, Germany
FPLC	GE Healthcare, USA
Gallenkamp Orbital Incubator shaker	Gemini BV, Netherlands
GATAN K2 Summit detector	Gatan, USA

Gatan K3 BioQuantum detector	Gatan, USA
Gatan Solarus II 955	Gatan, USA
Horizontal electrophoresis	Sigma-Aldrich, USA
Incubator	MELAG Medizintechnik, Germany
JEOL JEM 2100-plus EM	Akishima, Japan
Laboratory scales HF-200g	And, USA
NanoDrop One	Thermo scientific, USA
P-class nanophotometer	Implen GmbH, Germany
Peristaltic pump Ecoline	Ismatec, Germany
Shaker Multitron	Infors AG, Switzerland
Sonicator 3000	Misonix, Inc., USA
Source for vertical electrophoresis	Bio-Rad Laboratories, USA
Talos Arctica EM	Thermo scientific, USA
TemCam–XF416 4K CMOS camera	TVIPS GmbH, Germany
Thermal block	Grant, UK
timsTOF Pro mass spectrometer	Bruker Daltonics, Germany
Titan Krios EM	Thermo scientific, USA
Vertical electrophoresis	Bio-Rad Laboratories, USA
Vitrobot Mark IV System	Thermo scientific, USA
Vortex ZX3	VELP Scientifica, Italy

3.2 Protein expression and purification

3.2.1 ASK1 constructs

A total of six ASK1 constructs were repeatedly prepared, corresponding to the isolated domains ASK1-TBD (residues 88-267), ASK1-CRR (residues 268-658), ASK1-KD (residues 659-973), and their combinations - ASK1-TBD-CRR (residues 88-658), ASK1-CRR-KD (residues 269-973), and finally ASK1-TBD-CRR-KD (88-973).

ASK1 DNA corresponding to ASK1-TBD, ASK1-CRR and ASK1-TBD-CRR was cloned into modified plasmid pRSFDuet-1 (kindly provided by Evžen Bouřa, Institute of Organic Chemistry and Biochemistry, Czech Academy of Sciences) using BamHI and NotI restriction enzymes. In the case of ASK1-KD, ASK1-CRR-KD and ASK1-TBD-

CRR-KD, the corresponding DNA was cloned into plasmid pST39 using XbaI and BamHI restriction enzymes. The constructs were expressed as N-terminal 6xHis-GB1-tagged fusion proteins (pRSF-Duet-1) or C-terminal 6xHis-tagged proteins (pST39) in *Escherichia Coli* BL21(DE3) cells and, in the case of ASK1-KD, in *Escherichia Coli* Rosetta^{TM} (DE3) cells. Expression was initiated by induction with isopropyl β-D-1-thiogalactopyranoside (IPTG) at a final concentration of 0.5 mM. ASK1-KD was expressed by leakage expression. Expression of ASK1-TBD, ASK1-CRR, ASK1-KD and ASK1-TBD-CRR was performed overnight at 25 °C, and expression of ASK1-CRR-KD and ASK1-TBD-CRR-KD was also performed overnight (after one hour of cooling down at 4°C) at 18 °C. The bacterial cultures were centrifuged (20 min at 2,073 *g*), the pellets were resuspended in lysis buffer (1 x PBS, 1 M NaCl, 4 mM β-ME, 2 mM imidazole), and the lysate was frozen. After thawing, the cells were further disrupted by incubation with lysozyme and sonication in the presence of phenylmethylsulfonyl fluoride (PMSF), serine protease inhibitors, at a final concentration of 1 mM. The sonicate was then centrifuged (45 min at 19,561 *g* and 4 °C) and the supernatant was used to purify the protein.

The first purification step was performed by immobilized metal affinity chromatography (IMAC) using a standard protocol and the protein was eluted from the column with a buffer consisting of 1 x PBS, 0.5 M NaCl, 2 mM β-ME and 400 mM imidazole. IMAC was followed by overnight protein dialysis to remove excess imidazole and to cleave the affinity tag (together with the GB1 fusion protein) for those constructs containing a specific sequence for TEV (tobacco etch virus) protease cleavage (250 U TEV/1 mg protein). The dialysis buffer contained 50 mM Tris-HCl (pH 8.0), 0.5 M NaCl, 80 mM imidazole, 4 mM 2-ME, 10% (w/V) glycerol for ASK1-TBD, 50 mM Tris-HCl (7. 5), 200 mM NaCl, 5 mM EDTA, 2 mM β-ME for ASK1-KD, and 20 mM Tris-HCl (7.5), 0.5 M NaCl, 1 mM EDTA, 2 mM β-ME and 10% (w/v) glycerol for all other ASK1 constructs. Purification of ASK1-TBD after dialysis was followed by a second IMAC to ensure removal of the 6xHis-tagged TEV protease and the 6xHis-GB1 fusion. For all other protein constructs, protein concentration and size-exclusion chromatography (SEC) immediately followed as the second and final purification step using a buffer 20 mM Tris-HCl (7.5), 150 mM NaCl, 5 mM dithiothreitol (DTT) and 10% (w/v) glycerol. For this purpose, HiLoad 26/600 Superdex75/200 pg columns were used.

3.2.2 Thioredoxin

N-terminally 6xHis-tagged TRX1 C73S in plasmid pQE-30 was kindly provided by Katja Becker (Justus-Liebig-Universität, Giessen, Germany). It was cultured in *Escherichia Coli* BL21(DE3) cells, and its expression was initiated by induction with 0.5 mM IPTG, followed by overnight incubation at 30 °C. The bacterial culture was centrifuged (20 min at 2,073 *g*), the pellet was resuspended in lysis buffer (1 x PBS, 1 M NaCl, 4 mM β-ME, 2 mM imidazole), and the lysate was frozen. After thawing, the cells were further disrupted by incubation with lysozyme and sonication in the presence of PMSF at a final concentration of 1 mM. The sonicate was then centrifuged (45 min at 19,561 *g* and 4 °C) and the supernatant was used for protein purification.

IMAC was the first purification step and a standard protocol was used. The protein was eluted from the column with a buffer consisting of 1 x PBS, 0.5 M NaCl, 2 mM β-ME and 600 mM imidazole and was diluted 2 x in a SEC buffer (20 mM Tris-HCl (7.5), 1 mM EDTA, 150 mM NaCl, 5 mM DTT and 10% (w/v) glycerol) immediately after elution from the column. Following IMAC, the protein was concentrated and subjected to SEC as the second and final purification step. A Superdex™ 75 Increase 10/300 GL column was used for this purpose.

3.2.3 CaMKK1 and CaMKK2

DNA corresponding to CaMKK1 (residues 67-480) and CaMKK2 (93-517) was cloned into modified plasmid pRSFDuet-1 using NcoI and NotI restriction enzymes in case of CaMKK1 and BamHI and NotI in case of CaMKK2. Kinase dead mutants of both CaMKK1 (D293A) and CaMKK2 (D330A) were prepared using QuikChange site-directed mutagenesis kit (Stratagene). Inserted mutations were confirmed by sequencing. Both CaMKKs were expressed as N-terminal 6xHis-GB1-tagged fusion proteins in *Escherichia Coli* BL21(DE3) using autoinduction media. The expression was initiated by temperature decrease to 18 °C and 20 °C in CaMKK1 and CaMKK2, respectively, and was performed overnight. The bacterial cultures were centrifuged (20 min at 2,073 *g*), the pellets were resuspended in lysis buffer (1 x PBS, 1 M NaCl, 4 mM β-ME, 2 mM imidazole), and the lysates were frozen. After thawing, the cells were further disrupted by incubation with lysozyme and sonication in the presence of 1 mM PMSF. The sonicate was then centrifuged (45 min at 19,561 *g* and 4 °C) and the supernatant was used for protein purification.

IMAC was the first purification step. The protein was eluted with a buffer containing 1 x PBS, 0.5 M NaCl, 2 mM β-ME and 400 mM imidazole. IMAC was followed by overnight protein dialysis to remove excess imidazole and to cleave the 6xHis-GB1, therefore TEV protease was added (250 U TEV/1 mg protein). The dialysis buffer contained 50 mM Tris-HCl (pH 7.5), 5 mM EDTA, 0.5 M NaCl, 4 mM β-ME and 10 % (w/V) glycerol. The second purification step was SEC using a buffer 50 mM Tris-HCl (pH 8.0), 0.5 M NaCl, 5 mM DTT, 10 % (w/V) glycerol and a HiLoad 26/600 Superdex75/200 pg column.

To prepare phosphorylated CaMKK1 and CaMKK2, both proteins were subjected to a phosphorylation reaction with 20 mM $MgCl_2$, 750 µM ATP and 2000 U PKA/mg protein. The reaction ran at a temperature of 30 °C for 4 h and then continued overnight at 4 °C. Finally, to remove ATP and PKA the proteins were subjected to a second SEC using a buffer 20 mM Tris-HCl (pH 7.5), 0.15 M NaCl, 5 mM DTT, 10 % (w/V) glycerol and a HiLoad 26/600 Superdex75/200 pg column.

3.2.4 14-3-3γ

N-terminally 6xHis-tagged 14-3-3γ in plasmid pET15b was grown in *Escherichia Coli* BL21(DE3) cells, and its expression was initiated by induction with 0.5 mM IPTG, followed by overnight incubation at 30 °C. The bacterial culture was centrifuged (20 min at 2,073 *g*), the pellet was resuspended in lysis buffer (1 x PBS, 1 M NaCl, 4 mM β-ME, 2 mM imidazole), and the lysate was frozen. After thawing, the cells were further disrupted by incubation with lysozyme and sonication in the presence of PMSF at a final concentration of 1 mM. The sonicate was then centrifuged (45 min at 19,561 *g* and 4 °C) and the supernatant was used for protein purification.

Firstly, the protein was purified by IMAC using a standard protocol. 6xHis-tagged 14-3-3γ was eluted from the column with a buffer 1 x PBS, 0.5 M NaCl, 2 mM β-ME and 600 mM imidazole. It was then dialyzed for two hours to remove imidazole excess in a dialysis buffer containing 20 mM Tris-HCl (7.5), 2 mM EDTA, 2 mM β-ME and 10% (w/v) glycerol. After that, TEV protease (250 U/mg protein) was added and the protein was further dialyzed overnight in 20 mM Tris-HCl (8.0), 1 mM EDTA, 1 mM DTT and 10% (w/v) glycerol. It was then subjected to anion exchange chromatography using MonoQ 10/100 GL column. The eluted protein was concentrated and subjected to SEC

which ran on HiLoad 26/600 Superdex75 pg in in 20 mM Tris-HCl (7.5), 1 mM EDTA, 150 mM NaCl, 5 mM DTT and 10% (w/v) glycerol.

3.3 Cryo-electron microscopy

Cryo-electron microscopy (Cryo-EM) has evolved significantly in recent years and is now one of three fundamental structural biology techniques capable of providing atomic resolution structures. (Nakane et al., 2020). As the name implies, this method involves the imaging of samples at cryogenic temperatures, which reduces the radiation damage to the samples by up to six times compared to room temperature, thus allowing the acquisition of high resolution structures (Dubochet et al., 1988). Cryo-EM encompasses several methods, including cryo-EM single-particle analysis (SPA), cryo-electron tomography, and electron crystallography. Cryo-EM SPA is based on the vitrification of a sample containing many copies of the same protein (generally a molecule or a molecular assembly), which is then imaged. This process produces two-dimensional (2D) images of the molecules in a variety of orientations, which can be processed to produce a three-dimensional (3D) reconstruction of the original molecule (Milne et al., 2013).

3.3.1 Sample preparation and data collection

SEC on a Superdex 200 10/300 GL column was performed on ASK1-TBD-CRR-KD protein sample, the peak fraction was selected and mixed 1:1 with the SEC buffer (20 mM Tris-HCl (pH 7.5), 150 mM NaCl, and 2 mM β-ME) supplemented with CHAPSO (3-[(3-cholamidopropyl)dimethylammonio]-2-hydroxy-1-propanesulfonate) so that the final protein and CHAPSO concentrations were 0.9 mg/ml and 3.9 mM, respectively. UltrAuFoil holey grids R1.2/1.3 were prepared for sample application by a 45 s glow discharge using a Gatan Solarus II 955. 3.5 ul of the applied sample was blotted using a Vitrobot Mark IV. The temperature and humidity were set to 20 °C, and 100%, respectively, and the blotting time was 4 s. The grids were frozen by immersion in liquid ethane and then kept in liquid nitrogen for storage. Screening was conducted using either the JEOL JEM 2100-plus electron microscope, equipped with a TVIPS TemCam-XF416 4K CMOS camera, or Talos Arctica equipped with a GATAN K2 Summit detector, both operating at 200 keV. For the data collection, Titan Krios working at 300 keV was utilized in conjunction with a GATAN K3 BioQuantum detector. Movies were recorded

at a magnification of 105,000 with a calibrated resolution of 0.834 Å/pixel. Defocus values were between -0.7 to -2.8 um, and a total exposure of 40 electrons per $Å^2$ was used. A total of 11,395 movies were collected, with 8,691 of them acquired under a 40 ° tilt. Each movie was composed of 40 frames.

3.3.2 Data processing

All collected data were processed in CryoSPARC 4.1.2 (Punjani et al., 2017). Movies were first imported and gain correction, patch motion correction and CTF estimation were performed. Those images with estimated CTF resolution greater than 5 Å, full-frame motion distance greater than 20 Å, and relative ice thickness greater than 1.2 were discarded. Visual curation was performed, further discarding micrographs with heavily aggregated proteins, artifacts in the ice, or power spectra. A preliminary batch of particles was selected from 200 micrographs chosen at random, employing a blob picker configured with a particle size range of 60-180 Å. Following a visual examination, particles were isolated using a box size of 320x320 pixels. 2D classification was applied to the selected particles, and the compliant classes were used to create templates, which were subsequently used for another round of picking. The selected particles were extracted using a box size of 340x340 pixels. The particles were again 2D classified and the selected classes were subjected to ab-initio reconstruction. Several refinement procedures followed as next steps. First heterogeneous, then homogeneous, and finally non-uniform refinement on separate classes. To determine the final map resolution, the gold standard Fourier shell correlation (GSFSC) was calculated. The final map was sharpened using the phenix.autosharpen program (Liebschner et al., 2019).

3.3.3 Model building

Since the structures of the separate domains were already known, they were used for ASK1-TBD-CRR-KD model building. The crystal structures of ASK1-KD (PDB ID: 2CLQ (Bunkoczi et al., 2007)) and ASK1-CRR (PDB ID: 5ULM (Weijman et al., 2017)) and the AlphaFold predicted ASK1-TBD model were “jiggle-fitted” into the final map using Coot 0.9.8. (Emsley & Cowtan, 2004). These domains were connected to each other where possible and adjusted based on the map. The model was excluded in regions where the map could not be resolved in sufficient quality. Phenix.real_space_refine from the Phenix package 1.19.1 (Liebschner et al., 2019) was used for the atomic

refinement and MolProbity (Williams et al., 2018) was used for the validation of the final model, which was deposited in PDB/EMDB under accession ID: 8QGY/EMD-18396.

3.4 Analytical ultracentrifugation

Analytical ultracentrifugation (AUC) is used to study the hydrodynamic or thermodynamic properties of biomolecules. The advantage of AUC is that biomolecules are studied in solution (no complications due to interaction with surface/matrix) and do not require affinity/fluorescence tagging. Another advantage of this method is that it can be applied to a relatively wide concentration range of the molecules under investigation (Cole et al., 2008). In the AUC experiment, the solution with molecules of interest is loaded into special centrifugation cuvettes. The distribution of the molecules is then monitored by an optical system using absorption, interference or fluorescence. The most commonly used methods are sedimentation velocity (SV AUC) and sedimentation equilibrium (Lebowitz et al., 2002). In SV AUC, the experiment is performed at high angular velocities, applying large centrifugal forces to the sample. These cause a rapid sedimentation of the molecules creating a sharp interface between the protein-free region at the top of the cuvette and the region of constant protein concentration in the rest of the cuvette. This is a hydrodynamic technique that allows to determine the shape of a molecule of known mass, to determine the molecular weight or to confirm the presence of different molecules of different mass (oligomeric state analysis and characterization of PPIs in general) (Cole et al., 2008; Lebowitz et al., 2002).

3.4.1 SV AUC analysis of ASK1 constructs and the role of TRX

The oligomeric behavior of the ASK1 constructs was analyzed using the SV AUC method. Proteins were dialyzed overnight in a buffer composed of 20 mM Tris-HCl (pH 7.5), 0.15 M NaCl, and 2 mM β-ME. The final samples having a concentration of 4, 12, and 20 μM were loaded into a double-sector titanium centerpiece with a 1.2 cm optical pathlength. All measurements were conducted on a ProteomLab^{TM} XL-I analytical ultracentrifuge using a temperature of 20 °C, angular velocity in the range between 38,000-48,000 rpm, and using absorption or interference optics. Buffer parameters were calculated using SEDNTERP software (Laue et al., 1992), and sedimentation coefficient distributions were obtained using SEDFIT software (Schuck, 2000). The same procedure was used to analyze the effect of TRX on oligomerization of ASK1-TBD-CRR-KD. In this case,

the sedimentation of 12 μM ASK1-TBD-CRR-KD, 24 μM TRX and their combination were measured.

3.4.2 SV AUC analysis of the ERα/14-3-3ζ complex

The stoichiometry of the ERα/14-3-3ζ complex and the effect of ERα ligands on its stability were analyzed using SV AUC. Proteins were dialyzed in a buffer consisting of 20 mM HEPES (pH 7.5), 0.15 M NaCl, 0.5 mM tris(2-carboxyethyl)phosphine (TCEP), and 10 mM $MgCl_2$, and diluted to final concentration. ERα ligands were added to the samples where indicated. Samples were run on a ProteomLabTM XL-I analytical ultracentrifuge in double-sector titanium centerpieces with a 1.2 cm optical path and at a temperature of 20 °C. Angular velocity used was in the range between 43,000 and 45,000 rpm and the data was recorded using absorption optics. Buffer parameters were calculated in the SEDNTERP software (Laue et al., 1992), and the sedimentation coefficient distributions were obtained using the SEDFIT software (Schuck, 2000).

3.5 Hydrogen-deuterium exchange coupled to mass spectrometry

Hydrogen-deuterium exchange coupled to mass spectrometry (HDX-MS) is one of the methods of structural biology. Although it cannot provide us with the coordinates of individual atoms in space as some other methods can, it is a useful tool for gaining insight into both protein structure and protein dynamics, individual conformational states, and the influence of other molecules on a given protein (Trabjerg et al., 2018). The method takes advantage of the inherent lability of hydrogen atoms (these are hydrogen atoms in the O-H, S-H, N-H groups), which can exchange with their surroundings, such as water (Konermann et al., 2011). As the name suggests, HDX-MS exploits the exchange of hydrogen for deuterium, as this exchange involves a change in mass that can then be analyzed by mass spectrometry. In practice, because of the kinetic parameters, we monitor the rate of amide hydrogen exchange, which has two main advantages. The first is the uniform distribution of these hydrogens throughout the length of the protein, and the second is the fact that a secondary structure is formed by these hydrogens and the hydrogen bonds they mediate. The resulting exchange rate then reflects both solvent accessibility and the presence of intramolecular hydrogen bridges (Wales & Engen, 2006). Spatial resolution of HDX is achieved by protease cleavage upon termination of the HDX

reaction. The HDX is then resolved to the level of the resulting peptides or, in the case of an existing overlap, even to individual residues (Chalmers et al., 2011).

ASK1-TBD-CRR-KD and TRX proteins alone (20 μM each) or in mixture (20 μM ASK1 and 100 μM TRX or both 20 μM) were kept at a temperature of 4 °C for 20 min. The HDX reaction started with 10-fold sample dilution in a D_2O-containing buffer (20 mM Tris-HCl (pD 7.5), 0.15 M NaCl, 2 mM β-ME, 10% glycerol). The reaction was run at 4 °C. Samples were collected and quenched at 2 s, 10 s, 1 min and 10 min timepoints; 2 s and 10 min aliquots were prepared in triplicates. The quench was achieved by adding ice-cold 1 M Glycine-HCl (pH 2.3), 400 mM TCEP, 2 M thiourea, and 6 M urea, in a ratio 1:1. Collected samples were frozen in liquid nitrogen. Thawed samples were injected into LC system with a custom-made pepsin/nepenthesin-2 protease column. The resultant peptides were captured and desalted using a SecurityGuard™ precolumn for 3 min under a flow of 0.4% formic acid (FA) in water and at a flow rate of 0.2 mL/min. A reversed-phase analytical column (LUNA Omega Polar C18 Column, 100 Å, 1.6 μm, 100 mm × 1.0 mm) was used to separate the desalted peptides at a flow rate of 40 μl/min and a 10-40% linear gradient of solvent B (A: 2% acetonitrile/0.1% FA in water; B: 98% acetonitrile/0.1% FA in water). To avoid back-exchange, the temperature was kept at 0 °C. The timsTOF Pro mass spectrometer with PASEF and electrospray ionization was used. Data analysis was performed using Data Analysis v. 5.3 and in-house DeutEx software. Peptide identification for both proteins was achieved using data-dependent LC–MS/MS with the same LC setup, completing a MASCOT search against a custom database with sequences of ASK1, TRX1 and contaminants from the cRAP database.

3.6 Small-angle X-ray scattering

Small Angle X-ray Scattering (SAXS) is a technique that analyzes the elastic scattering of X-rays at low angles. It is a powerful method for studying the structural properties of proteins in solution. SAXS is versatile, accommodating a wide range of molecular sizes from kilodaltons to gigadaltons, and its efficiency is particularly pronounced when coupled with intense synchrotron X-ray radiation. In the experiment itself, a protein solution with a concentration typically greater than 1 mg/ml and a volume in the range of 50-100 μl is irradiated with a collimated beam of monochromatic X-rays, and the intensity of the scattered radiation is then recorded as a function of the scattering angle. The intensity of the radiation scattered by the solvent alone is subtracted from

the intensity of the sample in solution. The resulting scattering curve provides information about the shape and size of the particles being studied (Jacques & Trewhella, 2010; Kikhney & Svergun, 2015).

3.6.1 Sample preparation and data collection

All SAXS measurements were performed at beamline P12 operated by EMBL Hamburg at the PETRA III storage ring (DESY, Hamburg, Germany). The SEC-SAXS format was used, i.e. the actual scattering of X-rays on the sample was preceded by injection of the sample on a SEC column. In our case, Superdex 200 Increase 5/150 GL and 0.3 ml/min flowrate were used. Prior to measurement, both proteins and protein complexes (pCaMKK1, pCaMKK2 and their complexes with 14-3-3γ in a 1:2 ratio) were dialyzed in a buffer of the following composition: 50 mM Tris-HCl (pH 7.5), 0.15 M NaCl, 3% (w/v) glycerol and 1 mM TCEP. The determination of forward scattering, I_0, and radius of gyration, R_g, was achieved using the Guinier approximation for the s ($s = 4\pi\sin(\theta)/\lambda$, where 2θ is the scattering angle and λ is the wavelength) region that meets the $sR_g < 1.3$ condition. CHROMIXS software was used to process the SEC-SAXS data (Panjkovich & Svergun, 2018). The selection of data was based on the criterion of maintaining a constant R_g. Calculation of the distance distribution functions, $P(r)$, and determination of the maximum particle dimensions, D_{max}, were performed using GNOM (D. I. Svergun, 1992). Calculation of the excluded volume of the hydrated particle, known as the Porod volume, V_p, was performed utilizing PRIMUS (Konarev et al., 2003). Calculation of the V_C was carried out using the ScÅtter IV program (available at https://bl1231.als.lbl.gov/scatter/).

3.6.2 Model calculations

DAMMIF (Franke & Svergun, 2009) was utilized to derive ab initio molecular envelopes, and the results of fifteen iterations were then averaged in DAMAVER (Volkov & Svergun, 2003). The resulting averaged and filtered envelope was refined by a single run of DAMMIN (D. I. Svergun, 1999). Alignment of the calculated molecular envelope with structural models was performed in SUPCOMB (Kozin & Svergun, 2001). Theoretical scattering curves were derived using the structural models and subjected to fitting against experimental scattering data, a process facilitated by the use of CRYSOL (D. Svergun et al., 1995) and FoXS (Schneidman-Duhovny et al., 2013). The initial model for all-atom

modeling was constructed using the previously obtained crystal structures of CaMKK phosphopeptides bound to 14-3-3γ (PDB IDs: 6FEL and 6EWW (Psenakova et al., 2018) and the kinase domains of both CaMKKs (PDB IDs: 6CD6 and 5UY6). The mutual orientation confined the N- and C-terminal 14-3-3 binding motifs in the 14-3-3 binding groove as seen in the crystal structure of the complex between the respective CaMKK phosphopeptides and 14-3-3γ. 10-30 simulation runs, each consisting of 101 conformations, were used for sampling the most likely conformations that are consistent with the initial structures (Schneidman-Duhovny et al., 2016). The final models were selected based on the $\chi 2$ value - the agreement between the calculated models and the SAXS data.

4 Results and discussion

I was personally involved in obtaining the results presented below. The published studies consist of many other biophysical and biochemical experiments, the results of which can be found in the publications included in the appendix.

4.1 Study of the structure of the N-terminal part of the protein kinase ASK1 and the role of TRX in its regulation

ASK1 belongs to the family of MAP3Ks and promotes the p38 and JNK signaling (Ichijo et al., 1997). ASK1 has been implicated in many serious diseases (Kamiyama et al., 2017; Nygaard et al., 2018). Due to the unsuccessful efforts to develop p38 and JNK inhibitors, ASK1 is now being considered a therapeutic target (Obsilova et al., 2021; Ogier et al., 2020). To develop therapeutics, it is necessary to first understand the molecular mechanism of its regulation. ASK1 can be regulated in various ways, including interactions with other proteins and degradation in the ubiquitin-proteasome system (Maruyama et al., 2014; Nishitoh et al., 1998; Saitoh et al., 1998; L. Zhang et al., 1999; Zhao et al., 2007). The aim of this study is to determine the structure of the ASK1 portion containing all three N-terminal domains critical for regulation of its activity, to analyze the oligomerization behavior of ASK1, and to assess the effect of TRX on the conformation of ASK1.

4.1.1 Expression and purification of ASK1 and TRX

The protein constructs were designed to contain one, two, or all three domains from the N-terminal portion of ASK1 playing a critical role in regulating its activity. All proteins were prepared by a procedure involving IMAC and SEC as explained in Chapter 3.2.1. The resulting purity of the proteins was determined by sodium dodecyl sulfate-polyacrylamide gel electrophoresis. (SDS-PAGE). The resulting purity and SEC chromatogram for all constructs are shown in Fig. 4.1-4.6 on pages 59-61. The indicated fractions were pooled and concentrated for further use. Final yields were in milligrams per 1 L of LB medium for the constructs ASK1-TBD, ASK1-CRR, and ASK1-TBD-CRR, and fractions of milligrams per 1 L of LB medium for the constructs ASK1-KD, ASK1-CRR-KD, and ASK1-TBD-CRR-KD.

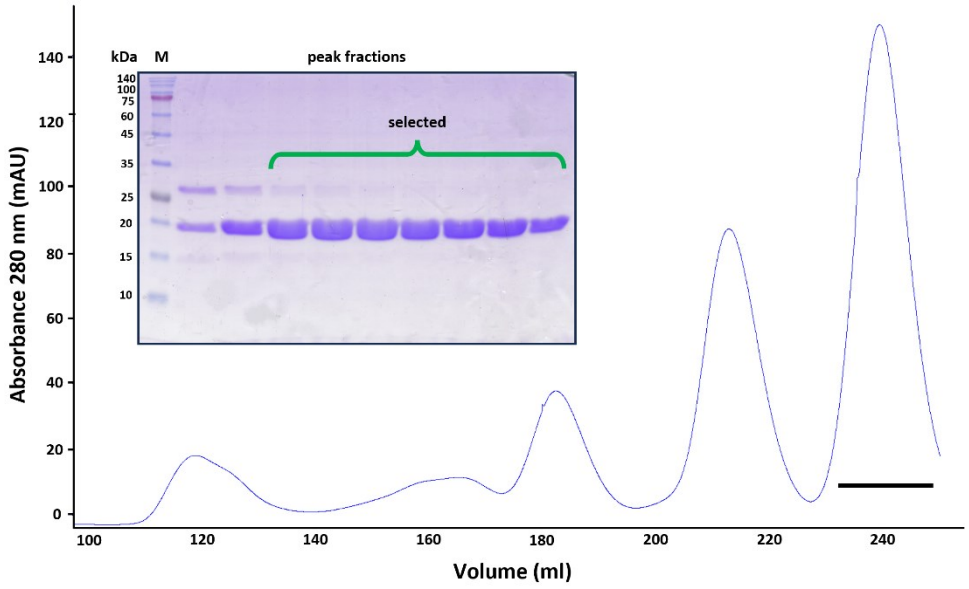

Figure 4.1 Purification of ASK1-TBD.
Chromatogram of ASK1-TBD from the last purification step (SEC) and the related 15 % SDS-PAGE gel demonstrating the purity of the fractions. The fractions loaded on SDS-PAGE are marked by the black bar and the fractions selected for further experiments are indicated in green. M - molecular weight standard.

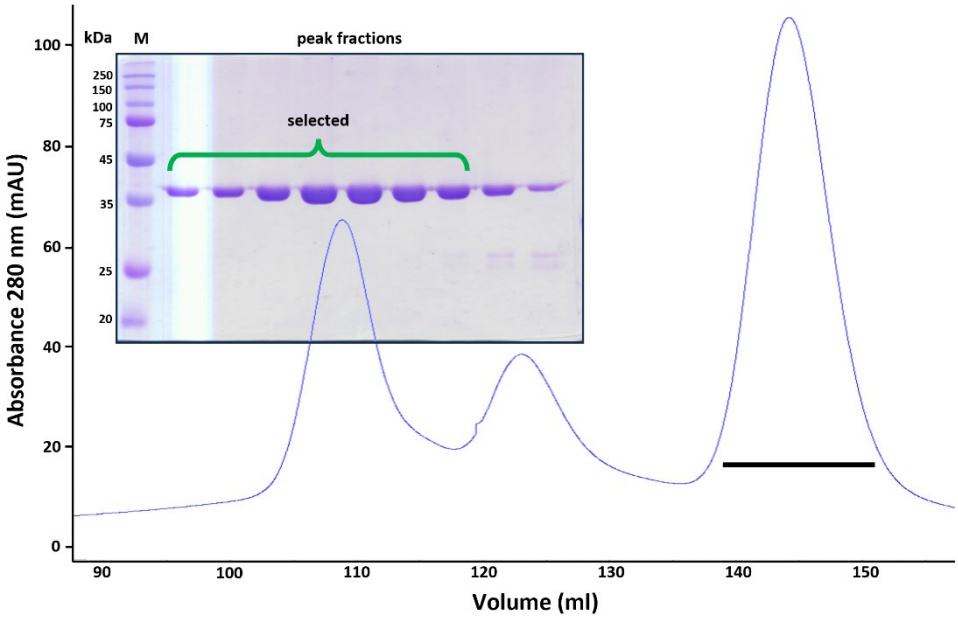

Figure 4.2 Purification of ASK1-CRR.
Chromatogram of ASK1-CRR from the last purification step (SEC) and the related 12 % SDS-PAGE gel demonstrating the purity of the fractions. The fractions loaded on SDS-PAGE are marked by the black bar and the fractions selected for further experiments are indicated in green. M - molecular weight standard.

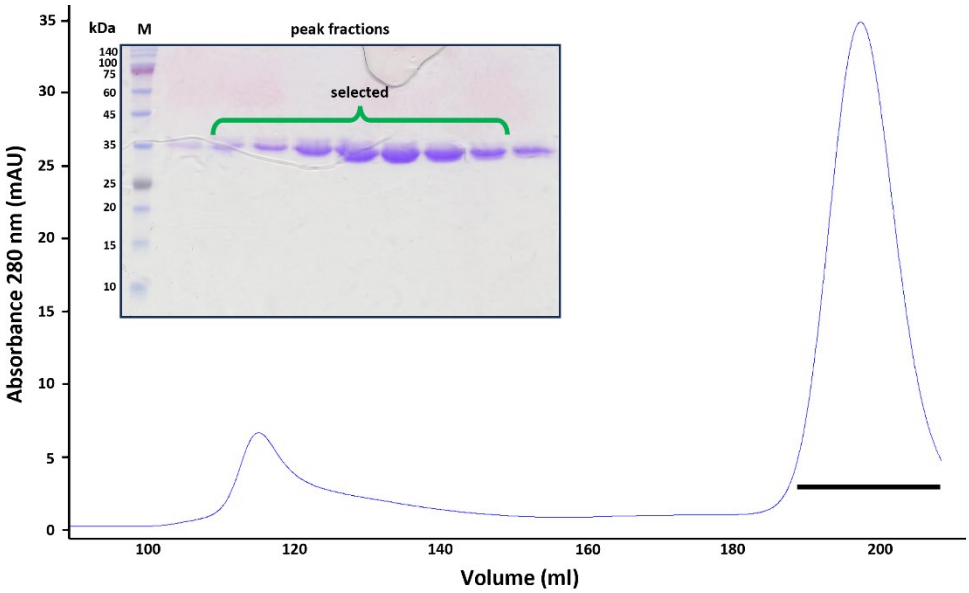

Figure 4.3 Purification of ASK1-KD.
Chromatogram of ASK1-KD from the last purification step (SEC) and the related 15 % SDS-PAGE gel demonstrating the purity of the fractions. The fractions loaded on SDS-PAGE are marked by the black bar and the fractions selected for further experiments are indicated in green. M - molecular weight standard.

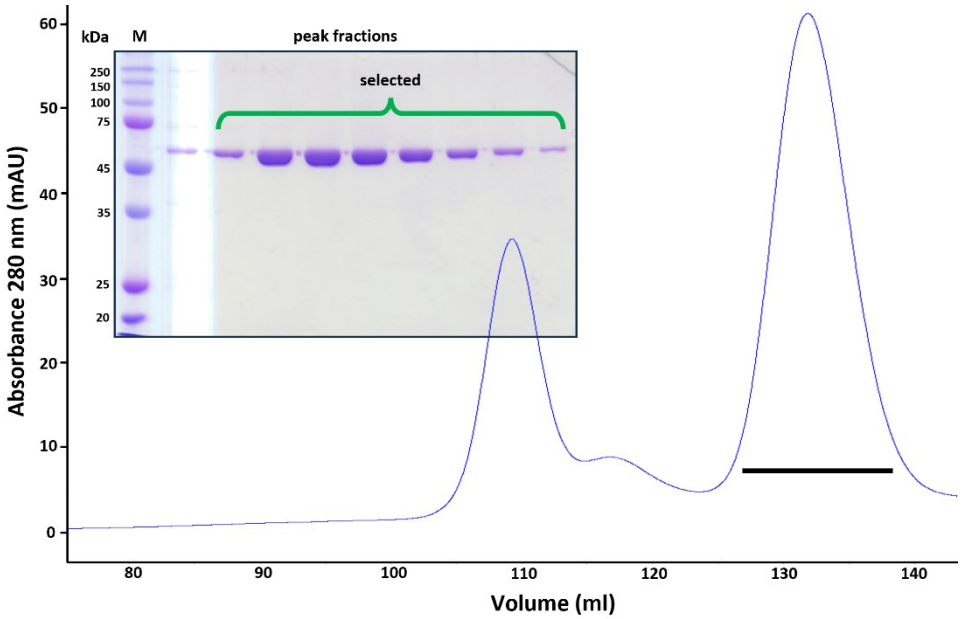

Figure 4.4 Purification of ASK1-TBD-CRR.
Chromatogram of ASK1-TBD-CRR from the last purification step (SEC) and the related 12 % SDS-PAGE gel demonstrating the purity of the fractions. The fractions loaded on SDS-PAGE are marked by the black and the fractions selected for further experiments are indicated in green. M - molecular weight standard.

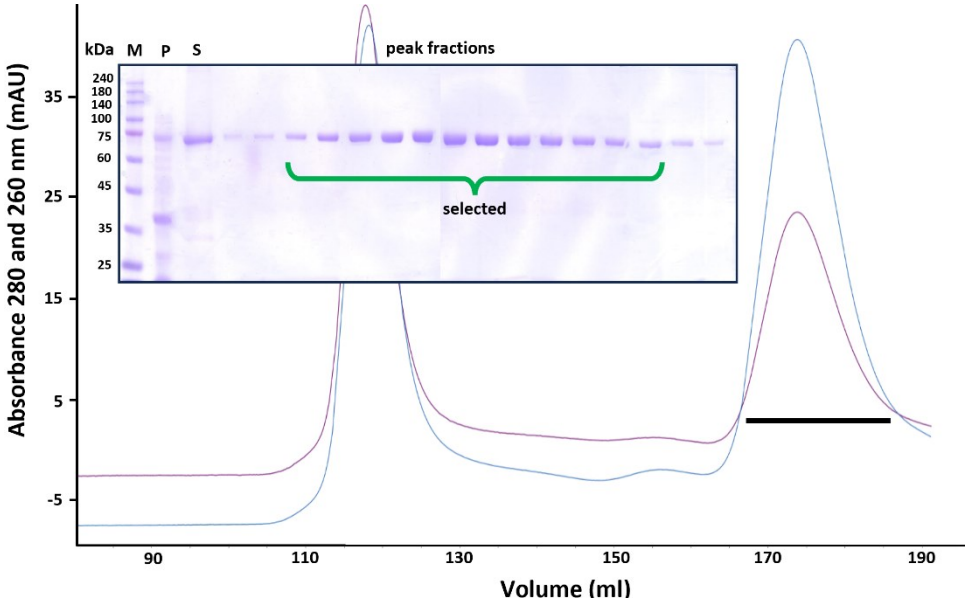

Figure 4.5 Purification of ASK1-CRR-KD.
Chromatogram of ASK1-CRR-KD from the last purification step (SEC) and the related 12 % SDS-PAGE gel demonstrating the purity of the fractions. The fractions loaded on SDS-PAGE are marked by the black bar and the fractions selected for further experiments are indicated in green. M - molecular weight standard, P – pellet, S – supernatant.

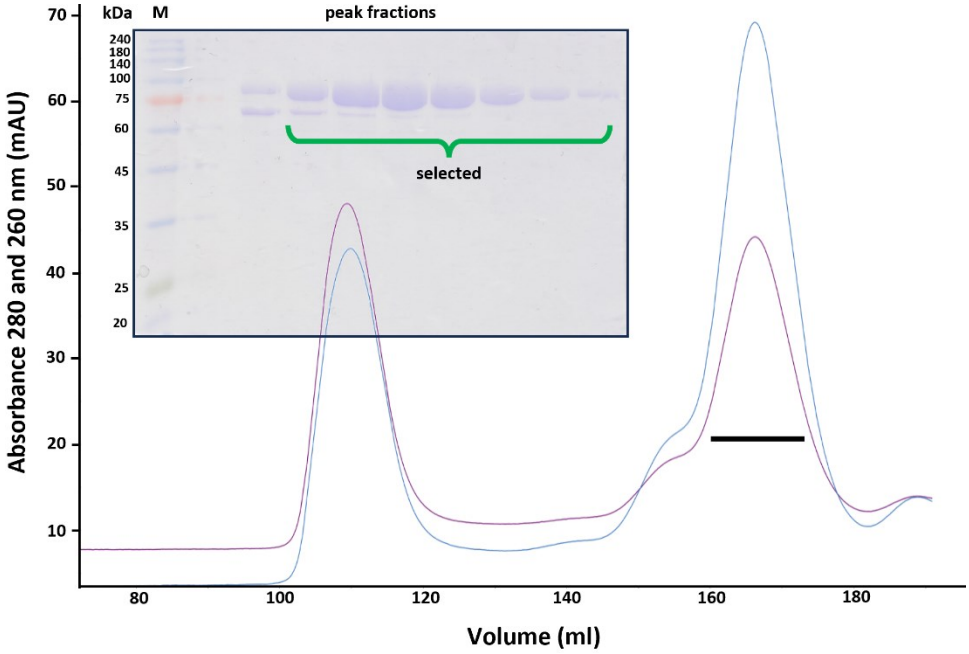

Figure 4.6 Purification of ASK1-TBD-CRR-KD.
Chromatogram of ASK1-CRR-KD from the last purification step (SEC) and the related 10 % SDS-PAGE gel with the purity of the fractions. The fractions loaded on SDS-PAGE are marked by the black bar and the fractions selected for further experiments are indicated in green. M - molecular weight standard.

TRX was expressed and purified using the procedure described in Chapter 3.2.2, i.e. a combination of IMAC and SEC. Final protein purity was visualized by SDS-PAGE and is shown with the chromatogram in Fig. 4.7. Final yields for this protein were in the tens of milligrams per 1L of LB medium.

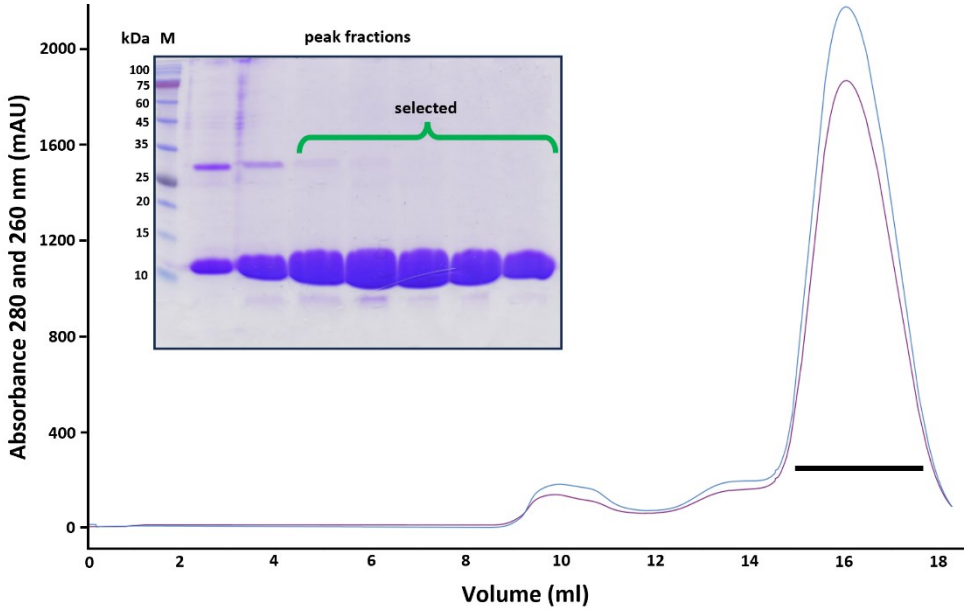

Figure 4.7 Purification of TRX.
Chromatogram of TRX from the last purification step (SEC) and the related 15 % SDS-PAGE gel with the purity of the fractions. The fractions loaded on SDS-PAGE are marked by the black and the fractions selected for further experiments are indicated in green. M - molecular weight standard

4.1.2 Structure of ASK1-TBD-CRR-KD

Up to now, only the structures of the separate domains of ASK1 have been determined. To better understand the regulation of this protein, we decided to use cryo-EM to solve the structure of the part comprising the TBD, CRR and KD domains, which are thought to be critical for both autoregulation and regulation mediated by other proteins.

Preparation of the ASK1-TBD-CRR-KD protein for final data collection included optimization of the protein construct, protein, and detergent concentrations, freezing parameters, and the grid used. A major improvement in the cryo-EM map and overcoming the preferential protein orientation was achieved by collecting the data at a tilt angle of 40°. The final cryo-EM map shows a GSFSC resolution of 3.7 Å. The entire sample preparation and data processing procedure is described in Chapter 3.3.1 and 3.3.2. The data processing is shown in Fig. 4.8 on page 63.

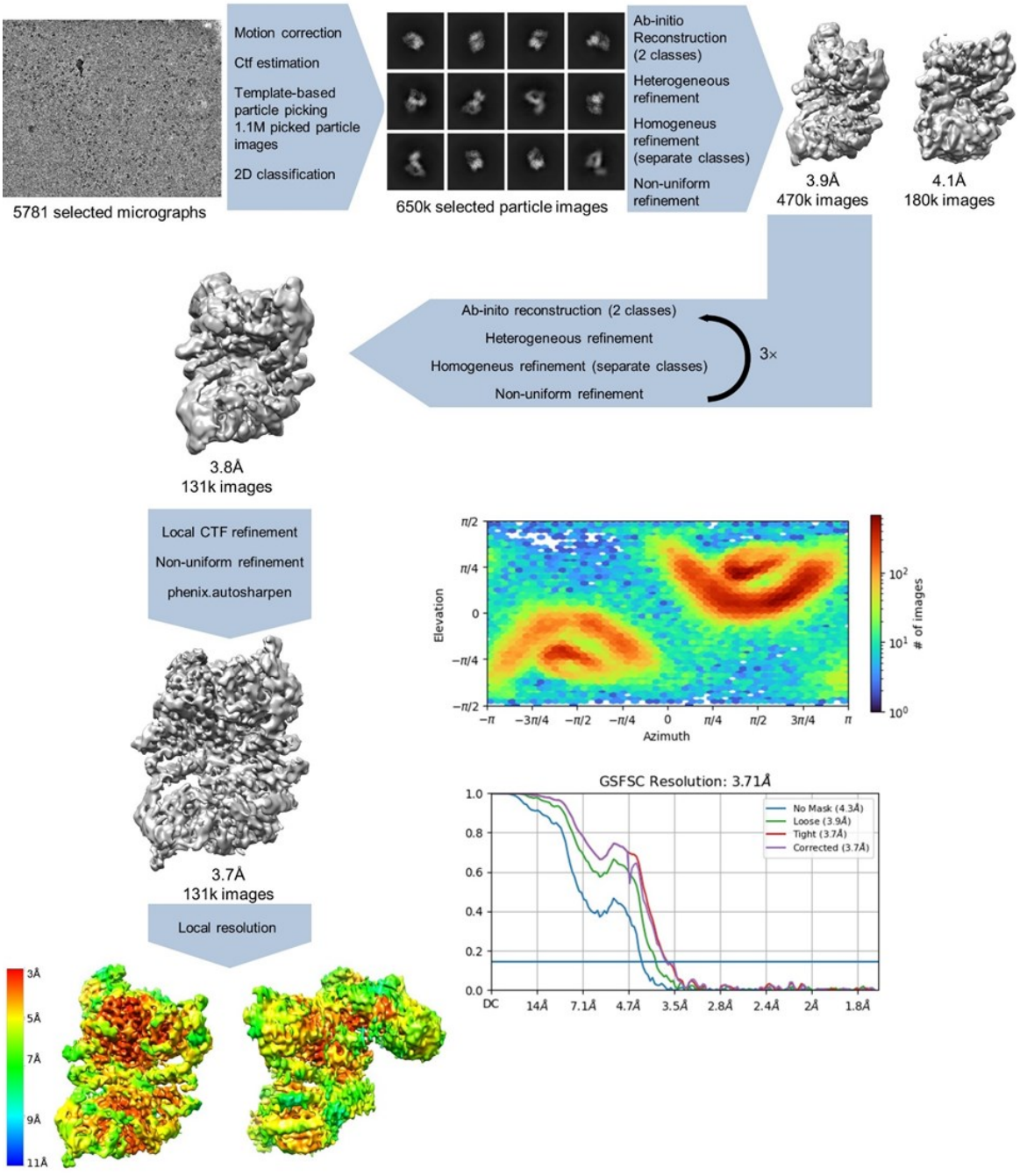

Figure 4.8 Cryo-EM data processing for ASK1-TBD-CRR-KD.
Shown is the procedure leading from the collected micrographs to the final cryo-EM map. All the processing steps are described in the scheme including the number of particle images and the respective resolution. CryoSPARC 4.1.2 output for GSFSC analysis and view distribution plots are shown. Maps were calculated using a threshold of 0.05-0.1 or 5 for sharpened maps.

The ASK1-TBD-CRR-KD model was built based on the obtained map, the crystal structures of ASK1-CRR and ASK1-KD, and the AlphaFold model of ASK1-TBD.

The model showed that ASK1-TBD-CRR-KD forms an asymmetric, compact dimer. One part of the dimer with twofold rotational symmetry is formed by the TBD and CRR domains (CRR subdivided into TPR and PH) and is funnel shaped. It contains dimerization interfaces between the TBD of one chain and the TPR of the opposite chain and another dimerization interface between PH_A and PH_B. Together, TPR_A and PH_A provide a scaffold for the binding of the second part of the protein, the KD dimer. The KD dimer binds asymmetrically to the first part - KD_B makes contacts with both TPR_A and PH_A, while KD_A is oriented away and makes no contacts with the rest of the molecule. KD_A and KD_B dimerize very similarly to the crystal structure, and their dimerization probably contributes to the stability of the dimer, as does the contact between KD_B and CRR_A (Fig. 4.9).

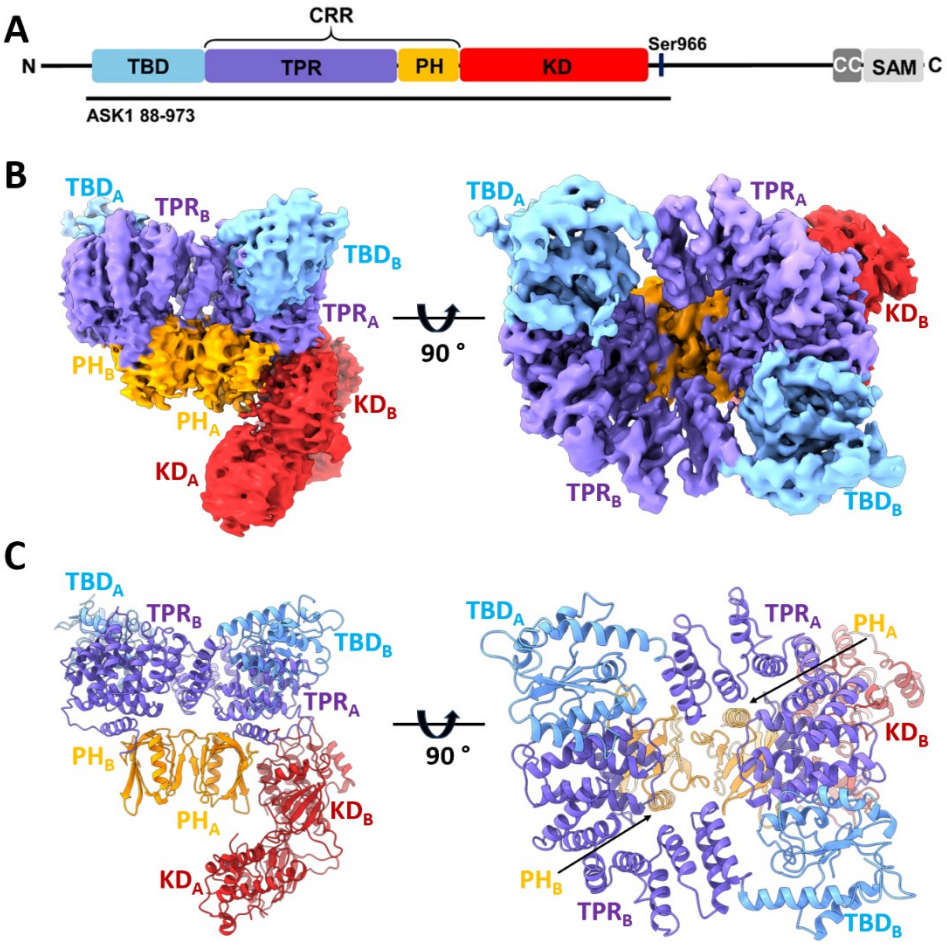

Figure 4.9 Structure of ASK1-TBD-CRR-KD.
A - Domain structure of ASK1. The construct analyzed by cryo-EM is indicated. TBD (blue) – TRX binding domain, TPR (violet) - tetratricopeptide repeat domain, PH – (orange) pleckstrin homology domain, CRR - central regulatory region, KD (red) - kinase domain, CC - coiled-coil domain, SAM - sterile alpha motif. B - cryo-EM density map for the dimeric ASK1-TBD-CRR-KD, C - cartoon representation of the structure.

TBD is a compact and globular domain formed by a mostly parallel beta sheet decorated by several alpha helices. It is rich in cysteine residues, which are assumed to be important for ASK1 regulation, both through oligomerization and interaction with TRX (Kylarova et al., 2016; Nadeau et al., 2007, 2009; Psenakova et al., 2020). C250 was previously identified as a critical residue for domain integrity and TRX binding (Psenakova et al., 2020). In our study, C250 forms a disulfide bridge with C225 in TBD_A. In TBD_B, which has a slightly lower cryo-EM map quality, both cysteine residues are also in close proximity. TBD forms a dimerization interface with the TPR from the opposite chain via its α3 helix and the loop between the α4 helix and β5. The α5 helix in TBD is then followed by the first helix in TPR of the same chain. The detailed view of TBD_A is in Fig. 4.10.

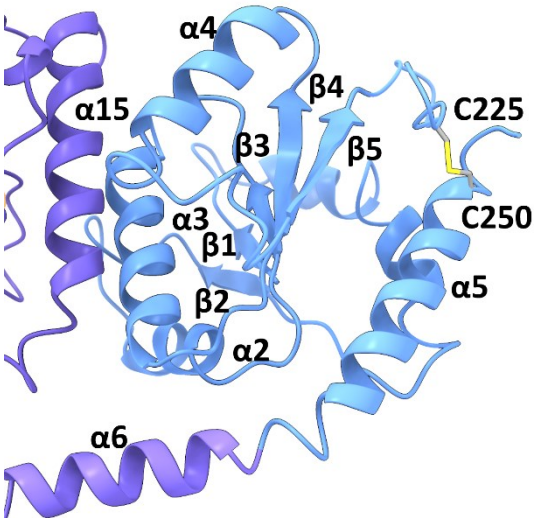

Figure 4.10 Structure of TBD_A.
The detailed view of the TBD_A structure with a focus on the dimerization interface between α3 of TBD_A and α15 of TPR_B.

CRR_A and CRR_B are almost identical to the previously solved crystal structure except for subtle shifts of the first helices (Fig 4.11A,B on page 66). TPR_A and TPR_B are embedded between the TBD domains, so they have no contact with each other. The two TPR domains are composed of 14 α-helices forming 7 TPR repeats. The second part of the CRR is represented by the interacting PH domains, which are composed of a β-sheet and two α-helices. Overall, the dimer of CRR domains has a twofold rotational symmetry.

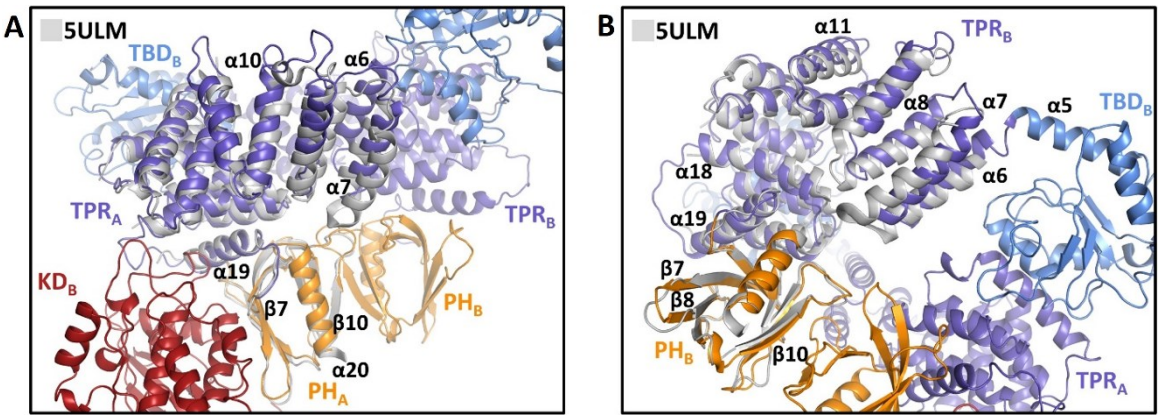

Figure 4.11 Structures of CRR$_A$ and CRR$_B$.
A, B – Comparison between the CRR$_A$/CRR$_B$ structures obtained from cryo-EM and the crystal structure of CRR obtained before. TPR domains and PH domains of the respective CRR are in violet and orange, respectively, and the crystal structure of CRR is in grey (PDB ID: 5uLM) (Weijman et al., 2017).

KD$_B$ interacts primarily via the C-lobe with helices α12, α13, α18 and α19 of TPR$_A$ and β-strands β6 and β7 of PH$_A$. KD$_B$ and KD$_A$ dimerize along their entire length in the same manner as observed in the crystal structure, i.e. head-to-tail. Compared to the crystal structure with the bound inhibitor staurosporine, the αC helix in our structure is shifted inwards and thus occupies an active position in both KDs, characterized by the active site K709 at a hydrogen bond distance from αC-E725 (Fig. 4.12). The activation segment resolved only in the KD$_B$ is in a conformation competent for substrate binding.

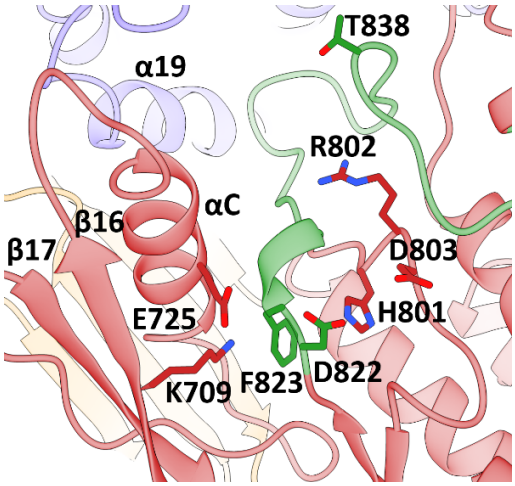

Figure 4.12 Detailed view of the active center in KD$_B$.
KD$_B$ is shown in red, TPR$_A$ in violet, PH$_A$ in orange. Activation segment is in green, the crucial T838 is shown in sticks and so is the conserved D822 and F823. Conserved H801, R802 and D803 from the catalytic loop are shown in sticks.

4.1.3 TBD and CRR are monomeric, but TBD-CRR tends to dimerize in solution

Oligomerization contributes to the regulation of many protein kinases (Pellicena & Kuriyan, 2006; Pike et al., 2008; Schwarz et al., 2003). It was previously shown that ASK1-KD not only crystallizes as a dimer but also forms dimers in solution with a dissociation constant K_D of ~220 nM (Bunkoczi et al., 2007). Later studies showed that both isolated TBD and isolated CRR are monomers in solution, and when the oligomeric state of the ASK1 construct comprising TBD, CRR and KD domains (amino acid range 88-941) was assessed, it was suggested that this construct also behaves as a monomer (Kosek et al., 2014; Weijman et al., 2017). Therefore, given the obtained cryo-EM structure of ASK1 dimer, we wanted to study the oligomerization behavior of different constructs in more detail and validate the interchain contacts observed in our structure.

For this purpose, we designed and prepared several ASK1 constructs - TBD, CRR, KD, and besides that constructs consisting of a combination of two domains TBD-CRR and CRR-KD or all three TBD-CRR-KD. Their oligomerization was studied by the sedimentation velocity method of analytical ultracentrifugation (SV AUC). The distribution of sedimentation coefficients shows us how many different species are present in the sample and their abundance. Based on the sedimentation coefficient and the molecular weight estimate, we can then determine which oligomer it is. While isolated TBD and CRR with sedimentation coefficients corrected to 20 °C and water $s_{w(20,w)}$ 2.2 S and 3.3 S and estimated M_w ~16 kDa and 38 kDa, respectively (Fig. 4.13A,B on page 68), are protomers in solution (theoretical M_w of TBD and CRR are 20.6 and 45.5 kDa), isolated KD with $s_{w(20,w)}$ 4.2 S and estimated M_w ~62 kDa (theoretical M_w 72.4 kDa) is a dimer (Fig. 4.13C on page 68). TBD-CRR shows a concentration-dependent dimerization as suggested by the bimodal distribution (Fig. 4.13D on page 68), CRR-KD with $s_{w(20,w)}$ 6.9 S and estimated M_w ~166 kDa (theoretical M_w 163 kDa) forms a stable dimer (Fig. 4.13E on page 68). Finally, TBD-CRR-KD with $s_{w(20,w)}$ 8.5 S forms a stable dimer and also some higher oligomers whose abundance increases with concentration (Fig. 4.13F on page 68). These results are in good agreement with our structure. Since KDs dimerize strongly and CRRs do not disturb the dimerization interface, but rather facilitate dimerization through interactions between PH domains, the dimerization of KD-containing protein constructs is expected. Furthermore, the interactions within the TBD-CRR module, where TBDs do not interact with each other, but only with TPR, are consistent

with the lack of dimerization of an isolated TBD. Isolated CRR also showed no dimerization. This suggests that the dimerization interface found in PH domains within the ASK1-TBD-CRR-KD structure is not sufficient for the formation of a stable CRR dimer. The dimerization interface between PHs may be a consequence of the dimerization of the KD.

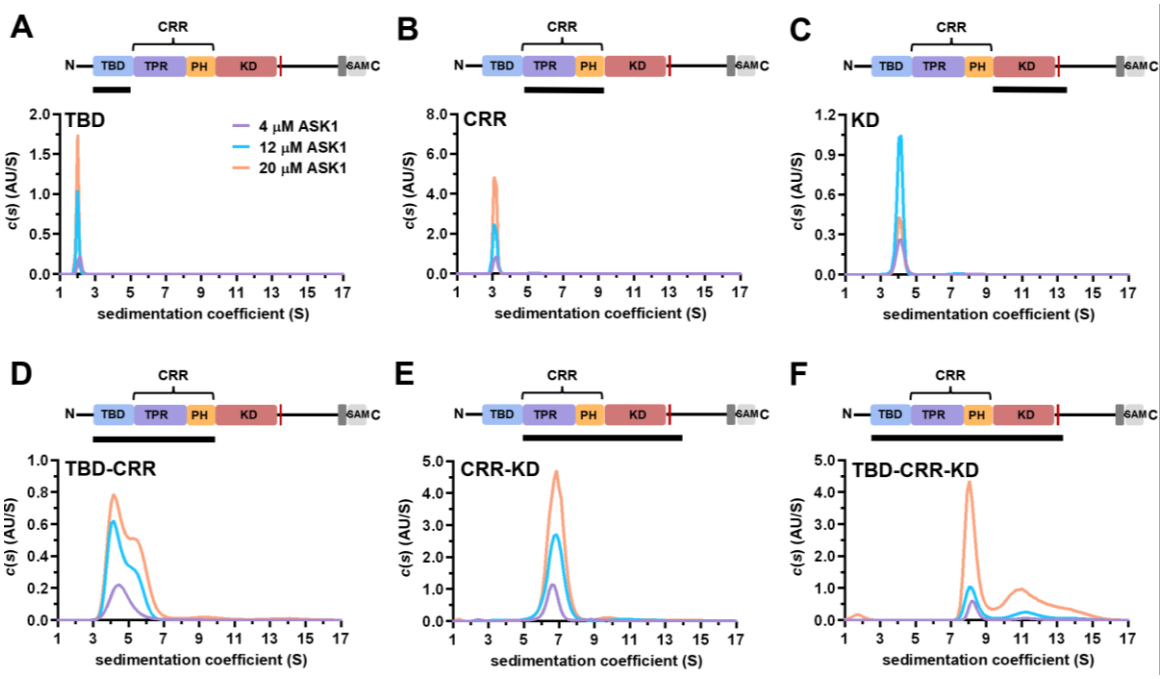

Figure 4.13 SV AUC analysis of the oligomerization of ASK1 constructs.
A-F – The sedimentation coefficients distributions (*c(s)*) for ASK1 constructs were measured at concentrations of 4, 12 and 20 μM. The identity of the constructs is indicated by the black bar in the schematic representation of the domain structure. TBD - TRX binding domain; TPR - tetratricopeptide repeats domain; PH – pleckstrin homology domain; CRR - central regulatory region; KD - kinase domain; SAM - sterile alpha motif domain.

4.1.4 TRX does not prevent the dimerization of ASK1

TRX was the first interaction partner discovered for ASK1, acting as its physiological inhibitor (Saitoh et al., 1998). The interaction between ASK1 and TRX is known to be affected by the redox environment, however, its nature has not been fully elucidated. Reportedly, TRX inhibits ASK1 by preventing homooligomerization of the N-terminal portion of ASK1, necessary for full activation, and by preventing TRAF2/6 from accessing the TRAF binding site (Fujino et al., 2007).

To determine if TRX's interaction with our dimeric N-terminal ASK1 construct, ASK1-TBD-CRR-KD, prevents dimerization, we conducted SV AUC measurements (Fig. 4.14). When comparing the distribution of sedimentation coefficients for ASK1-TBD-CRR-KD alone, TRX alone, and ASK1-TBD-CRR-KD in the presence of TRX, it is evident that the peak corresponding to the ASK1-TBD-CRR-KD dimer with $s_{w(20,w)}$ 8.5 S is preserved in the presence of TRX. Furthermore, its abundance is higher compared to the condition without TRX, presumably due to the loss of the fraction of higher oligomers of ASK1. This finding, combined with the absence of a lower sedimentation coefficient peak in the TRX condition, suggests that TRX does not impede the dimerization of ASK1-TBD-CRR-KD. While SV AUC does not provide sufficient resolution as a technique to exclude conformational changes in response to TRX binding, it does allow us to conclude that TRX binding does not block the dimerization of ASK1-TBD-CRR-KD completely.

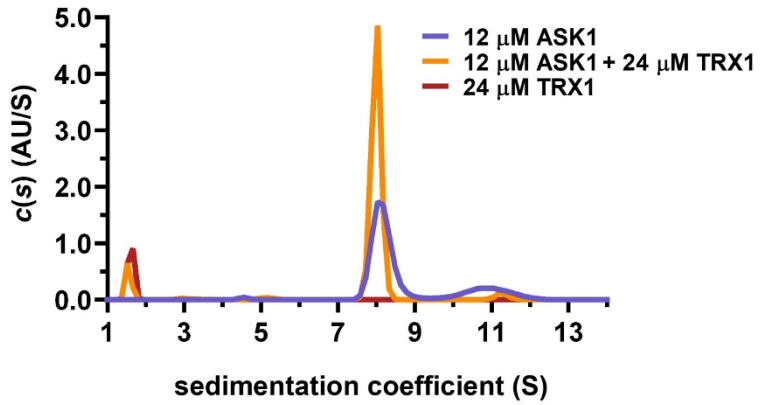

Figure 4.14 Analysis of the dimerization of ASK1-TBD-CRR-KD alone, or in presence of TRX by SV AUC.
The *c(s)* for 12 µM ASK1-TBD-CRR-KD in the absence (violet) and presence of 24 µM TRX (orange). *c(s)* for 24 µM TRX alone is shown in red.

4.1.5 TRX allosterically modulates ASK1, including the activation segment

To investigate TRX-induced structural changes on ASK1, we attempted to prepare the ASK1-TBD-CRR-KD complex with TRX and subsequently image it using cryo-EM. Probably due to the weak interaction of these proteins, our efforts were unsuccessful - we could not prepare a sufficiently stable complex. For this reason, we decided to map the effect of TRX on the structure of ASK1 using HDX-MS, a method that uses hydrogen-

deuterium exchange and monitors the rate of this process. Disordered regions accessible to the solvent are exchanged the fastest and, conversely, regions with stable secondary structure buried within the protein are exchanged the slowest (Wales & Engen, 2006).

To determine the effect of TRX on the structure of ASK1, we compared the percentage of ASK1-TBD-CRR-KD deuteration alone and in the presence of excess TRX. The resulting difference in deuteration is illustrated in Fig. 4.15A on page 71. It shows that the changes in deuteration are observed across the entire ASK1 molecule and that it is almost exclusively the lower deuteration that is observed in the presence of TRX (protection). This can be explained either by direct interaction with TRX or by TRX stabilizing the structure.

Significant protection within TBD is observed at residues 128-143, 184-195, and highest at 206-259. Many of these regions overlap with the region previously identified by NMR as the TRX binding site (Psenakova et al., 2020). At the same time, TRX-protected regions also include a flexible region between β-strand β5 and helix α5, which contains important residues C225 and C250. However, TRX-induced protection is by no means limited to TBD, quite the opposite. Significant protection in the presence of TRX also includes helices α13, α14, α15, and α19 as well as loops α13-α14, α14-α15, α17-α18, and α18-α19 in the TPR domains and the β-strand β9 and the loop connecting β8-β9 within the PH domains. The effect of TRX binding is transferred to the KD via a protected flexible linker comprising residues 655-670 at the interface between CRR and KD (not resolved in the cryo-EM structure). Surprisingly, the TRX effect is most pronounced within the KD in the region of the activation segment (residues 830-844). In addition, the region including the helices αEF (α24), αG (α26) and the loops αD-αE (α22-α23), αF-αG (α25-α26) and αG-αH (α26-α27) is also protected, i.e. stabilized/protected from solvent. The protections in ASK1-TBD-CRR-KD induced by TRX are shown in the context of the structure in Fig. 4.15B on page 71.

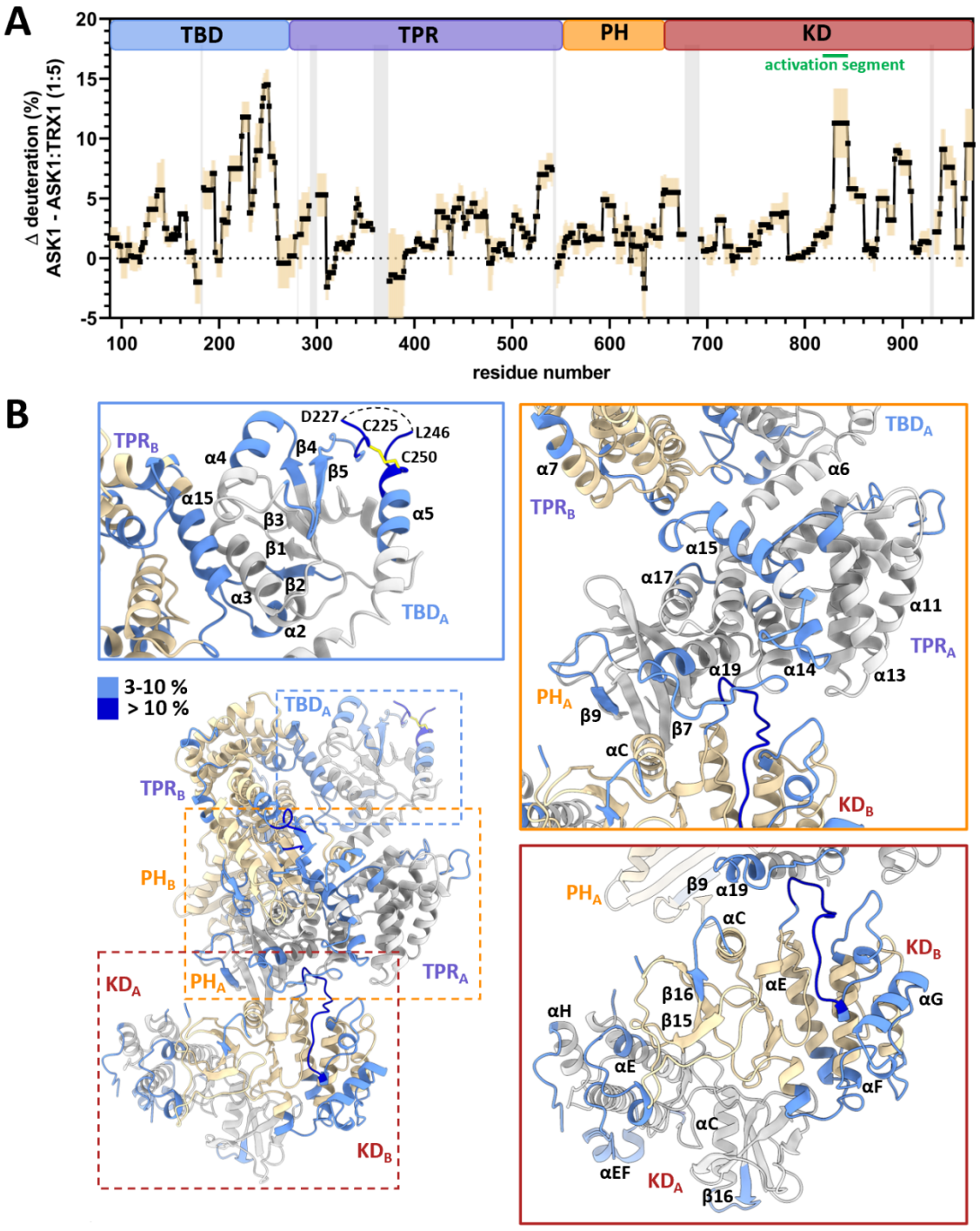

Figure 4.15 TRX-induced structural changes in ASK1-TBD-CRR-KD.
A – Difference in deuteration between ASK1 in absence and presence of TRX after 1 h. Positive values indicate protection by TRX. The black line is the average of three replicates, with standard deviations shown in beige. Regions not covered are grey. The domain structure is shown on top. TBD - TRX binding domain; TPR - tetratricopeptide repeats domain; PH – pleckstrin homology domain; KD - kinase domain. B – Changes in deuteration are mapped on the cartoon representation of ASK1-TBD-CRR-KD structure and are colored for the time 1 h. Chain A is depicted in grey, chain B in beige. Detail of TBD, CRR and KD is in blue, orange, and red squares, respectively.

Summarizing the HDX-MS results, we see that the TRX effect is by no means limited to the directly interacting TBD. On the contrary, the TRX effect is transmitted through regions in the CRR adjacent to the TBD and through the linker at the CRR-KD interface to the KD itself. The protection within the KD is concentrated both in the αEF and αG helix region and in the adjacent linkers between helices, and importantly, the greatest protection is found directly in the activation segment of the KD, which may be of great importance for the regulation of activity. The absence of major deprotection upon TRX binding also confirms the results from SV AUC that there is no disruption of homooligomerization.

4.1.6 TRX binds ASK1 via its active center

To determine the effect of ASK1 on the TRX molecule, we carried out a similar experiment. In this case, we were comparing the percentage of deuteration of TRX alone and TRX in the presence of ASK1. The greatest protection was observed in the β2, α2 and the connecting loop between them, which coincides with the $W^{31}CGPC^{35}$ motif - the catalytic center of TRX containing two key cysteine residues whose -SH groups are essential for the TRX-dependent oxidoreductase activity (Fig. 4.16A,B). These results agree with previous experiments (Kylarova et al., 2016; Psenakova et al., 2020).

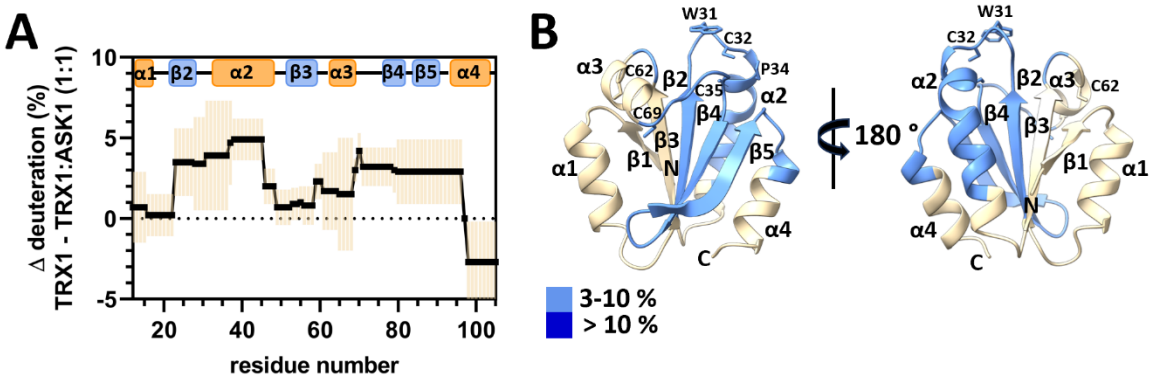

Figure 4.16 ASK1-TBD-CRR-KD-induced structural changes in TRX.
A - Difference in deuteration between TRX in absence and presence of ASK1 after 1 h. Positive values indicate protection by ASK1. The black line is the average of three replicates, standard deviations are shown in beige. The secondary structure of TRX is shown. B - Changes in deuteration are mapped on the cartoon representation of the structure of TRX and are colored for the incubation time 1 h.

4.1.7 Discussion

ASK1 belongs to the MAP3K family and is responsible for activating the p38 and JNK signaling pathways (Ichijo et al., 1997). Overexpression and activation of ASK1 can lead to inflammation and cell death (Ichijo et al., 1997; Iriyama et al., 2009; Takeda et al., 2003; Yoshikawa et al., 2020), and has been linked to various diseases, including neurodegenerative, inflammatory diseases, and cancer (Hsu et al., 2007; Kamiyama et al., 2017; Nygaard et al., 2018). Efforts have been made to develop inhibitors of both p38 and JNK, but these have been either ineffective or associated with side effects (Obsilova et al., 2021; Ogier et al., 2020). Therefore, ASK1 is now being considered as a target for therapeutic intervention. To develop such therapeutics, it is essential to first understand the molecular mechanisms of its regulation. This thesis focuses on two modes of ASK1 regulation: regulation via oligomerization and regulation via interaction with TRX. We determined the structure of the ASK1 portion containing all three N-terminal domains critical for regulating its activity using cryo-EM. Additionally, we analyzed the oligomerization behavior of ASK1 using SV AUC and assessed the effect of TRX on the dimerization and conformation of ASK1 using SV AUC and HDX-MS, respectively.

Oligomerization is often involved in the regulation of MAP3Ks and ASK1 is no exception (Chadee et al., 2002; H. Liu et al., 2000). Oligomerization of ASK1 is mediated by the C-terminal CC domain (covering residues 1236-1293) under non-stress conditions, and additionally by a region located within the first 384 residues, as shown by co-immunoprecipitation experiments. Oligomerization of the N-terminal part is assumed to be necessary for the activation of ASK1 (Fujino et al., 2007; Tobiume et al., 2002). Our cryo-EM structure shows that ASK1-TBD-CRR-KD forms a compact asymmetric dimer with large intra- and inter-chain interactions representing an approximation of the active state (Fig. 4.9 on page 64). At first glance, the surprising dimerization of the part encompassing the TBD and CRR domains - given that the isolated domains are monomeric - appears to be consistent with previously obtained data indicating oligomerization in the region of amino acids 1-384. The dimerization of ASK1-TBD-CRR is confirmed also by our SV AUC measurements (Fig. 4.13 on page 68). In addition, our cryo-EM structure shows that both PH domains and KD domains participate in ASK1-TBD-CRR-KD dimerization (Fig. 4.9 on page 64). The latter has been shown to be dimeric previously, but it was not clear if the dimerization persists in context of a full-length protein or if the dimerization is a truncation artifact (Bunkoczi et al., 2007). From our data, it seems

likely that dimerization of the kinase domain is the main driver of dimerization of the ASK1-TBD-CRR-KD construct and that dimerization of TBD and CRR only contribute to this dimerization. It is evident from the interactions between KD_B and CRR_A that all N-terminal domains are important for the conformation of the kinase domain and thus for protein kinase activity.

Our study is based on a protein construct that lacks both a short, disordered N-terminal portion and a longer mostly disordered C-terminal portion. The C-terminal portion contains the CC domain, which is known to mediate oligomerization (Fujino et al., 2007; Tobiume et al., 2002). It also contains a SAM domain at the C-terminus, which has been shown to heterodimerize with ASK2-SAM. This raises the possibility of the existence of an ASK1/ASK2 heterodimer, which has been reported previously (Federspiel et al., 2016; Trevelyan et al., 2020). Additionally, 14-3-3 proteins, interacting with ASK1 through the binding motif adjacent to the KD, may also affect oligomerization given their dimeric nature (L. Zhang et al., 1999). Finally, the role of the short, disordered N-terminus in the oligomerization of ASK1 is now completely missing. The role of these facts remains to be investigated, ideally in a full-length protein and in complex with relevant protein partners.

TRX was the first ASK1 interacting partner discovered, acting as its physiological inhibitor (Saitoh et al., 1998). The ASK1-TRX interaction is known to be affected by the redox environment, but its exact nature is not fully understood (Kosek et al., 2014; Kylarova et al., 2016; Nadeau et al., 2007, 2009; Psenakova et al., 2020). TRX inhibits ASK1 by preventing homooligomerization of the N-terminal portion of ASK1, necessary for full activation, and by preventing TRAF2/6 from accessing the TRAF binding site (Fujino et al., 2007). This study examines how TRX affects ASK1 oligomerization and structural conformation.

SV AUC measurements performed to assess the effect of TRX on the dimerization of ASK1-TBD-CRR-KD do not suggest any disruption of dimerization by TRX. The resulting *c(s)* do not show any decreased signal of the dimeric fraction of ASK1 in the presence of TRX, nor do they show any signal increase in the lower *s* range (which could suggest monomer occurrence – Fig. 4.14 on page 69). HDX-MS also did not reveal significant deprotection in the presence of TRX, thus supporting the same conclusion (Fig. 4.15 on page 71). Whether this effect translates to physiological conditions is unclear. As previously discussed, parts of the protein that are not part of the construct under study

could play a role in the dimerization. Given that TRX directly interacts with the TBD located near the N-terminus, it is entirely possible that this interaction, or the homooligomerization of the N-terminal part, may be influenced by the disordered N-terminus. Furthermore, dimerization may be affected by the local concentration of ASK1 directly in the cell and by the presence of many other proteins including other interaction partners.

HDX-MS results assessing the structural effect of TRX binding on ASK1-TBD-CRR-KD showed significant protections in TBD including the region containing C250 previously shown to be essential for maintaining structural integrity of TBD and for TRX binding (Fig. 4.15A on page 71) (Psenakova et al., 2020). Structurally varied, the TPR domains serve as scaffolding and binding modules, with certain ones exhibiting notable flexibility. This flexibility initiates allosteric effects and facilitates the functions of molecular switches ((Perez-Riba et al., 2018; Perez-Riba & Itzhaki, 2019). The effect of TRX is transferred through conformational changes in the TPR domain, adjacent to TBD, and PH domain, further through a linker at the interface between CRR and KD and ultimately ends in KD itself. Protections are present in the αEF and αG helix region within the KD, which is a crucial region for substrate binding in other MAP3Ks such is BRAF (Haling et al., 2014). The strongest effect of TRX was observed in the activation segment, a region crucial for kinase activation that commonly contains a regulatory phosphorylatable residue (Fig. 4.15B on page 71) (Johnson et al., 1996). In ASK1 it contains T838, which must be phosphorylated to achieve full ASK1 activity. Therefore, we hypothesize that TRX´s inhibitory effect on the regulation of ASK1 may be also due to its impact on the activation segment. TRX binding protects/stabilizes the activation segment, preventing the crucial T838 from being phosphorylated. To confirm this hypothesis, functional experiments are required.

Despite the shortcomings outlined above, our cryo-EM structure represents the first structural glimpse into ASK1 protein kinase comprising all N-terminal domains critical for its regulation. The structure reveals that all N-terminal domains participate in the dimerization and form a compact dimer with significant intra- and inter-chain interactions which stabilize the active conformation of the KD. The structural changes induced by TRX binding to ASK1 are not restricted solely to the directly interacting TBD, they are rather propagated through the entire molecule up to the activation segment and substrate binding region within KD. The results of our study thus open up

the possibility of targeting ASK1-specific interactions and designing drugs against diseases associated with ASK1 dysregulation.

4.2 Differential effect of 14-3-3γ on CaMKK1 and CaMKK2 activity

CaMKK1 and CaMKK2 are both upstream activators of substrates CaMKI and CaMKIV, regulating axon/dendrite outgrowth, aldosterone synthase expression, memory, immune and inflammatory responses (Condon et al., 2002; Racioppi & Means, 2008; Wayman et al., 2004; Wei et al., 2002). They share about 65% sequence homology, with the highest homology found in their KD (Anderson et al., 1998; Green et al., 2011; Tokumitsu et al., 1997). Despite the homology and their similar domain structure, their regulation is different (Tokumitsu et al., 2001). This study aims to explain the differential effect of the binding partner 14-3-3 on protein activity through structural analysis.

4.2.1 Expression and purification of CaMKKs and 14-3-3γ

CaMKKs were expressed and purified as explained in Chapter 3.2.3 using a combination of IMAC, SEC, phosphorylation reaction and another SEC where necessary. Final protein purity was visualized by SDS-PAGE and is shown with the chromatogram in Fig. 4.17 and Fig. 4.18 on page 77. Final yields for this protein were in the order of milligrams per 1L of autoinduction medium.

14-3-3γ was expressed and purified according to the procedure reported in Chapter 3.2.4, i.e. a combination of IMAC, followed by anion exchange chromatography and SEC. Final protein purity was visualized by SDS-PAGE and is illustrated in Fig. 4.19 on page 78. Final yields for this protein were in the tens of milligrams per 1L of LB medium.

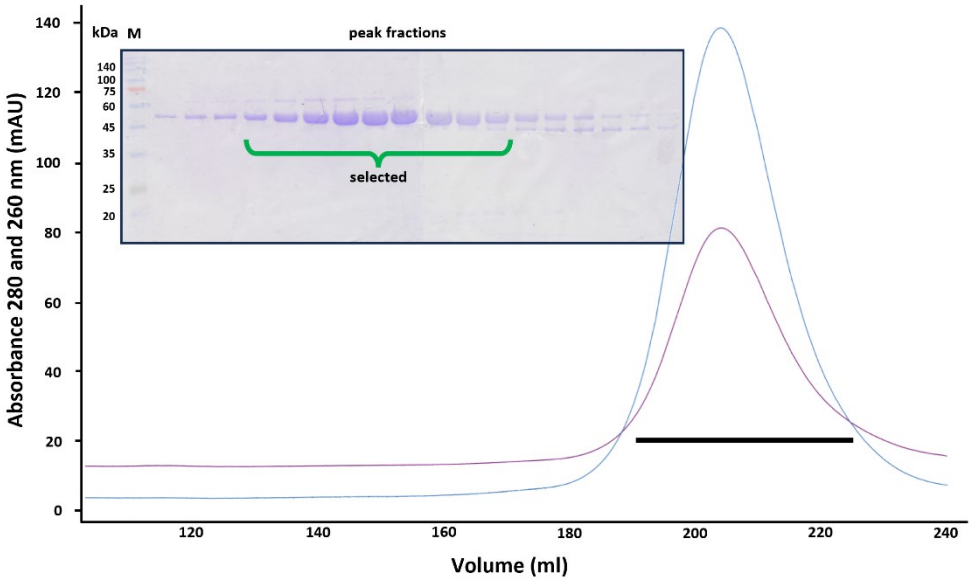

Figure 4.17 Purification of pCaMKK1
Chromatogram of pCaMKK1 from the last purification step (SEC) and the related 12 % SDS-PAGE gel with the purity of the fractions. The fractions loaded on SDS-PAGE are marked by the black bar and the fractions selected for further experiments are indicated in green. M - molecular weight standard.

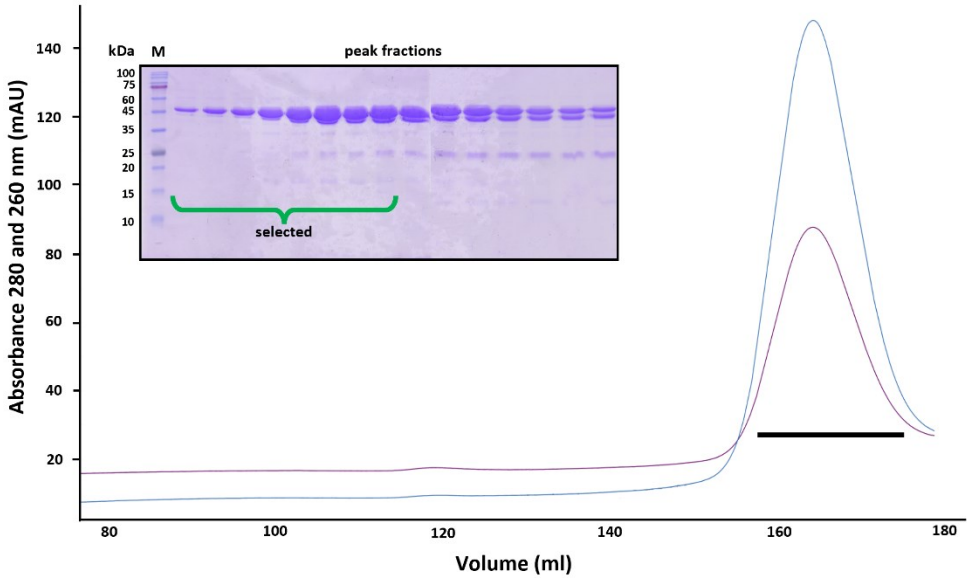

Figure 4.18 Purification of pCaMKK2
Chromatogram of pCaMKK2 from the last purification step (SEC) and the related 15 % SDS-PAGE gel with the purity of the fractions. The fractions loaded on SDS-PAGE are marked by the black bar and the fractions selected for further experiments are indicated in green. M - molecular weight standard.

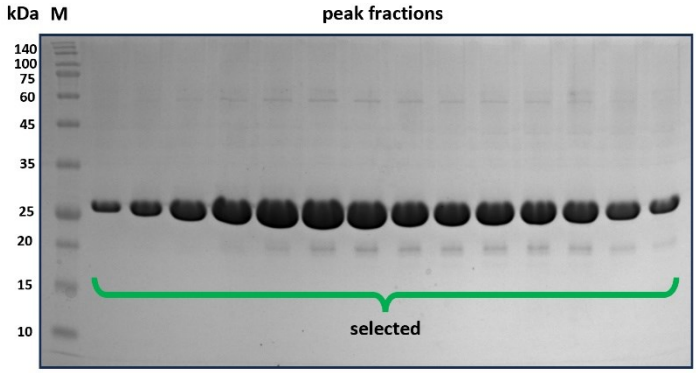

Figure 4.19 Final purity of 14-3-3γΔC
15 % SDS-PAGE gel demonstrating the purity of the fractions after SEC. The fractions selected for further experiments are indicated in green. M - molecular weight standard

4.2.2 The complex of pCaMKK1:14-3-3γ is less flexible than that-of pCaMKK2:14-3-3γ

pCaMKK1, pCaMKK2 and their complexes with 14-3-3γ protein were analyzed by the SEC-SAXS method. The complexes were prepared in a 2:1 ratio (14-3-3γ and the corresponding CaMKK, respectively) based on previous SV AUX experiments that are part of this study. The peak region that showed a constant R_g was selected for subsequent analysis. The analysis of the selected data proved that the complexes form with the expected stoichiometry. The experimental molecular masses agreed with the theoretical ones derived from the protein sequence (Tab. 1 on page 79). Several model-independent structural parameters indicated that the pCaMKK:14-3-3γ complex is more compact and less conformationally heterogeneous when compared to the same complex of pCaMKK2. The R_g and V_c (Rambo & Tainer, 2013) calculated from the Gunier approximation and GNOM were lower for pCaMKK1:14-3-3γ than for pCaMKK2:14-3-3γ (Tab. 1 on page 79). A dimensionless Kratky plot (showing the dependence of $(sR_g)2I(s)/I_0$ versus sR_g, where s is the momentum transfer, $I(s)$ is the scattering intensity, and I_0 is the extrapolated intensity at zero angle) was used to compare conformational flexibility, which also showed that the pCaMKK1:14-3-3γ complex is less conformationally heterogeneous, as indicated by the position of the maximum of the curve (1.10 at sR_g = 1.73 for the pCaMKK1 complex and 1.14 at sR_g = 1.84 for the pCaMKK2 complex) as shown in Fig. 4.20 on page 79.

Table 1 Structural parameters determined from SAXS measurements.

Sample	14-3-3γΔC (dimer)	pCaMKK1	pCaMKK2	pCaMKK1: 14-3-3γΔC (1:2)	pCaMKK2: 14-3-3γΔC (1:2)
Guinier Analysis					
$I(0)$ (cm^{-1})	0.06	0.02	0.041	0.283	0.253
R_g (Å)	28.4	29.5	30.1	33.5	36.5
P(r) analysis					
$I(0)$ (cm^{-1})	0.06	0.02	0.041	0.283	0.254
R_g (Å)	28.4	30.2	31.4	33.3	37
D_{max} (Å)	84	105	120	108	132
Other parameters					
Porod volume V_P ($Å^3$)	76600	87600	88600	152000	156800
Volume-of-correlation V_C ($Å^2$)	423	424	434	637	662
M from a consensus Bayesian assessment method (kDa)	50.9	47.7	53.2	101.1	94.2
M from chemical composition (kDa)	54.3	46.9	47.9	101.2	102.2

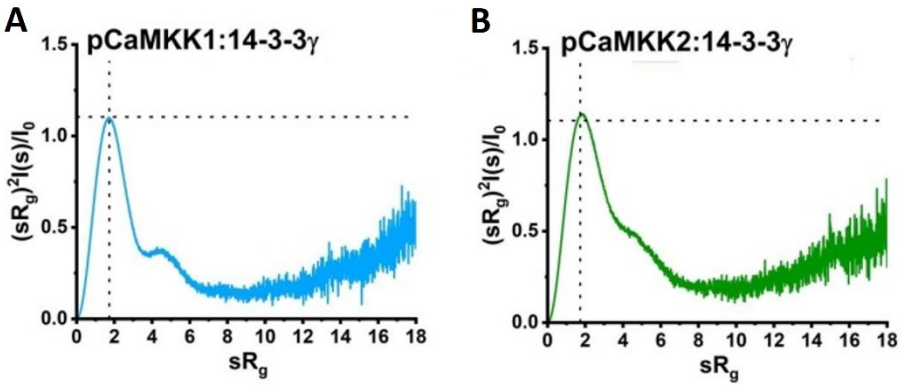

Figure 4.20 Dimensionless Kratky plots.
Dimensionless Kratky plots ($(sR_g)2I(s)/I_0$ versus sR_g, where s is the momentum transfer, $I(s)$ is the scattering intensity, and I_0 is the extrapolated intensity at zero angle) for A – pCaMKK1:14-3-3γ and B – pCaMKK2:14-3-3γ. Adapted from Petrvalska et al., 2023.

4.2.3 14-3-3γ interacts with the N-lobe of the kinase domain of pCaMKK1, blocking access to the active site

To gain more insight into the structure of the pCaMKK1/2:14-3-3γ complexes and to understand the differential effect of 14-3-3γ on their activity, we attempted to crystallize both complexes. However, despite extensive screening of crystallization conditions, successful crystallization was not achieved. This is not surprising, as 14-3-3

protein complexes are notoriously difficult to crystallize - mainly due to the frequent occurrence of 14-3-3 binding motifs in the unstructured regions of 14-3-3 protein partners (X. Yang et al., 2006). Thus, to gain better structural insight into both complexes, we instead used all-atom modeling based on the SAXS data obtained.

Both complexes were modeled using the AllosMod-FoXS method (Schneidman-Duhovny et al., 2013). The best-scoring model of the pCaMKK1:14-3-3γ complex agreed with the experimental data with χ^2 =1.18. According to this model, the KD of pCaMKK1 interacts asymmetrically with the 14-3-3γ dimer. The kinase domain is located on the side, near the C-terminal helices H8 and H9 of one of the protomers of 14-3-3γ outside its central channel. pCaMKK1 interacts with 14-3-3γ via the N-lobe - specifically through the β-strands forming the binding site for ATP and through the phosphate binding loop (between β1 and β2) and the β5-αE loop taking part in substrate binding. The figure showing the model of the pCaMKK1:14-3-3γ complex also illustrate the deuteration changes between isolated pCaMKK1 and pCaMKK1 in complex with 14-3-3γ, which were derived from HDX-MS measurements (Fig. 4.21 on page 81). The results show that the regions protected during complex formation, shown in blue, overlap with the regions where contacts occur between proteins in the complex. HDX-MS thus confirms our SAXS-based structural model.

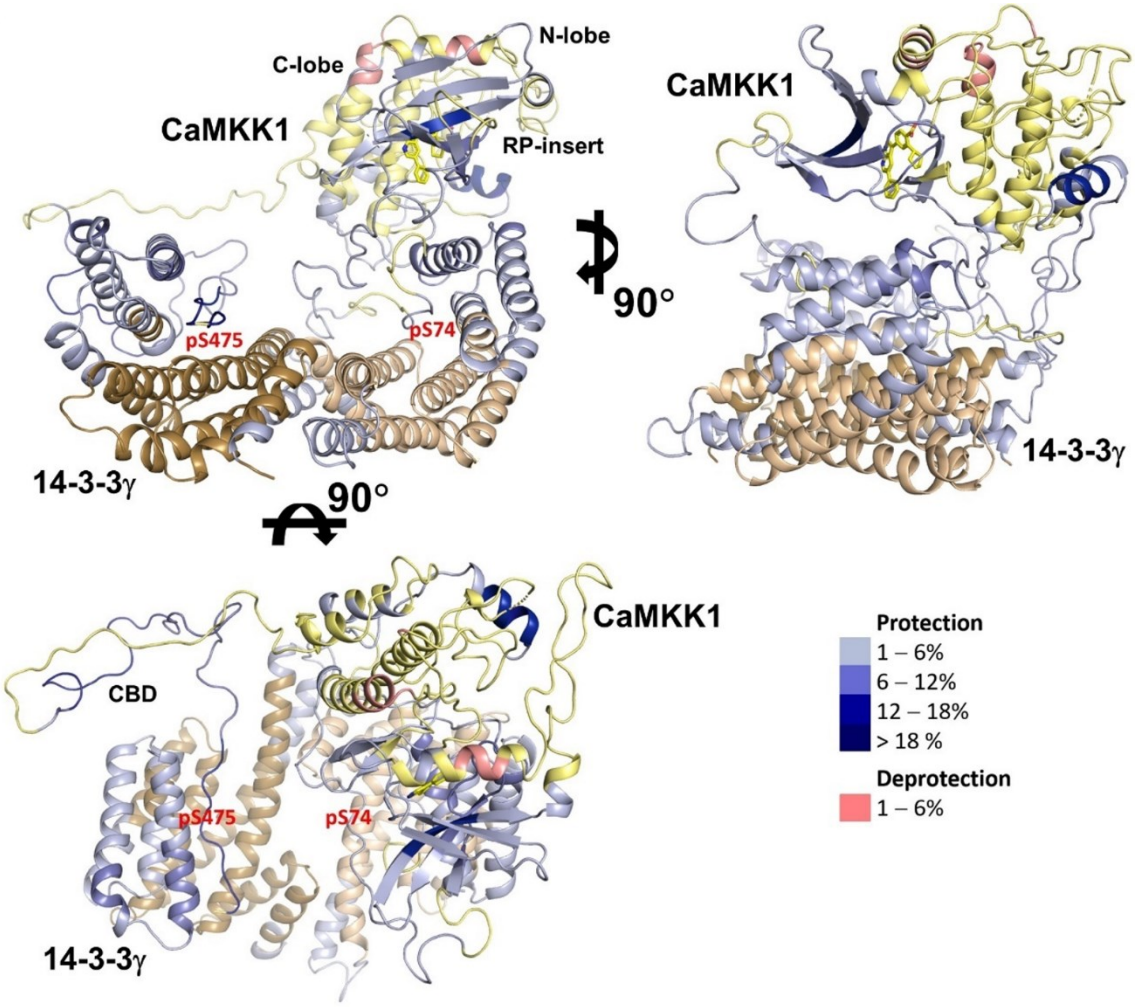

Figure 4.21 AllosMod-FoXS model of the pCaMKK1:14-3-3γ complex.
Cartoon representation of the best-scoring model of the pCaMKK1:14-3-3γ complex at different orientations. 14-3-3γ is shown in brown, pCaMKK1 is in yellow. Changes in deuteration after 120 s are illustrated. Protections and deprotections upon complex formation are depicted in shades of blue and pink, respectively. Adapted from Petrvalska et al., 2023.

On the other hand, all-atom modelling of pCaMKK2:14-3-3γ complex using AllosModFoXS provided the best-scoring model that fits the obtained data with χ^2 =2.13. The obtained model reveals that the KD of pCaMKK2 is located at the very edge of the central channel of the 14-3-3γ dimer and has limited contact with it. When viewed from the side, the kinase domain of pCaMKK2 tilts away from the 14-3-3γ dimer. These results are supported by data from HDX-MS. Changes in deuteration are mapped onto a model of the complex. In comparison to the pCaMKK1:14-3-3γ complex, we observe fewer protected areas during complex formation, and the degree of protection is weaker (Fig. 4. 22 on page 82).

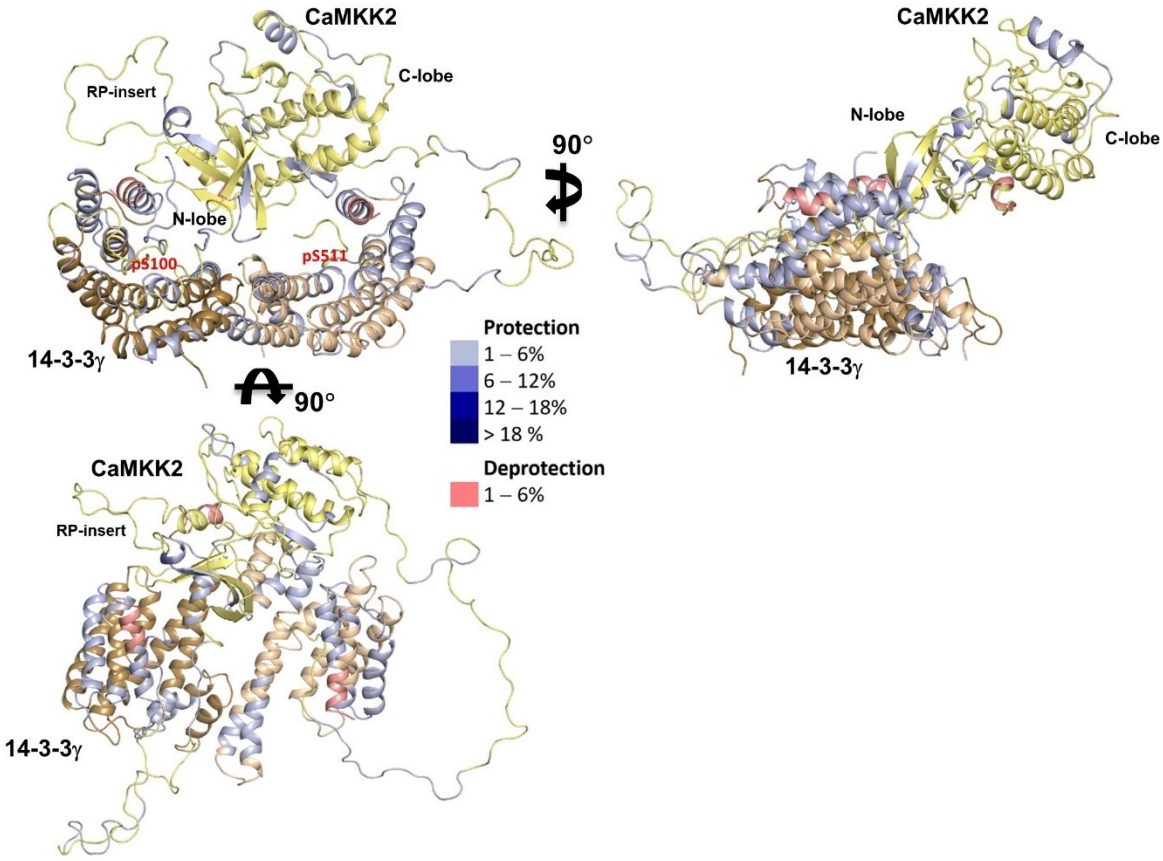

Figure 4.22 AllosMod-FoXS model of the pCaMKK2:14-3-3γ complex.
Cartoon representation of the best-scoring model of the pCaMKK2:14-3-3γ complex at different orientations. 14-3-3γ is shown in brown, pCaMKK1 is in yellow. Changes in deuteration after 20 min are illustrated. Protections and deprotections upon complex formation are depicted in shades of blue and pink, respectively. Adapted from Petrvalska et al., 2023.

4.2.4 Discussion

CaMKK1 and CaMKK2 regulate important processes such as immune and inflammatory responses, energy balance maintenance, and cell survival (Hawley et al., 1995; Racioppi & Means, 2008; Szewczuk et al., 2020; Yano et al., 1998). They share a considerable sequence homology, especially within their kinase domain. Their activity is promoted by Ca^{2+}/CaM, while phosphorylation by PKA inhibits it (Langendorf et al., 2020; Matsushita & Nairn, 1999; Takabatake et al., 2019; Tokumitsu et al., 2001; Wayman et al., 1997). Phosphorylation by PKA makes the binding motifs for 14-3-3 proteins exposed, which further inhibit the activity of CaMKKs (Obsilova & Obsil, 2022). This study aims to explain the difference in the magnitude of the effect of 14-3-3 binding between CaMKK1 and CaMKK2 using structural analysis.

In exploring the interaction between pCaMKK1 and 14-3-3γ, we prepared a SAXS-based structural model which unveiled a direct engagement of the active site and substrate-binding region of pCaMKK1 with H8 and H9 in 14-3-3γ (Fig. 4.21 on page 81). The interaction is in line with the participation of helices 8 and 9 of 14-3-3γ in the binding of other proteins, as evidenced for example in structures with AANAT or Nth1 (Alblova et al., 2017; Obsil et al., 2001). Our HDX-MS data lent additional support, revealing reduced deuteration in the N-lobe of the KD and β strands constituting the ATP-binding pocket, including the P-loop. By contrast, the SAXS-based structural model of the pCaMKK2:14-3-3γ complex shows a comparatively modest binding interface between the two proteins, which was corroborated by weaker deuteration changes after 14-3-3 binding (Fig. 4.22 on page 82). These observations align with the smaller effect of 14-3-3 on the catalytic activity of pCaMKK2. The model-independent structural parameters obtained from SAXS further underline the difference indicating lower R_g, D_{max} and V_c values in the pCaMKK1 complex (Tab. 1 on page 79).

Although we were not able to obtain high-resolution structures that could give more detailed information on the interaction of pCaMKK1/2 and 14-3-3γ, we successfully used the low-resolution information provided by SAXS. The structural models obtained give us an idea of how the different interaction between pCaMKK1/2 and 14-3-3γ look like and explain the different effect on the activity of CaMKKs, but they do not tell us why these differences occur. This may be due to the difference in length of the unstructured segments located between the KD and the N-terminal binding motif or by the other insertions that are present in the CaMKK2 sequence when compared to CaMKK1. In any case, the example of these two complexes illustrates how small changes in protein properties can result in dramatically different outcomes. A recent study showed that the interaction between pCaMKK2 and 14-3-3 can be stabilized by the natural product fusicoccin (Lentini Santo et al., 2020). Further research is necessary to determine whether interaction with 14-3-3 can be an alternative method of regulating CaMKKs and downstream signaling.

4.3 Interaction of nuclear receptor ERα with 14-3-3ζ

ERα is one of 48 members of the NR family of transcription factors that regulate gene transcription and thereby many cellular processes (Escriva et al., 2000; Frigo et al., 2021). Dysregulation of NRs has been linked to the pathogenesis of a number of diseases - cancer,

diabetes, and infertility included (Dhiman et al., 2018; Sever & Glass, 2013). ERα is associated with breast cancer, which can be treated with agents that block ERα activation, such as tamoxifen (Arnesen et al., 2021). One problem with treatment is the emergence of resistance (Arnesen et al., 2021; Paterni et al., 2014; Sharma et al., 2018). Reducing ERα activation through interactions with other proteins may be an alternative to this treatment. It has been shown that 14-3-3 proteins downregulate ERα activity and that stabilizing this interaction results in a reduction of ERα activity (De Vries-van Leeuwen et al., 2013). This study examines the interaction of 14-3-3ζ with ERα in the context of its LBD and C-terminal F domain.

4.3.1 ERα/14-3-3ζ complex is formed in 2:2 stoichiometry

Distributions of sedimentation coefficients (*c(s)*) showed weight-averaged sedimentation coefficients corrected for density and viscosity of water at 20 °C ($s_{w(20,w)}$) of 4.0 S and 3.8 S for ERα and 14-3-3ζ alone corresponding to estimated M_w of ~55 kD and ~58 kD, respectively (theoretical M_w is 66 kD for ERα dimer and 58 kD for 14-3-3ζ dimer). The ERα/14-3-3ζ complex sedimented as two species - the major peak having $s_{w(20,w)}$ 6.3 S and estimated M_w of ~124 kD corresponds to a complex with 2:2 stoichiometry, the minor peak with $s_{w(20,w)}$ corresponds to isolated 14-3-3ζ and ERα representing small amounts of uncomplexed components (Fig. 4.23A on page 85). Overtitration of ERα with up to six equivalents of 14-3-3ζ did not result in the formation of other complexes such as 14-3-3ζ/ERα in a 2:1 stoichiometry, suggesting that ERα binds 14-3-3 as a stable dimer (Fig. 4.23B on page 85). It is hypothesized that the binding of ERα monomer to 14-3-3ζ brings the other ERα monomer into proximity of 14-3-3ζ, resulting in a local concentration increase. Once the ERα/14-3-3ζ tetramer is formed, dissociation is more difficult as the complex is held by two binding interfaces that must be rapidly disrupted one after the other.

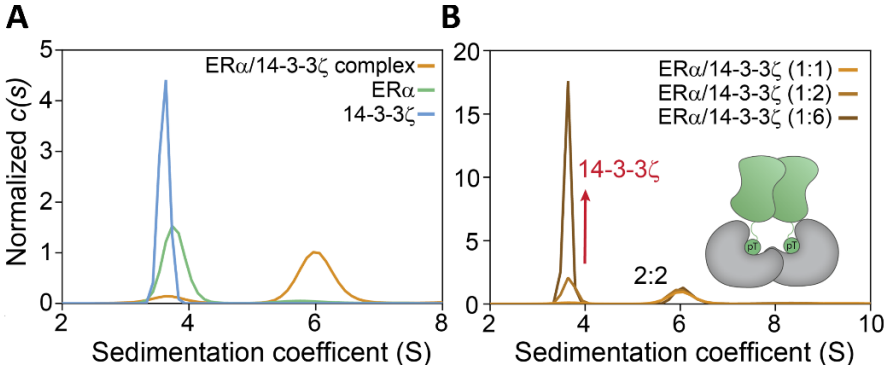

Figure 4.23 SV AUC analysis of the stoichiometry of ERα/14-3-3ζ complex
A – Normalized *c(s)* distribution comparing the sedimentation of ERα (10 µM) and 14-3-3ζ (10 µM) alone, and in complex (30 µM). B Normalized *c(s)* distribution exploring the effect of excess 14-3-3ζ (addition of 5 and 25 µM 14-3-3ζ to the initial 10 µM complex) Adapted from Somsen et al., 2023.

4.3.2 Binding of the ERα dimer to 14-3-3ζ improves the affinity of the complex

The idea of a more stable complex of ERα and 14-3-3ζ dimers is consistent with the observed dissociation constant K_D of this complex. The K_D was estimated using the steady-state equilibrium binding equation (K_D = [A][B]/[AB]), known input concentrations of each component assuming 100 % dimer formation, and calculated area under the curve for the peak of each protein as well as the tetrameric ERα/14-3-3ζ complex. Such a calculation, performed for three replicates, provided us with a K_D ~32 ± 6 nM, which is about ten times lower than the K_D obtained analogically for ERα phosphopeptide, showing that binding of ERα dimer promotes the affinity of the ERα/14-3-3ζ complex.

4.3.3 Effect of Y537S mutation and ligand binding on the ERα/14-3-3ζ complex

The emergence of the Y537 mutation in ERα is closely associated with drug resistance and occurs as a consequence of antiestrogen treatment (Arnesen et al., 2021). To determine whether the mutation affects ERα/14-3-3ζ complex formation, we performed SV AUC measurements and compared complex sedimentation for wild-type and mutant ERα. The results showed that the ERα Y537S is still 14-3-3 binding competent, as can be seen in the *c(s)* in Fig. 4.24 on page 86. Since ERα ligands play an important role in its regulation, we also wanted to assess their ability to bind/destabilize the ERα/14-3-3ζ

complex. Data obtained from SV AUC in combination with differential scanning fluorimetry (DSF) data show us that ERα is fully capable of forming a complex with 14-3-3ζ even when binding the ERα ligands estradiol (E2) and 4-hydroxytamoxifen (4-OHT) as shown in Fig. 4.25.

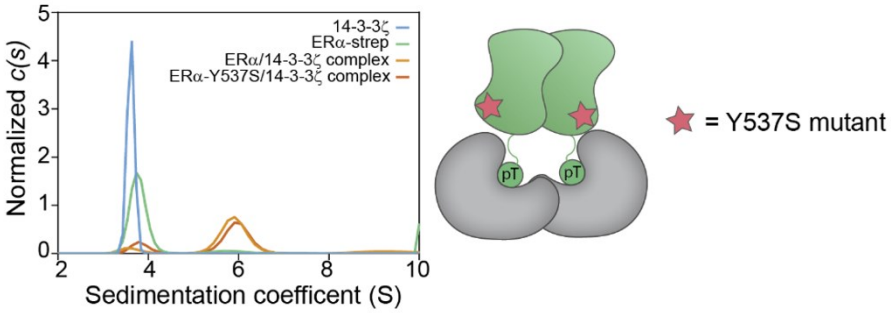

Figure 4.24 Analysis of the ERα/ERα-Y537S complex with 14-3-3ζ.
Normalized *c(s)* distributions showing the effect of ERα-Y537S mutation on complex stability. Shown are distributions for 10 μM ERα, 10 μM 14-3-3ζ and 10 μM complex. Adapted from Somsen et al., 2023.

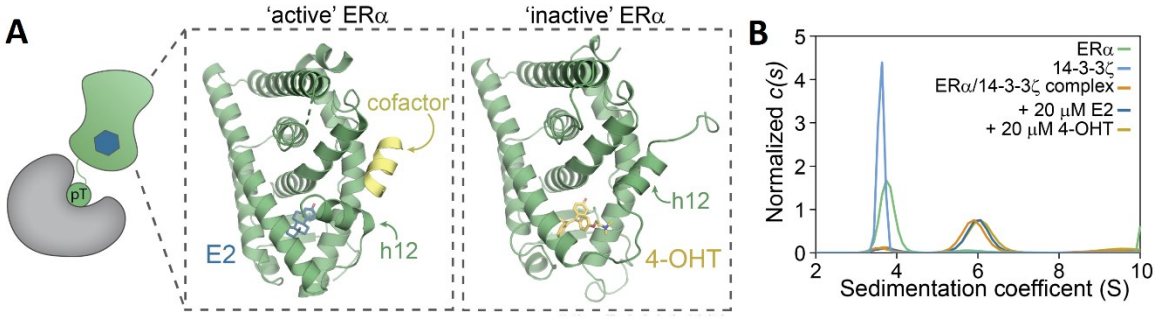

Figure 4.25 ERα/14-3-3ζ complex and the effect of ligands.
A - Schematic representation of the ER/14-3-3ζ complex. The blue hexagon represents the ligand binding to the LBD. Crystal structures of the LBD (green) of the ERα with E2 and 4-OHT ligands bound and shown in blue and yellow sticks, respectively. Ligand binding modifies helix 12´s conformation and enables cofactor binding in the case of E2. (yellow cartoon), PDB: 5WGD & 3ERT. B – Normalized *c(s)* showing the effect of added ligands. Shown are distributions for 10 μM ERα, 10 μM 14-3-3ζ, and 10 μM ERα/14-3-3ζ complex. The complex was also analyzed in the presence of 20 μM E2 and 20 μM 4-OHT. Adapted from Somsen et al., 2023.

4.3.4 Discussion

Efforts to design compounds targeting NRs currently focus on the ligand binding pocket within the LBD (Gronemeyer et al., 2004). However, this approach often leads to the development of resistance, not only in ERα studied in breast cancer but also in other

receptors such as the androgen receptor implicated in prostate cancer (Antonarakis et al., 2016; Paterni et al., 2014; Sharma et al., 2018; Xiang & Wang, 2022). One way to address this issue is to focus on PPIs that are distinct to each protein, which can provide the necessary specificity that is often missing in the traditional approach.

This study analyzed the ERα and 14-3-3ζ complex and found that the two proteins form a high-affinity tetrameric complex consisting of homodimers of both proteins (Fig. 23A on page 85). The complex remains stable even in the presence of ERα ligands, such as the E2 agonist and the 4-OHT antagonist (Fig. 4.25 on page 86), and the Y537S mutation (Fig. 4.24 on page 86), which is known to cause drug resistance in ERα. It was found that the interaction between ERα and 14-3-3ζ is stabilized by the natural product FC-A even under conditions of bound ligands or the Y537S mutation. This suggests that the conformational changes in ERα resulting from ligand binding or the presence of the Y537S mutation are not dependent on the formation of the ERα/14-3-3ζ complex or its stabilization by FC-A. Targeting this protein-protein interaction (PPI) thus represents a viable alternative approach that can be combined with established traditional methods.

Although the results were obtained using a truncated construct, and the use of the full-length protein would add even more value to the results, they still represent a significant advance over earlier studies that are based solely on peptides (Munier et al., 2021; Sijbesma et al., 2019, 2020). It may be possible to apply these findings to other proteins in the NR family, but further detailed studies are necessary to confirm this.

5 Conclusions

The goal of this thesis was to provide mechanistic insights into the function and regulation of several protein complexes. This was done using a combination of biochemical and biophysical methods the results of which are listed below:

1. Study of the structure of the N-terminal part of the protein kinase ASK1 and the role of thioredoxin in its regulation.
   - ASK1-TBD-CRR-KD forms a compact asymmetric dimer with substantial intra- and interchain interactions.
   - All N-terminal domains are involved in the oligomerization.
   - The interdomain contacts are important for stabilization of the active conformation of the KD.
   - Thioredoxin does not disrupt the dimerization of ASK1-TBD-CRR-KD.
   - Thioredoxin strongly affects the region containing C250 in ASK1.
   - Thioredoxin allosterically affects ASK1-KD, most significantly in the activation segment.
   - Thioredoxin binds ASK1 via its active center.

2. Study of the differential effect of 14-3-3γ on CaMKK1 and CaMKK2 activity
   - pCaMKK2 forms a more flexible complex with 14-3-3γ than pCaMKK1.
   - pCaMKK1 interacts with the last two C-terminal helices of one of the protomers within the 14-3-3γ dimer.
   - pCaMKK2 is located at the very edge of the central channel of the 14-3-3γ dimer and has limited contact with it.

3. Study of the interaction between the nuclear receptor ERα and 14-3-3ζ
   - The ERα:14-3-3ζ complex is formed in 2:2 stoichiometry (dimer of ERα interacts with a dimer of 14-3-3ζ).
   - Binding of the ERα dimer to 14-3-3ζ improves the affinity of the complex.
   - The ERα-Y537S mutation does not affect the stability of the complex. Neither do the ligands.

References

Alberts, B., Johnson, A., Lewis, J., Raff, M., Roberts, K., & Walter, P. (2002). *Molecular biology of the cell* (4th ed). Garland Science.

Alblova, M., Smidova, A., Docekal, V., Vesely, J., Herman, P., Obsilova, V., & Obsil, T. (2017). Molecular basis of the 14-3-3 protein-dependent activation of yeast neutral trehalase Nth1. *Proceedings of the National Academy of Sciences of the United States of America*, *114*(46), E9811–E9820. https://doi.org/10.1073/pnas.1714491114

Alessi, D. R., Gomez, N., Moorhead, G., Lewis, T., Keyse, S. M., & Cohen, P. (1995). Inactivation of p42 MAP kinase by protein phosphatase 2A and a protein tyrosine phosphatase, but not CL100, in various cell lines. *Current Biology: CB*, *5*(3), 283–295. https://doi.org/10.1016/s0960-9822(95)00059-5

Alzyoud, L., Bryce, R. A., Al Sorkhy, M., Atatreh, N., & Ghattas, M. A. (2022). Structure-based assessment and druggability classification of protein-protein interaction sites. *Scientific Reports*, *12*(1), 7975. https://doi.org/10.1038/s41598-022-12105-8

Anderson, K. A., Means, R. L., Huang, Q. H., Kemp, B. E., Goldstein, E. G., Selbert, M. A., Edelman, A. M., Fremeau, R. T., & Means, A. R. (1998). Components of a calmodulin-dependent protein kinase cascade. Molecular cloning, functional characterization and cellular localization of Ca2+/calmodulin-dependent protein kinase kinase beta. *The Journal of Biological Chemistry*, *273*(48), 31880–31889. https://doi.org/10.1074/jbc.273.48.31880

Andrews, C., Xu, Y., Kirberger, M., & Yang, J. J. (2020). Structural Aspects and Prediction of Calmodulin-Binding Proteins. *International Journal of Molecular Sciences*, *22*(1), 308. https://doi.org/10.3390/ijms22010308

Antonarakis, E. S., Armstrong, A. J., Dehm, S. M., & Luo, J. (2016). Androgen receptor variant-driven prostate cancer: Clinical implications and therapeutic targeting. *Prostate Cancer and Prostatic Diseases*, *19*(3), 231–241. https://doi.org/10.1038/pcan.2016.17

Araki, K., Yagi, N., Aoyama, K., Choong, C.-J., Hayakawa, H., Fujimura, H., Nagai, Y., Goto, Y., & Mochizuki, H. (2019). Parkinson's disease is a type of amyloidosis featuring accumulation of amyloid fibrils of α-synuclein. *Proceedings of the National Academy of Sciences of the United States of America*, *116*(36), 17963–17969. https://doi.org/10.1073/pnas.1906124116

Arnér, E. S., & Holmgren, A. (2000). Physiological functions of thioredoxin and thioredoxin reductase. *European Journal of Biochemistry*, *267*(20), 6102–6109. https://doi.org/10.1046/j.1432-1327.2000.01701.x

Arnesen, S., Blanchard, Z., Williams, M. M., Berrett, K. C., Li, Z., Oesterreich, S., Richer, J. K., & Gertz, J. (2021). Estrogen Receptor Alpha Mutations in Breast Cancer Cells Cause Gene Expression Changes through Constant Activity and Secondary Effects. *Cancer Research*, *81*(3), 539–551. https://doi.org/10.1158/0008-5472.CAN-20-1171

Atchison, D. K., & Beierwaltes, W. H. (2013). The influence of extracellular and intracellular calcium on the secretion of renin. *Pflugers Archiv: European Journal of Physiology*, *465*(1), 59–69. https://doi.org/10.1007/s00424-012-1107-x

Babu, Y. S., Bugg, C. E., & Cook, W. J. (1988). Structure of calmodulin refined at 2.2 A resolution. *Journal of Molecular Biology*, *204*(1), 191–204. https://doi.org/10.1016/0022-2836(88)90608-0

Bhullar, K. S., Lagarón, N. O., McGowan, E. M., Parmar, I., Jha, A., Hubbard, B. P., & Rupasinghe, H. P. V. (2018). Kinase-targeted cancer therapies: Progress, challenges and future directions. *Molecular Cancer*, *17*(1), 48. https://doi.org/10.1186/s12943-018-0804-2

Bogan, A. A., & Thorn, K. S. (1998). Anatomy of hot spots in protein interfaces. *Journal of Molecular Biology*, *280*(1), 1–9. https://doi.org/10.1006/jmbi.1998.1843

Bootman, M. D. (2012). Calcium signaling. *Cold Spring Harbor Perspectives in Biology*, *4*(7), a011171. https://doi.org/10.1101/cshperspect.a011171

Bootman, M. D., Collins, T. J., Peppiatt, C. M., Prothero, L. S., MacKenzie, L., De Smet, P., Travers, M., Tovey, S. C., Seo, J. T., Berridge, M. J., Ciccolini, F., & Lipp, P. (2001). Calcium signalling—An overview. *Seminars in Cell & Developmental Biology*, *12*(1), 3–10. https://doi.org/10.1006/scdb.2000.0211

Bossemeyer, D. (1995). Protein kinases—Structure and function. *FEBS Letters*, *369*(1), 57–61. https://doi.org/10.1016/0014-5793(95)00580-3

Bunkoczi, G., Salah, E., Filippakopoulos, P., Fedorov, O., Müller, S., Sobott, F., Parker, S. A., Zhang, H., Min, W., Turk, B. E., & Knapp, S. (2007). Structural and functional characterization of the human protein kinase ASK1. *Structure (London, England: 1993)*, *15*(10), 1215–1226. https://doi.org/10.1016/j.str.2007.08.011

Caboni, L., & Lloyd, D. G. (2013). Beyond the ligand-binding pocket: Targeting alternate sites in nuclear receptors. *Medicinal Research Reviews*, *33*(5), 1081–1118. https://doi.org/10.1002/med.21275

Carafoli, E. (2002). Calcium signaling: A tale for all seasons. *Proceedings of the National Academy of Sciences of the United States of America*, *99*(3), 1115–1122. https://doi.org/10.1073/pnas.032427999

Cargnello, M., & Roux, P. P. (2011). Activation and function of the MAPKs and their substrates, the MAPK-activated protein kinases. *Microbiology and Molecular Biology Reviews: MMBR*, *75*(1), 50–83. https://doi.org/10.1128/MMBR.00031-10

Chadee, D. N., Yuasa, T., & Kyriakis, J. M. (2002). Direct Activation of Mitogen-Activated Protein Kinase Kinase Kinase MEKK1 by the Ste20p Homologue GCK and the Adapter Protein TRAF2. *Molecular and Cellular Biology*, *22*(3), 737–749. https://doi.org/10.1128/MCB.22.3.737-749.2002

Chalmers, M. J., Busby, S. A., Pascal, B. D., West, G. M., & Griffin, P. R. (2011). Differential hydrogen/deuterium exchange mass spectrometry analysis of protein-ligand interactions. *Expert Review of Proteomics*, *8*(1), 43–59. https://doi.org/10.1586/epr.10.109

Chen, M., Qu, X., Zhang, Z., Wu, H., Qin, X., Li, F., Liu, Z., Tian, L., Miao, J., & Shu, W. (2016). Cross-talk between Arg methylation and Ser phosphorylation modulates apoptosis signal-regulating kinase 1 activation in endothelial cells. *Molecular Biology of the Cell*, *27*(8), 1358–1366. https://doi.org/10.1091/mbc.E15-10-0738

Cheng, H. L., & Feldman, E. L. (1998). Bidirectional regulation of p38 kinase and c-Jun N-terminal protein kinase by insulin-like growth factor-I. *The Journal of Biological Chemistry*, *273*(23), 14560–14565. https://doi.org/10.1074/jbc.273.23.14560

Cheng, R., Takeda, K., Naguro, I., Hatta, T., Iemura, S.-I., Natsume, T., Ichijo, H., & Hattori, K. (2018). β-TrCP-dependent degradation of ASK1 suppresses the induction of the apoptotic response by oxidative stress. *Biochimica Et Biophysica Acta. General Subjects*, *1862*(10), 2271–2280. https://doi.org/10.1016/j.bbagen.2018.07.015

Cherkasov, A., Hsing, M., Zoraghi, R., Foster, L. J., See, R. H., Stoynov, N., Jiang, J., Kaur, S., Lian, T., Jackson, L., Gong, H., Swayze, R., Amandoron, E., Hormozdiari, F., Dao, P., Sahinalp, C., Santos-Filho, O., Axerio-Cilies, P., Byler, K., … Reiner, N. E. (2011). Mapping the protein interaction network in methicillin-resistant Staphylococcus aureus. *Journal of Proteome Research*, *10*(3), 1139–1150. https://doi.org/10.1021/pr100918u

Chin, D., & Means, A. R. (2000). Calmodulin: A prototypical calcium sensor. *Trends in Cell Biology*, *10*(8), 322–328. https://doi.org/10.1016/s0962-8924(00)01800-6

Cho, J.-H., Lee, M.-K., Yoon, K. W., Lee, J., Cho, S.-G., & Choi, E.-J. (2012). Arginine methylation-dependent regulation of ASK1 signaling by PRMT1. *Cell Death and Differentiation*, *19*(5), 859–870. https://doi.org/10.1038/cdd.2011.168

Cho, Y.-C., Park, J. E., Park, B. C., Kim, J.-H., Jeong, D. G., Park, S. G., & Cho, S. (2015). Cell cycle-dependent Cdc25C phosphatase determines cell survival by regulating apoptosis signal-regulating kinase 1. *Cell Death and Differentiation*, *22*(10), 1605–1617. https://doi.org/10.1038/cdd.2015.2

Clapham, D. E. (2007). Calcium signaling. *Cell*, *131*(6), 1047–1058. https://doi.org/10.1016/j.cell.2007.11.028

Cockrell, L. M., Puckett, M. C., Goldman, E. H., Khuri, F. R., & Fu, H. (2010). Dual engagement of 14-3-3 proteins controls signal relay from ASK2 to the ASK1 signalosome. *Oncogene*, *29*(6), 822–830. https://doi.org/10.1038/onc.2009.382

Cohen, P. (2002). Protein kinases—The major drug targets of the twenty-first century? *Nature Reviews. Drug Discovery*, *1*(4), 309–315. https://doi.org/10.1038/nrd773

Colbran, R. J. (2004). Targeting of calcium/calmodulin-dependent protein kinase II. *The Biochemical Journal*, *378*(Pt 1), 1–16. https://doi.org/10.1042/BJ20031547

Cole, J. L., Lary, J. W., P Moody, T., & Laue, T. M. (2008). Analytical ultracentrifugation: Sedimentation velocity and sedimentation equilibrium. *Methods in Cell Biology*, *84*, 143–179. https://doi.org/10.1016/S0091-679X(07)84006-4

Condon, J. C., Pezzi, V., Drummond, B. M., Yin, S., & Rainey, W. E. (2002). Calmodulin-dependent kinase I regulates adrenal cell expression of aldosterone synthase. *Endocrinology*, *143*(9), 3651–3657. https://doi.org/10.1210/en.2001-211359

Dahlman-Wright, K., Cavailles, V., Fuqua, S. A., Jordan, V. C., Katzenellenbogen, J. A., Korach, K. S., Maggi, A., Muramatsu, M., Parker, M. G., & Gustafsson, J.-A. (2006). International Union of Pharmacology. LXIV. Estrogen receptors. *Pharmacological Reviews*, *58*(4), 773–781. https://doi.org/10.1124/pr.58.4.8

Davare, M. A., Saneyoshi, T., Guire, E. S., Nygaard, S. C., & Soderling, T. R. (2004). Inhibition of calcium/calmodulin-dependent protein kinase kinase by protein 14-3-3. *The Journal of Biological Chemistry*, *279*(50), 52191–52199. https://doi.org/10.1074/jbc.M409873200

De Vries-van Leeuwen, I. J., da Costa Pereira, D., Flach, K. D., Piersma, S. R., Haase, C., Bier, D., Yalcin, Z., Michalides, R., Feenstra, K. A., Jiménez, C. R., de Greef, T. F. A., Brunsveld, L., Ottmann, C., Zwart, W., & de Boer, A. H. (2013). Interaction of 14-3-3 proteins with the estrogen receptor alpha F domain provides a drug target interface. *Proceedings of the National Academy of Sciences of the United States of America*, *110*(22), 8894–8899. https://doi.org/10.1073/pnas.1220809110

Deiss, S., Hernandez Alvarez, B., Bär, K., Ewers, C. P., Coles, M., Albrecht, R., & Hartmann, M. D. (2014). Your personalized protein structure: Andrei N. Lupas fused to GCN4 adaptors. *Journal of Structural Biology*, *186*(3), 380–385. https://doi.org/10.1016/j.jsb.2014.01.013

Dhiman, V. K., Bolt, M. J., & White, K. P. (2018). Nuclear receptors in cancer—Uncovering new and evolving roles through genomic analysis. *Nature Reviews. Genetics*, *19*(3), 160–174. https://doi.org/10.1038/nrg.2017.102

Dubochet, J., Adrian, M., Chang, J. J., Homo, J. C., Lepault, J., McDowall, A. W., & Schultz, P. (1988). Cryo-electron microscopy of vitrified specimens. *Quarterly Reviews of Biophysics*, *21*(2), 129–228. https://doi.org/10.1017/s0033583500004297

Dunn, L. L., Buckle, A. M., Cooke, J. P., & Ng, M. K. C. (2010). The emerging role of the thioredoxin system in angiogenesis. *Arteriosclerosis, Thrombosis, and Vascular Biology*, *30*(11), 2089–2098. https://doi.org/10.1161/ATVBAHA.110.209643

Eid, S., Turk, S., Volkamer, A., Rippmann, F., & Fulle, S. (2017). KinMap: A web-based tool for interactive navigation through human kinome data. *BMC Bioinformatics*, *18*(1), 16. https://doi.org/10.1186/s12859-016-1433-7

Emsley, P., & Cowtan, K. (2004). Coot: Model-building tools for molecular graphics. *Acta Crystallographica. Section D, Biological Crystallography*, *60*(Pt 12 Pt 1), 2126–2132. https://doi.org/10.1107/S0907444904019158

Endo, M. (2006). Calcium ion as a second messenger with special reference to excitation-contraction coupling. *Journal of Pharmacological Sciences*, *100*(5), 519–524. https://doi.org/10.1254/jphs.cpj06004x

Escriva, H., Delaunay, F., & Laudet, V. (2000). Ligand binding and nuclear receptor evolution. *BioEssays: News and Reviews in Molecular, Cellular and Developmental Biology*, *22*(8), 717–727. https://doi.org/10.1002/1521-1878(200008)22:8<717::AID-BIES5>3.0.CO;2-I

Federspiel, J. D., Codreanu, S. G., Palubinsky, A. M., Winland, A. J., Betanzos, C. M., McLaughlin, B., & Liebler, D. C. (2016). Assembly Dynamics and Stoichiometry of the Apoptosis Signal-regulating Kinase (ASK) Signalosome in Response to Electrophile Stress. *Molecular & Cellular Proteomics: MCP*, *15*(6), 1947–1961. https://doi.org/10.1074/mcp.M115.057364

Ferrell, J. E. (1996). Tripping the switch fantastic: How a protein kinase cascade can convert graded inputs into switch-like outputs. *Trends in Biochemical Sciences*, *21*(12), 460–466. https://doi.org/10.1016/s0968-0004(96)20026-x

Forman-Kay, J. D., Clore, G. M., Stahl, S. J., & Gronenborn, A. M. (1992). 1H and 15N resonance assignments and secondary structure of the human thioredoxin C62A, C69A, C73A mutant. *Journal of Biomolecular NMR*, *2*(5), 431–445. https://doi.org/10.1007/BF02192807

Franke, D., & Svergun, D. I. (2009). DAMMIF, a program for rapid ab-initio shape determination in small-angle scattering. *Journal of Applied Crystallography*, *42*(Pt 2), 342–346. https://doi.org/10.1107/S0021889809000338

Frigo, D. E., Bondesson, M., & Williams, C. (2021). Nuclear receptors: From molecular mechanisms to therapeutics. *Essays in Biochemistry*, *65*(6), 847–856. https://doi.org/10.1042/EBC20210020

Fu, H., Subramanian, R. R., & Masters, S. C. (2000). 14-3-3 proteins: Structure, function, and regulation. *Annual Review of Pharmacology and Toxicology*, *40*, 617–647. https://doi.org/10.1146/annurev.pharmtox.40.1.617

Fujino, G., Noguchi, T., Matsuzawa, A., Yamauchi, S., Saitoh, M., Takeda, K., & Ichijo, H. (2007). Thioredoxin and TRAF family proteins regulate reactive oxygen species-dependent activation of ASK1 through reciprocal modulation of the N-terminal homophilic interaction of ASK1. *Molecular and Cellular Biology*, *27*(23), 8152–8163. https://doi.org/10.1128/MCB.00227-07

Ganguly, S., Weller, J. L., Ho, A., Chemineau, P., Malpaux, B., & Klein, D. C. (2005). Melatonin synthesis: 14-3-3-dependent activation and inhibition of arylalkylamine N-acetyltransferase mediated by phosphoserine-205. *Proceedings of the National Academy of Sciences of the United States of America*, *102*(4), 1222–1227. https://doi.org/10.1073/pnas.0406871102

Gigante, A., Sijbesma, E., Sánchez-Murcia, P. A., Hu, X., Bier, D., Bäcker, S., Knauer, S., Gago, F., Ottmann, C., & Schmuck, C. (2020). A Supramolecular Stabilizer of the 14-3-3ζ/ERα Protein-Protein Interaction with a Synergistic Mode of Action. *Angewandte Chemie (International Ed. in English)*, *59*(13), 5284–5287. https://doi.org/10.1002/anie.201914517

Goldberg, J., Nairn, A. C., & Kuriyan, J. (1996). Structural basis for the autoinhibition of calcium/calmodulin-dependent protein kinase I. *Cell*, *84*(6), 875–887. https://doi.org/10.1016/s0092-8674(00)81066-1

Goldman, E. H., Chen, L., & Fu, H. (2004). Activation of apoptosis signal-regulating kinase 1 by reactive oxygen species through dephosphorylation at serine 967 and 14-3-3 dissociation. *The Journal of Biological Chemistry*, *279*(11), 10442–10449. https://doi.org/10.1074/jbc.M311129200

Gonzalez, M. W., & Kann, M. G. (2012). Chapter 4: Protein interactions and disease. *PLoS Computational Biology*, *8*(12), e1002819. https://doi.org/10.1371/journal.pcbi.1002819

Gotoh, Y., & Cooper, J. A. (1998). Reactive oxygen species- and dimerization-induced activation of apoptosis signal-regulating kinase 1 in tumor necrosis factor-alpha signal transduction. *The Journal of Biological Chemistry*, *273*(28), 17477–17482. https://doi.org/10.1074/jbc.273.28.17477

Green, M. F., Scott, J. W., Steel, R., Oakhill, J. S., Kemp, B. E., & Means, A. R. (2011). Ca2+/Calmodulin-dependent protein kinase kinase beta is regulated by multisite phosphorylation. *The Journal of Biological Chemistry*, *286*(32), 28066–28079. https://doi.org/10.1074/jbc.M111.251504

Gronemeyer, H., Gustafsson, J.-A., & Laudet, V. (2004). Principles for modulation of the nuclear receptor superfamily. *Nature Reviews. Drug Discovery*, *3*(11), 950–964. https://doi.org/10.1038/nrd1551

Guo, X., Harada, C., Namekata, K., Matsuzawa, A., Camps, M., Ji, H., Swinnen, D., Jorand-Lebrun, C., Muzerelle, M., Vitte, P.-A., Rückle, T., Kimura, A., Kohyama, K., Matsumoto, Y., Ichijo, H., & Harada, T. (2010). Regulation of the severity of neuroinflammation and demyelination by TLR-ASK1-p38 pathway. *EMBO Molecular Medicine*, *2*(12), 504–515. https://doi.org/10.1002/emmm.201000103

Hagen, N., Bayer, K., Rösch, K., & Schindler, M. (2014). The intraviral protein interaction network of hepatitis C virus. *Molecular & Cellular Proteomics: MCP*, *13*(7), 1676–1689. https://doi.org/10.1074/mcp.M113.036301

Haling, J. R., Sudhamsu, J., Yen, I., Sideris, S., Sandoval, W., Phung, W., Bravo, B. J., Giannetti, A. M., Peck, A., Masselot, A., Morales, T., Smith, D., Brandhuber, B. J., Hymowitz, S. G., & Malek, S. (2014). Structure of the BRAF-MEK complex reveals a kinase activity independent role for BRAF in MAPK signaling. *Cancer Cell*, *26*(3), 402–413. https://doi.org/10.1016/j.ccr.2014.07.007

Han, T., Gao, J., Wang, L., Qu, Y., Sun, A., Peng, K., Zhu, J., Liu, H., Yang, W., Shao, G., & Lin, Q. (2020). ASK1 inhibits proliferation and migration of lung cancer cells via inactivating TAZ. *American Journal of Cancer Research*, *10*(9), 2785–2799.

Hanks, S. K., & Hunter, T. (1995). The eukaryotic protein kinase superfamily: Kinase (catalytic) domain structure and classification1. *The FASEB Journal*, *9*(8), 576–596. https://doi.org/10.1096/fasebj.9.8.7768349

Hanks, S. K., Quinn, A. M., & Hunter, T. (1988). The protein kinase family: Conserved features and deduced phylogeny of the catalytic domains. *Science (New York, N.Y.)*, *241*(4861), 42–52. https://doi.org/10.1126/science.3291115

Hanson, P. I., & Schulman, H. (1992). Neuronal Ca2+/calmodulin-dependent protein kinases. *Annual Review of Biochemistry*, *61*, 559–601. https://doi.org/10.1146/annurev.bi.61.070192.003015

Harrison, S. A., Wong, V. W.-S., Okanoue, T., Bzowej, N., Vuppalanchi, R., Younes, Z., Kohli, A., Sarin, S., Caldwell, S. H., Alkhouri, N., Shiffman, M. L., Camargo, M., Li, G., Kersey, K., Jia, C., Zhu, Y., Djedjos, C. S., Subramanian, G. M., Myers, R. P., … STELLAR-3 and STELLAR-4 Investigators. (2020). Selonsertib for patients with bridging fibrosis or compensated cirrhosis due to NASH: Results from randomized phase III STELLAR trials. *Journal of Hepatology*, *73*(1), 26–39. https://doi.org/10.1016/j.jhep.2020.02.027

Hawley, S. A., Selbert, M. A., Goldstein, E. G., Edelman, A. M., Carling, D., & Hardie, D. G. (1995). 5'-AMP activates the AMP-activated protein kinase cascade, and Ca2+/calmodulin activates the calmodulin-dependent protein kinase I cascade, via three independent mechanisms. *The Journal of Biological Chemistry*, *270*(45), 27186–27191. https://doi.org/10.1074/jbc.270.45.27186

Heldring, N., Pike, A., Andersson, S., Matthews, J., Cheng, G., Hartman, J., Tujague, M., Ström, A., Treuter, E., Warner, M., & Gustafsson, J.-A. (2007). Estrogen receptors: How do they signal

and what are their targets. *Physiological Reviews*, *87*(3), 905–931. https://doi.org/10.1152/physrev.00026.2006

Hoeflich, K. P., & Ikura, M. (2002). Calmodulin in action: Diversity in target recognition and activation mechanisms. *Cell*, *108*(6), 739–742. https://doi.org/10.1016/s0092-8674(02)00682-7

Holmgren, A. (1985). Thioredoxin. *Annual Review of Biochemistry*, *54*, 237–271. https://doi.org/10.1146/annurev.bi.54.070185.001321

Holmgren, A. (1995). Thioredoxin structure and mechanism: Conformational changes on oxidation of the active-site sulfhydryls to a disulfide. *Structure (London, England: 1993)*, *3*(3), 239–243. https://doi.org/10.1016/s0969-2126(01)00153-8

Hsu, M.-J., Hsu, C. Y., Chen, B.-C., Chen, M.-C., Ou, G., & Lin, C.-H. (2007). Apoptosis signal-regulating kinase 1 in amyloid beta peptide-induced cerebral endothelial cell apoptosis. *The Journal of Neuroscience: The Official Journal of the Society for Neuroscience*, *27*(21), 5719–5729. https://doi.org/10.1523/JNEUROSCI.1874-06.2007

Ichijo, H., Nishida, E., Irie, K., ten Dijke, P., Saitoh, M., Moriguchi, T., Takagi, M., Matsumoto, K., Miyazono, K., & Gotoh, Y. (1997). Induction of apoptosis by ASK1, a mammalian MAPKKK that activates SAPK/JNK and p38 signaling pathways. *Science (New York, N.Y.)*, *275*(5296), 90–94. https://doi.org/10.1126/science.275.5296.90

Ichimura, T., Isobe, T., Okuyama, T., Takahashi, N., Araki, K., Kuwano, R., & Takahashi, Y. (1988). Molecular cloning of cDNA coding for brain-specific 14-3-3 protein, a protein kinase-dependent activator of tyrosine and tryptophan hydroxylases. *Proceedings of the National Academy of Sciences of the United States of America*, *85*(19), 7084–7088. https://doi.org/10.1073/pnas.85.19.7084

Ichimura, T., Taoka, M., Hozumi, Y., Goto, K., & Tokumitsu, H. (2008). 14-3-3 Proteins directly regulate Ca(2+)/calmodulin-dependent protein kinase kinase alpha through phosphorylation-dependent multisite binding. *FEBS Letters*, *582*(5), 661–665. https://doi.org/10.1016/j.febslet.2008.01.037

Iriyama, T., Takeda, K., Nakamura, H., Morimoto, Y., Kuroiwa, T., Mizukami, J., Umeda, T., Noguchi, T., Naguro, I., Nishitoh, H., Saegusa, K., Tobiume, K., Homma, T., Shimada, Y., Tsuda, H., Aiko, S., Imoto, I., Inazawa, J., Chida, K., … Ichijo, H. (2009). ASK1 and ASK2 differentially regulate the counteracting roles of apoptosis and inflammation in tumorigenesis. *The EMBO Journal*, *28*(7), 843–853. https://doi.org/10.1038/emboj.2009.32

Jacques, D. A., & Trewhella, J. (2010). Small-angle scattering for structural biology—Expanding the frontier while avoiding the pitfalls. *Protein Science: A Publication of the Protein Society*, *19*(4), 642–657. https://doi.org/10.1002/pro.351

Jin, L., Li, D., Lee, J. S., Elf, S., Alesi, G. N., Fan, J., Kang, H.-B., Wang, D., Fu, H., Taunton, J., Boggon, T. J., Tucker, M., Gu, T.-L., Chen, Z. G., Shin, D. M., Khuri, F. R., & Kang, S. (2013). P90 RSK2 mediates antianoikis signals by both transcription-dependent and -independent mechanisms. *Molecular and Cellular Biology*, *33*(13), 2574–2585. https://doi.org/10.1128/MCB.01677-12

Johnson, L. N., & Barford, D. (1993). The effects of phosphorylation on the structure and function of proteins. *Annual Review of Biophysics and Biomolecular Structure*, *22*, 199–232. https://doi.org/10.1146/annurev.bb.22.060193.001215

Johnson, L. N., Noble, M. E., & Owen, D. J. (1996). Active and inactive protein kinases: Structural basis for regulation. *Cell*, *85*(2), 149–158. https://doi.org/10.1016/s0092-8674(00)81092-2

Jumper, J., Evans, R., Pritzel, A., Green, T., Figurnov, M., Ronneberger, O., Tunyasuvunakool, K., Bates, R., Žídek, A., Potapenko, A., Bridgland, A., Meyer, C., Kohl, S. A. A., Ballard, A. J., Cowie, A., Romera-Paredes, B., Nikolov, S., Jain, R., Adler, J., … Hassabis, D. (2021). Highly accurate protein structure prediction with AlphaFold. *Nature*, *596*(7873), 583–589. https://doi.org/10.1038/s41586-021-03819-2

Jung, H., Seong, H.-A., & Ha, H. (2008). Murine protein serine/threonine kinase 38 activates apoptosis signal-regulating kinase 1 via Thr 838 phosphorylation. *The Journal of Biological Chemistry*, *283*(50), 34541–34553. https://doi.org/10.1074/jbc.M807219200

Junn, E., Han, S. H., Im, J. Y., Yang, Y., Cho, E. W., Um, H. D., Kim, D. K., Lee, K. W., Han, P. L., Rhee, S. G., & Choi, I. (2000). Vitamin D3 up-regulated protein 1 mediates oxidative stress via suppressing the thioredoxin function. *Journal of Immunology (Baltimore, Md.: 1950)*, *164*(12), 6287–6295. https://doi.org/10.4049/jimmunol.164.12.6287

Kadowaki, H., Nishitoh, H., Urano, F., Sadamitsu, C., Matsuzawa, A., Takeda, K., Masutani, H., Yodoi, J., Urano, Y., Nagano, T., & Ichijo, H. (2005). Amyloid beta induces neuronal cell death through ROS-mediated ASK1 activation. *Cell Death and Differentiation*, *12*(1), 19–24. https://doi.org/10.1038/sj.cdd.4401528

Kaji, T., Yoshida, S., Kawai, K., Fuchigami, Y., Watanabe, W., Kubodera, H., & Kishimoto, T. (2010). ASK3, a novel member of the apoptosis signal-regulating kinase family, is essential for stress-induced cell death in HeLa cells. *Biochemical and Biophysical Research Communications*, *395*(2), 213–218. https://doi.org/10.1016/j.bbrc.2010.03.164

Kamiyama, M., Naguro, I., & Ichijo, H. (2015). In vivo gene manipulation reveals the impact of stress-responsive MAPK pathways on tumor progression. *Cancer Science*, *106*(7), 785–796. https://doi.org/10.1111/cas.12676

Kamiyama, M., Shirai, T., Tamura, S., Suzuki-Inoue, K., Ehata, S., Takahashi, K., Miyazono, K., Hayakawa, Y., Sato, T., Takeda, K., Naguro, I., & Ichijo, H. (2017). ASK1 facilitates tumor metastasis through phosphorylation of an ADP receptor P2Y12 in platelets. *Cell Death and Differentiation*, *24*(12), 2066–2076. https://doi.org/10.1038/cdd.2017.114

Kaneshige, R., Ohtsuka, S., Harada, Y., Kawamata, I., Magari, M., Kanayama, N., Hatano, N., Sakagami, H., & Tokumitsu, H. (2022). Substrate recognition by Arg/Pro-rich insert domain in calcium/calmodulin-dependent protein kinase kinase for target protein kinases. *The FEBS Journal*, *289*(19), 5971–5984. https://doi.org/10.1111/febs.16467

Kassouf, T., & Sumara, G. (2020). Impact of Conventional and Atypical MAPKs on the Development of Metabolic Diseases. *Biomolecules*, *10*(9), 1256. https://doi.org/10.3390/biom10091256

Keyse, S. M. (2000). Protein phosphatases and the regulation of mitogen-activated protein kinase signalling. *Current Opinion in Cell Biology*, *12*(2), 186–192. https://doi.org/10.1016/s0955-0674(99)00075-7

Kikhney, A. G., & Svergun, D. I. (2015). A practical guide to small angle X-ray scattering (SAXS) of flexible and intrinsically disordered proteins. *FEBS Letters*, *589*(19 Pt A), 2570–2577. https://doi.org/10.1016/j.febslet.2015.08.027

Kim, A. H., Khursigara, G., Sun, X., Franke, T. F., & Chao, M. V. (2001). Akt phosphorylates and negatively regulates apoptosis signal-regulating kinase 1. *Molecular and Cellular Biology*, *21*(3), 893–901. https://doi.org/10.1128/MCB.21.3.893-901.2001

Knapp, S. (2018). New opportunities for kinase drug repurposing and target discovery. *British Journal of Cancer*, *118*(7), 936–937. https://doi.org/10.1038/s41416-018-0045-6

Knighton, D. R., Zheng, J. H., Ten Eyck, L. F., Ashford, V. A., Xuong, N. H., Taylor, S. S., & Sowadski, J. M. (1991). Crystal structure of the catalytic subunit of cyclic adenosine monophosphate-dependent protein kinase. *Science (New York, N.Y.)*, *253*(5018), 407–414. https://doi.org/10.1126/science.1862342

Konarev, P. V., Volkov, V. V., Sokolova, A. V., Koch, M. H. J., & Svergun, D. I. (2003). PRIMUS: A Windows PC-based system for small-angle scattering data analysis. *Journal of Applied Crystallography*, *36*(5), 1277–1282. https://doi.org/10.1107/S0021889803012779

Kondoh, K., Terasawa, K., Morimoto, H., & Nishida, E. (2006). Regulation of nuclear translocation of extracellular signal-regulated kinase 5 by active nuclear import and export mechanisms. *Molecular and Cellular Biology*, *26*(5), 1679–1690. https://doi.org/10.1128/MCB.26.5.1679-1690.2006

Konermann, L., Pan, J., & Liu, Y.-H. (2011). Hydrogen exchange mass spectrometry for studying protein structure and dynamics. *Chemical Society Reviews*, *40*(3), 1224–1234. https://doi.org/10.1039/c0cs00113a

Kosek, D., Kylarova, S., Psenakova, K., Rezabkova, L., Herman, P., Vecer, J., Obsilova, V., & Obsil, T. (2014). Biophysical and structural characterization of the thioredoxin-binding domain of protein kinase ASK1 and its interaction with reduced thioredoxin. *The Journal of Biological Chemistry*, *289*(35), 24463–24474. https://doi.org/10.1074/jbc.M114.583807

Kozin, M. B., & Svergun, D. I. (2001). Automated matching of high- and low-resolution structural models. *Journal of Applied Crystallography*, *34*(1), 33–41. https://doi.org/10.1107/S0021889800014126

Krebs, J. (1998). Calmodulin-dependent protein kinase IV: Regulation of function and expression. *Biochimica Et Biophysica Acta*, *1448*(2), 183–189. https://doi.org/10.1016/s0167-4889(98)00142-6

Krishna, M., & Narang, H. (2008). The complexity of mitogen-activated protein kinases (MAPKs) made simple. *Cellular and Molecular Life Sciences: CMLS*, *65*(22), 3525–3544. https://doi.org/10.1007/s00018-008-8170-7

Kukimoto-Niino, M., Yoshikawa, S., Takagi, T., Ohsawa, N., Tomabechi, Y., Terada, T., Shirouzu, M., Suzuki, A., Lee, S., Yamauchi, T., Okada-Iwabu, M., Iwabu, M., Kadowaki, T., Minokoshi, Y., & Yokoyama, S. (2011). Crystal structure of the Ca^{2+}/calmodulin-dependent protein kinase kinase in complex with the inhibitor STO-609. *The Journal of Biological Chemistry*, *286*(25), 22570–22579. https://doi.org/10.1074/jbc.M111.251710

Kutuzov, M. A., Bennett, N., & Andreeva, A. V. (2010). Protein phosphatase with EF-hand domains 2 (PPEF2) is a potent negative regulator of apoptosis signal regulating kinase-1 (ASK1). *The International Journal of Biochemistry & Cell Biology*, *42*(11), 1816–1822. https://doi.org/10.1016/j.biocel.2010.07.014

Kuzmanov, U., & Emili, A. (2013). Protein-protein interaction networks: Probing disease mechanisms using model systems. *Genome Medicine*, *5*(37). https://doi.org/10.1186/gm441

Kylarova, S., Kosek, D., Petrvalska, O., Psenakova, K., Man, P., Vecer, J., Herman, P., Obsilova, V., & Obsil, T. (2016). Cysteine residues mediate high-affinity binding of thioredoxin to ASK1. *The FEBS Journal*, *283*(20), 3821–3838. https://doi.org/10.1111/febs.13893

Kyriakis, J. M., & Avruch, J. (2001). Mammalian mitogen-activated protein kinase signal transduction pathways activated by stress and inflammation. *Physiological Reviews*, *81*(2), 807–869. https://doi.org/10.1152/physrev.2001.81.2.807

Langendorf, C. G., O'Brien, M. T., Ngoei, K. R. W., McAloon, L. M., Dhagat, U., Hoque, A., Ling, N. X. Y., Dite, T. A., Galic, S., Loh, K., Parker, M. W., Oakhill, J. S., Kemp, B. E., & Scott, J. W. (2020). CaMKK2 is inactivated by cAMP-PKA signaling and 14-3-3 adaptor proteins. *The Journal of Biological Chemistry*, *295*(48), 16239–16250. https://doi.org/10.1074/jbc.RA120.013756

Laue, T. M., Shah, B. D., Ridgeway, T. M., & Pelletier, S. L. (1992). Computer-aided interpretation of analytical sedimentation data for proteins. *Analytical Ultracentrifugation in Biochemistry and Polymer Science.*, 90–125.

Laurent, T. C., Moore, E. C., & Reichard, P. (1964). ENZYMATIC SYNTHESIS OF DEOXYRIBONUCLEOTIDES. IV. ISOLATION AND CHARACTERIZATION OF THIOREDOXIN, THE HYDROGEN DONOR FROM ESCHERICHIA COLI B. *The Journal of Biological Chemistry*, *239*, 3436–3444.

Le Gal, K., Schmidt, E. E., & Sayin, V. I. (2021). Cellular Redox Homeostasis. *Antioxidants (Basel, Switzerland)*, *10*(9), 1377. https://doi.org/10.3390/antiox10091377

Lebowitz, J., Lewis, M. S., & Schuck, P. (2002). Modern analytical ultracentrifugation in protein science: A tutorial review. *Protein Science: A Publication of the Protein Society*, *11*(9), 2067–2079. https://doi.org/10.1110/ps.0207702

Lentini Santo, D., Petrvalska, O., Obsilova, V., Ottmann, C., & Obsil, T. (2020). Stabilization of Protein-Protein Interactions between CaMKK2 and 14-3-3 by Fusicoccins. *ACS Chemical Biology*, *15*(11), 3060–3071. https://doi.org/10.1021/acschembio.0c00821

Leung, A. K.-W., Ramesh, N., Vogel, C., & Unniappan, S. (2019). Nucleobindins and encoded peptides: From cell signaling to physiology. *Advances in Protein Chemistry and Structural Biology*, *116*, 91–133. https://doi.org/10.1016/bs.apcsb.2019.02.001

Leung, I. W., & Lassam, N. (1998). Dimerization via tandem leucine zippers is essential for the activation of the mitogen-activated protein kinase kinase kinase, MLK-3. *The Journal of Biological Chemistry*, *273*(49), 32408–32415. https://doi.org/10.1074/jbc.273.49.32408

Lewit-Bentley, A., & Réty, S. (2000). EF-hand calcium-binding proteins. *Current Opinion in Structural Biology*, *10*(6), 637–643. https://doi.org/10.1016/s0959-440x(00)00142-1

Liebschner, D., Afonine, P. V., Baker, M. L., Bunkóczi, G., Chen, V. B., Croll, T. I., Hintze, B., Hung, L. W., Jain, S., McCoy, A. J., Moriarty, N. W., Oeffner, R. D., Poon, B. K., Prisant, M. G., Read, R. J., Richardson, J. S., Richardson, D. C., Sammito, M. D., Sobolev, O. V., … Adams, P. D. (2019). Macromolecular structure determination using X-rays, neutrons and electrons: Recent developments in Phenix. *Acta Crystallographica. Section D, Structural Biology*, *75*(Pt 10), 861–877. https://doi.org/10.1107/S2059798319011471

Lin, A., Minden, A., Martinetto, H., Claret, F. X., Lange-Carter, C., Mercurio, F., Johnson, G. L., & Karin, M. (1995). Identification of a dual specificity kinase that activates the Jun kinases and p38-Mpk2. *Science (New York, N.Y.)*, *268*(5208), 286–290. https://doi.org/10.1126/science.7716521

Liu, D., Bienkowska, J., Petosa, C., Collier, R. J., Fu, H., & Liddington, R. (1995). Crystal structure of the zeta isoform of the 14-3-3 protein. *Nature*, *376*(6536), 191–194. https://doi.org/10.1038/376191a0

Liu, D.-H., Yuan, F.-G., Hu, S.-Q., Diao, F., Wu, Y.-P., Zong, Y.-Y., Song, T., Li, C., & Zhang, G.-Y. (2013). Endogenous nitric oxide induces activation of apoptosis signal-regulating kinase 1 via S-nitrosylation in rat hippocampus during cerebral ischemia-reperfusion. *Neuroscience*, *229*, 36–48. https://doi.org/10.1016/j.neuroscience.2012.10.055

Liu, H., Nishitoh, H., Ichijo, H., & Kyriakis, J. M. (2000). Activation of apoptosis signal-regulating kinase 1 (ASK1) by tumor necrosis factor receptor-associated factor 2 requires prior dissociation of the ASK1 inhibitor thioredoxin. *Molecular and Cellular Biology*, *20*(6), 2198–2208. https://doi.org/10.1128/MCB.20.6.2198-2208.2000

Liu, J., Zheng, Q., Deng, Y., Cheng, C.-S., Kallenbach, N. R., & Lu, M. (2006). A seven-helix coiled coil. *Proceedings of the National Academy of Sciences of the United States of America*, *103*(42), 15457–15462. https://doi.org/10.1073/pnas.0604871103

Liu, Y., & Min, W. (2002). Thioredoxin promotes ASK1 ubiquitination and degradation to inhibit ASK1-mediated apoptosis in a redox activity-independent manner. *Circulation Research*, *90*(12), 1259–1266. https://doi.org/10.1161/01.res.0000022160.64355.62

Lu, H., Zhou, Q., He, J., Jiang, Z., Peng, C., Tong, R., & Shi, J. (2020). Recent advances in the development of protein-protein interactions modulators: Mechanisms and clinical trials. *Signal Transduction and Targeted Therapy*, *5*(1), 213. https://doi.org/10.1038/s41392-020-00315-3

Luck, K., Kim, D.-K., Lambourne, L., Spirohn, K., Begg, B. E., Bian, W., Brignall, R., Cafarelli, T., Campos-Laborie, F. J., Charloteaux, B., Choi, D., Coté, A. G., Daley, M., Deimling, S.,

Desbuleux, A., Dricot, A., Gebbia, M., Hardy, M. F., Kishore, N., … Calderwood, M. A. (2020). A reference map of the human binary protein interactome. *Nature*, *580*(7803), Article 7803. https://doi.org/10.1038/s41586-020-2188-x

Luo, Tzivion, G., Belshaw, P. J., Vavvas, D., Marshall, M., & Avruch, J. (1996). Oligomerization activates c-Raf-1 through a Ras-dependent mechanism. *Nature*, *383*(6596), 181–185. https://doi.org/10.1038/383181a0

Luo, Y., Gao, S., Hao, Z., Yang, Y., Xie, S., Li, D., Liu, M., & Zhou, J. (2016). Apoptosis signal-regulating kinase 1 exhibits oncogenic activity in pancreatic cancer. *Oncotarget*, *7*(46), 75155–75164. https://doi.org/10.18632/oncotarget.12090

Lupas, A., Van Dyke, M., & Stock, J. (1991). Predicting coiled coils from protein sequences. *Science (New York, N.Y.)*, *252*(5009), 1162–1164. https://doi.org/10.1126/science.252.5009.1162

Manning, G., Plowman, G. D., Hunter, T., & Sudarsanam, S. (2002). Evolution of protein kinase signaling from yeast to man. *Trends in Biochemical Sciences*, *27*(10), 514–520. https://doi.org/10.1016/s0968-0004(02)02179-5

Manning, G., Whyte, D. B., Martinez, R., Hunter, T., & Sudarsanam, S. (2002). The protein kinase complement of the human genome. *Science (New York, N.Y.)*, *298*(5600), 1912–1934. https://doi.org/10.1126/science.1075762

Maruyama, T., Araki, T., Kawarazaki, Y., Naguro, I., Heynen, S., Aza-Blanc, P., Ronai, Z., Matsuzawa, A., & Ichijo, H. (2014). Roquin-2 promotes ubiquitin-mediated degradation of ASK1 to regulate stress responses. *Science Signaling*, *7*(309), ra8. https://doi.org/10.1126/scisignal.2004822

Masters, S. C., Pederson, K. J., Zhang, L., Barbieri, J. T., & Fu, H. (1999). Interaction of 14-3-3 with a nonphosphorylated protein ligand, exoenzyme S of Pseudomonas aeruginosa. *Biochemistry*, *38*(16), 5216–5221. https://doi.org/10.1021/bi982492m

Mathien, S., Tesnière, C., & Meloche, S. (2021). Regulation of Mitogen-Activated Protein Kinase Signaling Pathways by the Ubiquitin-Proteasome System and Its Pharmacological Potential. *Pharmacological Reviews*, *73*(4), 263–296. https://doi.org/10.1124/pharmrev.120.000170

Matsushita, M., & Nairn, A. C. (1999). Inhibition of the Ca2+/calmodulin-dependent protein kinase I cascade by cAMP-dependent protein kinase. *The Journal of Biological Chemistry*, *274*(15), 10086–10093. https://doi.org/10.1074/jbc.274.15.10086

Matsuzawa, A., Saegusa, K., Noguchi, T., Sadamitsu, C., Nishitoh, H., Nagai, S., Koyasu, S., Matsumoto, K., Takeda, K., & Ichijo, H. (2005). ROS-dependent activation of the TRAF6-ASK1-p38 pathway is selectively required for TLR4-mediated innate immunity. *Nature Immunology*, *6*(6), 587–592. https://doi.org/10.1038/ni1200

Meijer, F. A., Leijten-van de Gevel, I. A., de Vries, R. M. J. M., & Brunsveld, L. (2019). Allosteric small molecule modulators of nuclear receptors. *Molecular and Cellular Endocrinology*, *485*, 20–34. https://doi.org/10.1016/j.mce.2019.01.022

Meijles, D. N., Cull, J. J., Markou, T., Cooper, S. T. E., Haines, Z. H. R., Fuller, S. J., O'Gara, P., Sheppard, M. N., Harding, S. E., Sugden, P. H., & Clerk, A. (2020). Redox Regulation of Cardiac ASK1 (Apoptosis Signal-Regulating Kinase 1) Controls p38-MAPK (Mitogen-Activated Protein Kinase) and Orchestrates Cardiac Remodeling to Hypertension. *Hypertension (Dallas, Tex.: 1979)*, *76*(4), 1208–1218. https://doi.org/10.1161/HYPERTENSIONAHA.119.14556

Milne, J. L. S., Borgnia, M. J., Bartesaghi, A., Tran, E. E. H., Earl, L. A., Schauder, D. M., Lengyel, J., Pierson, J., Patwardhan, A., & Subramaniam, S. (2013). Cryo-electron microscopy: A primer for the non-microscopist. *The FEBS Journal*, *280*(1), 28–45. https://doi.org/10.1111/febs.12078

Mnich, S. J., Blanner, P. M., Hu, L. G., Shaffer, A. F., Happa, F. A., O'Neil, S., Ukairo, O., Weiss, D., Welsh, E., Storer, C., Mbalaviele, G., Ichijo, H., Monahan, J. B., Hardy, M. M., & Eda, H. (2010). Critical role for apoptosis signal-regulating kinase 1 in the development of inflammatory

K/BxN serum-induced arthritis. *International Immunopharmacology*, *10*(10), 1170–1176. https://doi.org/10.1016/j.intimp.2010.06.023

Moore, B. E., & Perez, V. J. (1967). *Specific acidic proteins of the nervous system. Physiological and Biochemical aspects of Nervous integration. A symposium*. Prentice Hall, Englewood Cliffs, NJ.

Moore, T. W., Mayne, C. G., & Katzenellenbogen, J. A. (2010). Minireview: Not picking pockets: nuclear receptor alternate-site modulators (NRAMs). *Molecular Endocrinology (Baltimore, Md.)*, *24*(4), 683–695. https://doi.org/10.1210/me.2009-0362

Morita, K., Saitoh, M., Tobiume, K., Matsuura, H., Enomoto, S., Nishitoh, H., & Ichijo, H. (2001). Negative feedback regulation of ASK1 by protein phosphatase 5 (PP5) in response to oxidative stress. *The EMBO Journal*, *20*(21), 6028–6036. https://doi.org/10.1093/emboj/20.21.6028

Munier, C. C., De Maria, L., Edman, K., Gunnarsson, A., Longo, M., MacKintosh, C., Patel, S., Snijder, A., Wissler, L., Brunsveld, L., Ottmann, C., & Perry, M. W. D. (2021). Glucocorticoid receptor Thr524 phosphorylation by MINK1 induces interactions with 14-3-3 protein regulators. *The Journal of Biological Chemistry*, *296*, 100551. https://doi.org/10.1016/j.jbc.2021.100551

Muslin, A. J., Tanner, J. W., Allen, P. M., & Shaw, A. S. (1996). Interaction of 14-3-3 with signaling proteins is mediated by the recognition of phosphoserine. *Cell*, *84*(6), 889–897. https://doi.org/10.1016/s0092-8674(00)81067-3

Nadeau, P. J., Charette, S. J., & Landry, J. (2009). REDOX reaction at ASK1-Cys250 is essential for activation of JNK and induction of apoptosis. *Molecular Biology of the Cell*, *20*(16), 3628–3637. https://doi.org/10.1091/mbc.e09-03-0211

Nadeau, P. J., Charette, S. J., Toledano, M. B., & Landry, J. (2007). Disulfide Bond-mediated multimerization of Ask1 and its reduction by thioredoxin-1 regulate H(2)O(2)-induced c-Jun NH(2)-terminal kinase activation and apoptosis. *Molecular Biology of the Cell*, *18*(10), 3903–3913. https://doi.org/10.1091/mbc.e07-05-0491

Naguro, I., Umeda, T., Kobayashi, Y., Maruyama, J., Hattori, K., Shimizu, Y., Kataoka, K., Kim-Mitsuyama, S., Uchida, S., Vandewalle, A., Noguchi, T., Nishitoh, H., Matsuzawa, A., Takeda, K., & Ichijo, H. (2012). ASK3 responds to osmotic stress and regulates blood pressure by suppressing WNK1-SPAK/OSR1 signaling in the kidney. *Nature Communications*, *3*, 1285. https://doi.org/10.1038/ncomms2283

Nakane, T., Kotecha, A., Sente, A., McMullan, G., Masiulis, S., Brown, P. M. G. E., Grigoras, I. T., Malinauskaite, L., Malinauskas, T., Miehling, J., Uchański, T., Yu, L., Karia, D., Pechnikova, E. V., de Jong, E., Keizer, J., Bischoff, M., McCormack, J., Tiemeijer, P., … Scheres, S. H. W. (2020). Single-particle cryo-EM at atomic resolution. *Nature*, *587*(7832), 152–156. https://doi.org/10.1038/s41586-020-2829-0

Nelson, D. L., Cox, M. M., & Lehninger, A. L. (2017). *Lehninger principles of biochemistry* (Seventh edition). W.H. Freeman and Company ; Macmillan Higher Education.

Nishida, T., Hattori, K., & Watanabe, K. (2017). The regulatory and signaling mechanisms of the ASK family. *Advances in Biological Regulation*, *66*, 2–22. https://doi.org/10.1016/j.jbior.2017.05.004

Nishitoh, H., Matsuzawa, A., Tobiume, K., Saegusa, K., Takeda, K., Inoue, K., Hori, S., Kakizuka, A., & Ichijo, H. (2002). ASK1 is essential for endoplasmic reticulum stress-induced neuronal cell death triggered by expanded polyglutamine repeats. *Genes & Development*, *16*(11), 1345–1355. https://doi.org/10.1101/gad.992302

Nishitoh, H., Saitoh, M., Mochida, Y., Takeda, K., Nakano, H., Rothe, M., Miyazono, K., & Ichijo, H. (1998). ASK1 is essential for JNK/SAPK activation by TRAF2. *Molecular Cell*, *2*(3), 389–395. https://doi.org/10.1016/s1097-2765(00)80283-x

Nishiyama, A., Matsui, M., Iwata, S., Hirota, K., Masutani, H., Nakamura, H., Takagi, Y., Sono, H., Gon, Y., & Yodoi, J. (1999). Identification of thioredoxin-binding protein-2/vitamin D(3) up-regulated protein 1 as a negative regulator of thioredoxin function and expression. *The Journal of Biological Chemistry*, *274*(31), 21645–21650. https://doi.org/10.1074/jbc.274.31.21645

Noguchi, T., Takeda, K., Matsuzawa, A., Saegusa, K., Nakano, H., Gohda, J., Inoue, J.-I., & Ichijo, H. (2005). Recruitment of tumor necrosis factor receptor-associated factor family proteins to apoptosis signal-regulating kinase 1 signalosome is essential for oxidative stress-induced cell death. *The Journal of Biological Chemistry*, *280*(44), 37033–37040. https://doi.org/10.1074/jbc.M506771200

Nygaard, G., Di Paolo, J. A., Hammaker, D., Boyle, D. L., Budas, G., Notte, G. T., Mikaelian, I., Barry, V., & Firestein, G. S. (2018). Regulation and function of apoptosis signal-regulating kinase 1 in rheumatoid arthritis. *Biochemical Pharmacology*, *151*, 282–290. https://doi.org/10.1016/j.bcp.2018.01.041

Obsil, T., Ghirlando, R., Klein, D. C., Ganguly, S., & Dyda, F. (2001). Crystal structure of the 14-3-3zeta:serotonin N-acetyltransferase complex. A role for scaffolding in enzyme regulation. *Cell*, *105*(2), 257–267. https://doi.org/10.1016/s0092-8674(01)00316-6

Obsilova, V., Honzejkova, K., & Obsil, T. (2021). Structural Insights Support Targeting ASK1 Kinase for Therapeutic Interventions. *International Journal of Molecular Sciences*, *22*(24), 13395. https://doi.org/10.3390/ijms222413395

Obsilova, V., & Obsil, T. (2020). The 14-3-3 Proteins as Important Allosteric Regulators of Protein Kinases. *International Journal of Molecular Sciences*, *21*(22), 8824. https://doi.org/10.3390/ijms21228824

Obsilova, V., & Obsil, T. (2022). Structural insights into the functional roles of 14-3-3 proteins. *Frontiers in Molecular Biosciences*, *9*, 1016071. https://doi.org/10.3389/fmolb.2022.1016071

Ogier, J. M., Nayagam, B. A., & Lockhart, P. J. (2020). ASK1 inhibition: A therapeutic strategy with multi-system benefits. *Journal of Molecular Medicine (Berlin, Germany)*, *98*(3), 335–348. https://doi.org/10.1007/s00109-020-01878-y

Ottmann, C., Yasmin, L., Weyand, M., Veesenmeyer, J. L., Diaz, M. H., Palmer, R. H., Francis, M. S., Hauser, A. R., Wittinghofer, A., & Hallberg, B. (2007). Phosphorylation-independent interaction between 14-3-3 and exoenzyme S: From structure to pathogenesis. *The EMBO Journal*, *26*(3), 902–913. https://doi.org/10.1038/sj.emboj.7601530

Panjkovich, A., & Svergun, D. I. (2018). CHROMIXS: Automatic and interactive analysis of chromatography-coupled small-angle X-ray scattering data. *Bioinformatics (Oxford, England)*, *34*(11), 1944–1946. https://doi.org/10.1093/bioinformatics/btx846

Park, H.-S., Yu, J.-W., Cho, J.-H., Kim, M.-S., Huh, S.-H., Ryoo, K., & Choi, E.-J. (2004). Inhibition of apoptosis signal-regulating kinase 1 by nitric oxide through a thiol redox mechanism. *The Journal of Biological Chemistry*, *279*(9), 7584–7590. https://doi.org/10.1074/jbc.M304183200

Paterni, I., Granchi, C., Katzenellenbogen, J. A., & Minutolo, F. (2014). Estrogen receptors alpha (ERα) and beta (ERβ): Subtype-selective ligands and clinical potential. *Steroids*, *90*, 13–29. https://doi.org/10.1016/j.steroids.2014.06.012

Pearson, G., Robinson, F., Beers Gibson, T., Xu, B. E., Karandikar, M., Berman, K., & Cobb, M. H. (2001). Mitogen-activated protein (MAP) kinase pathways: Regulation and physiological functions. *Endocrine Reviews*, *22*(2), 153–183. https://doi.org/10.1210/edrv.22.2.0428

Pellicena, P., & Kuriyan, J. (2006). Protein-protein interactions in the allosteric regulation of protein kinases. *Current Opinion in Structural Biology*, *16*(6), 702–709. https://doi.org/10.1016/j.sbi.2006.10.007

Pennington, K. L., Chan, T. Y., Torres, M. P., & Andersen, J. L. (2018). The dynamic and stress-adaptive signaling hub of 14-3-3: Emerging mechanisms of regulation and context-dependent

protein-protein interactions. *Oncogene*, *37*(42), 5587–5604. https://doi.org/10.1038/s41388-018-0348-3

Perez-Riba, A., & Itzhaki, L. S. (2019). The tetratricopeptide-repeat motif is a versatile platform that enables diverse modes of molecular recognition. *Current Opinion in Structural Biology*, *54*, 43–49. https://doi.org/10.1016/j.sbi.2018.12.004

Perez-Riba, A., Synakewicz, M., & Itzhaki, L. S. (2018). Folding cooperativity and allosteric function in the tandem-repeat protein class. *Philosophical Transactions of the Royal Society of London. Series B, Biological Sciences*, *373*(1749), 20170188. https://doi.org/10.1098/rstb.2017.0188

Peterson, A. F., Ingram, K., Huang, E. J., Parksong, J., McKenney, C., Bever, G. S., & Regot, S. (2022). Systematic analysis of the MAPK signaling network reveals MAP3K-driven control of cell fate. *Cell Systems*, *13*(11), 885-894.e4. https://doi.org/10.1016/j.cels.2022.10.003

Peterson, A. J., Kyba, M., Bornemann, D., Morgan, K., Brock, H. W., & Simon, J. (1997). A domain shared by the Polycomb group proteins Scm and ph mediates heterotypic and homotypic interactions. *Molecular and Cellular Biology*, *17*(11), 6683–6692. https://doi.org/10.1128/MCB.17.11.6683

Petrvalska, O., Honzejkova, K., Koupilova, N., Herman, P., Obsilova, V., & Obsil, T. (2023). 14-3-3 protein inhibits CaMKK1 by blocking the kinase active site with its last two C-terminal helices. *Protein Science: A Publication of the Protein Society*, *32*(11), e4805. https://doi.org/10.1002/pro.4805

Petrvalska, O., Kosek, D., Kukacka, Z., Tosner, Z., Man, P., Vecer, J., Herman, P., Obsilova, V., & Obsil, T. (2016). Structural Insight into the 14-3-3 Protein-dependent Inhibition of Protein Kinase ASK1 (Apoptosis Signal-regulating kinase 1). *The Journal of Biological Chemistry*, *291*(39), 20753–20765. https://doi.org/10.1074/jbc.M116.724310

Pike, A. C. W., Rellos, P., Niesen, F. H., Turnbull, A., Oliver, A. W., Parker, S. A., Turk, B. E., Pearl, L. H., & Knapp, S. (2008). Activation segment dimerization: A mechanism for kinase autophosphorylation of non-consensus sites. *The EMBO Journal*, *27*(4), 704–714. https://doi.org/10.1038/emboj.2008.8

Psenakova, K., Hexnerova, R., Srb, P., Obsilova, V., Veverka, V., & Obsil, T. (2020). The redox-active site of thioredoxin is directly involved in apoptosis signal-regulating kinase 1 binding that is modulated by oxidative stress. *The FEBS Journal*, *287*(8), 1626–1644. https://doi.org/10.1111/febs.15101

Psenakova, K., Petrvalska, O., Kylarova, S., Lentini Santo, D., Kalabova, D., Herman, P., Obsilova, V., & Obsil, T. (2018). 14-3-3 protein directly interacts with the kinase domain of calcium/calmodulin-dependent protein kinase kinase (CaMKK2). *Biochimica Et Biophysica Acta. General Subjects*, *1862*(7), 1612–1625. https://doi.org/10.1016/j.bbagen.2018.04.006

Puckett, M. C., Goldman, E. H., Cockrell, L. M., Huang, B., Kasinski, A. L., Du, Y., Wang, C.-Y., Lin, A., Ichijo, H., Khuri, F., & Fu, H. (2013). Integration of apoptosis signal-regulating kinase 1-mediated stress signaling with the Akt/protein kinase B-IκB kinase cascade. *Molecular and Cellular Biology*, *33*(11), 2252–2259. https://doi.org/10.1128/MCB.00047-13

Punjani, A., Rubinstein, J. L., Fleet, D. J., & Brubaker, M. A. (2017). cryoSPARC: Algorithms for rapid unsupervised cryo-EM structure determination. *Nature Methods*, *14*(3), 290–296. https://doi.org/10.1038/nmeth.4169

Racioppi, L., & Means, A. R. (2008). Calcium/calmodulin-dependent kinase IV in immune and inflammatory responses: Novel routes for an ancient traveller. *Trends in Immunology*, *29*(12), 600–607. https://doi.org/10.1016/j.it.2008.08.005

Rambo, R. P., & Tainer, J. A. (2013). Accurate assessment of mass, models and resolution by small-angle scattering. *Nature*, *496*(7446), 477–481. https://doi.org/10.1038/nature12070

Rigden, D. J., & Galperin, M. Y. (2004). The DxDxDG motif for calcium binding: Multiple structural contexts and implications for evolution. *Journal of Molecular Biology*, *343*(4), 971–984. https://doi.org/10.1016/j.jmb.2004.08.077

Rittinger, K., Budman, J., Xu, J., Volinia, S., Cantley, L. C., Smerdon, S. J., Gamblin, S. J., & Yaffe, M. B. (1999). Structural analysis of 14-3-3 phosphopeptide complexes identifies a dual role for the nuclear export signal of 14-3-3 in ligand binding. *Molecular Cell*, *4*(2), 153–166. https://doi.org/10.1016/s1097-2765(00)80363-9

Roe, J. L., Durfee, T., Zupan, J. R., Repetti, P. P., McLean, B. G., & Zambryski, P. C. (1997). TOUSLED is a nuclear serine/threonine protein kinase that requires a coiled-coil region for oligomerization and catalytic activity. *The Journal of Biological Chemistry*, *272*(9), 5838–5845. https://doi.org/10.1074/jbc.272.9.5838

Roskoski, R. (2023). Properties of FDA-approved small molecule protein kinase inhibitors: A 2023 update. *Pharmacological Research*, *187*, 106552. https://doi.org/10.1016/j.phrs.2022.106552

Saito, J., Toriumi, S., Awano, K., Ichijo, H., Sasaki, K., Kobayashi, T., & Tamura, S. (2007). Regulation of apoptosis signal-regulating kinase 1 by protein phosphatase 2Cepsilon. *The Biochemical Journal*, *405*(3), 591–596. https://doi.org/10.1042/BJ20070231

Saitoh, M., Nishitoh, H., Fujii, M., Takeda, K., Tobiume, K., Sawada, Y., Kawabata, M., Miyazono, K., & Ichijo, H. (1998). Mammalian thioredoxin is a direct inhibitor of apoptosis signal-regulating kinase (ASK) 1. *The EMBO Journal*, *17*(9), 2596–2606. https://doi.org/10.1093/emboj/17.9.2596

Schaeffer, H. J., & Weber, M. J. (1999). Mitogen-activated protein kinases: Specific messages from ubiquitous messengers. *Molecular and Cellular Biology*, *19*(4), 2435–2444. https://doi.org/10.1128/MCB.19.4.2435

Schneidman-Duhovny, D., Hammel, M., Tainer, J. A., & Sali, A. (2013). Accurate SAXS profile computation and its assessment by contrast variation experiments. *Biophysical Journal*, *105*(4), 962–974. https://doi.org/10.1016/j.bpj.2013.07.020

Schneidman-Duhovny, D., Hammel, M., Tainer, J. A., & Sali, A. (2016). FoXS, FoXSDock and MultiFoXS: Single-state and multi-state structural modeling of proteins and their complexes based on SAXS profiles. *Nucleic Acids Research*, *44*(W1), W424-429. https://doi.org/10.1093/nar/gkw389

Schuck, P. (2000). Size-distribution analysis of macromolecules by sedimentation velocity ultracentrifugation and lamm equation modeling. *Biophysical Journal*, *78*(3), 1606–1619. https://doi.org/10.1016/S0006-3495(00)76713-0

Schuster, S., & Feldstein, A. E. (2017). NASH: Novel therapeutic strategies targeting ASK1 in NASH. *Nature Reviews. Gastroenterology & Hepatology*, *14*(6), 329–330. https://doi.org/10.1038/nrgastro.2017.42

Schwarz, J. K., Lovly, C. M., & Piwnica-Worms, H. (2003). Regulation of the Chk2 protein kinase by oligomerization-mediated cis- and trans-phosphorylation. *Molecular Cancer Research: MCR*, *1*(8), 598–609.

Seger, R., & Krebs, E. G. (1995). The MAPK signaling cascade. *FASEB Journal: Official Publication of the Federation of American Societies for Experimental Biology*, *9*(9), 726–735.

Seimiya, H., Sawada, H., Muramatsu, Y., Shimizu, M., Ohko, K., Yamane, K., & Tsuruo, T. (2000). Involvement of 14-3-3 proteins in nuclear localization of telomerase. *The EMBO Journal*, *19*(11), 2652–2661. https://doi.org/10.1093/emboj/19.11.2652

Sekine, Y., Takeda, K., & Ichijo, H. (2006). The ASK1-MAP kinase signaling in ER stress and neurodegenerative diseases. *Current Molecular Medicine*, *6*(1), 87–97. https://doi.org/10.2174/156652406775574541

Sever, R., & Glass, C. K. (2013). Signaling by nuclear receptors. *Cold Spring Harbor Perspectives in Biology*, *5*(3), a016709. https://doi.org/10.1101/cshperspect.a016709

Sharma, D., Kumar, S., & Narasimhan, B. (2018). Estrogen alpha receptor antagonists for the treatment of breast cancer: A review. *Chemistry Central Journal*, *12*(1), 107. https://doi.org/10.1186/s13065-018-0472-8

Sijbesma, E., Hallenbeck, K. K., Leysen, S., de Vink, P. J., Skóra, L., Jahnke, W., Brunsveld, L., Arkin, M. R., & Ottmann, C. (2019). Site-Directed Fragment-Based Screening for the Discovery of Protein-Protein Interaction Stabilizers. *Journal of the American Chemical Society*, *141*(8), 3524–3531. https://doi.org/10.1021/jacs.8b11658

Sijbesma, E., Somsen, B. A., Miley, G. P., Leijten-van de Gevel, I. A., Brunsveld, L., Arkin, M. R., & Ottmann, C. (2020). Fluorescence Anisotropy-Based Tethering for Discovery of Protein-Protein Interaction Stabilizers. *ACS Chemical Biology*, *15*(12), 3143–3148. https://doi.org/10.1021/acschembio.0c00646

Sladek, F. (2011). What are nuclear receptor ligands? *Molecular and Cellular Endocrinology*, *334*(1–2), 3–13. https://doi.org/10.1016/j.mce.2010.06.018

Sluchanko, N. N., & Bustos, D. M. (2019). Intrinsic disorder associated with 14-3-3 proteins and their partners. *Progress in Molecular Biology and Translational Science*, *166*, 19–61. https://doi.org/10.1016/bs.pmbts.2019.03.007

Smoly, I., Shemesh, N., Ziv-Ukelson, M., Ben-Zvi, A., & Yeger-Lotem, E. (2017). An Asymmetrically Balanced Organization of Kinases versus Phosphatases across Eukaryotes Determines Their Distinct Impacts. *PLoS Computational Biology*, *13*(1), e1005221. https://doi.org/10.1371/journal.pcbi.1005221

Soderling, T. R., & Stull, J. T. (2001). Structure and regulation of calcium/calmodulin-dependent protein kinases. *Chemical Reviews*, *101*(8), 2341–2352. https://doi.org/10.1021/cr0002386

Somsen, B. A., Sijbesma, E., Leysen, S., Honzejkova, K., Visser, E. J., Cossar, P. J., Obšil, T., Brunsveld, L., & Ottmann, C. (2023). Molecular basis and dual ligand regulation of tetrameric estrogen receptor α/14-3-3ζ protein complex. *The Journal of Biological Chemistry*, *299*(7), 104855. https://doi.org/10.1016/j.jbc.2023.104855

Song, J. J., Rhee, J. G., Suntharalingam, M., Walsh, S. A., Spitz, D. R., & Lee, Y. J. (2002). Role of glutaredoxin in metabolic oxidative stress. Glutaredoxin as a sensor of oxidative stress mediated by H2O2. *The Journal of Biological Chemistry*, *277*(48), 46566–46575. https://doi.org/10.1074/jbc.M206826200

Sturgill, T. W., Ray, L. B., Erikson, E., & Maller, J. L. (1988). Insulin-stimulated MAP-2 kinase phosphorylates and activates ribosomal protein S6 kinase II. *Nature*, *334*(6184), 715–718. https://doi.org/10.1038/334715a0

Svergun, D., Barberato, C., & Koch, M. H. J. (1995). CRYSOL– a Program to Evaluate X-ray Solution Scattering of Biological Macromolecules from Atomic Coordinates. *Journal of Applied Crystallography*, *28*(6), 768–773. https://doi.org/10.1107/S0021889895007047

Svergun, D. I. (1992). Determination of the regularization parameter in indirect-transform methods using perceptual criteria. *Journal of Applied Crystallography*, *25*(4), 495–503. https://doi.org/10.1107/S0021889892001663

Svergun, D. I. (1999). Restoring low resolution structure of biological macromolecules from solution scattering using simulated annealing. *Biophysical Journal*, *76*(6), 2879–2886.

Swulius, M. T., & Waxham, M. N. (2008). Ca(2+)/calmodulin-dependent protein kinases. *Cellular and Molecular Life Sciences: CMLS*, *65*(17), 2637–2657. https://doi.org/10.1007/s00018-008-8086-2

Szewczuk, M., Boguszewska, K., Kaźmierczak-Barańska, J., & Karwowski, B. T. (2020). The role of AMPK in metabolism and its influence on DNA damage repair. *Molecular Biology Reports*, *47*(11), 9075–9086. https://doi.org/10.1007/s11033-020-05900-x

Takabatake, S., Ohtsuka, S., Sugawara, T., Hatano, N., Kanayama, N., Magari, M., Sakagami, H., & Tokumitsu, H. (2019). Regulation of Ca2+/calmodulin-dependent protein kinase kinase β by cAMP signaling. *Biochimica Et Biophysica Acta. General Subjects*, *1863*(4), 672–680. https://doi.org/10.1016/j.bbagen.2018.12.012

Takahashi, H., Honma, M., Miyauchi, Y., Nakamura, S., Ishida-Yamamoto, A., & Iizuka, H. (2004). Cyclic AMP differentially regulates cell proliferation of normal human keratinocytes through ERK activation depending on the expression pattern of B-Raf. *Archives of Dermatological Research*, *296*(2), 74–82. https://doi.org/10.1007/s00403-004-0478-z

Takeda, K., Matsuzawa, A., Nishitoh, H., & Ichijo, H. (2003). Roles of MAPKKK ASK1 in stress-induced cell death. *Cell Structure and Function*, *28*(1), 23–29. https://doi.org/10.1247/csf.28.23

Takeda, K., Matsuzawa, A., Nishitoh, H., Tobiume, K., Kishida, S., Ninomiya-Tsuji, J., Matsumoto, K., & Ichijo, H. (2004). Involvement of ASK1 in Ca2+-induced p38 MAP kinase activation. *EMBO Reports*, *5*(2), 161–166. https://doi.org/10.1038/sj.embor.7400072

Takeda, K., Shimozono, R., Noguchi, T., Umeda, T., Morimoto, Y., Naguro, I., Tobiume, K., Saitoh, M., Matsuzawa, A., & Ichijo, H. (2007). Apoptosis signal-regulating kinase (ASK) 2 functions as a mitogen-activated protein kinase kinase kinase in a heteromeric complex with ASK1. *The Journal of Biological Chemistry*, *282*(10), 7522–7531. https://doi.org/10.1074/jbc.M607177200

Tanaka, T. (1988). Calmodulin-dependent calcium signal transduction. *Japanese Journal of Pharmacology*, *46*(2), 101–107. https://doi.org/10.1254/jjp.46.101

Tanaka, T., Hosoi, F., Yamaguchi-Iwai, Y., Nakamura, H., Masutani, H., Ueda, S., Nishiyama, A., Takeda, S., Wada, H., Spyrou, G., & Yodoi, J. (2002). Thioredoxin-2 (TRX-2) is an essential gene regulating mitochondria-dependent apoptosis. *The EMBO Journal*, *21*(7), 1695–1703. https://doi.org/10.1093/emboj/21.7.1695

Taylor, S. S., Keshwani, M. M., Steichen, J. M., & Kornev, A. P. (2012). Evolution of the eukaryotic protein kinases as dynamic molecular switches. *Philosophical Transactions of the Royal Society of London. Series B, Biological Sciences*, *367*(1602), 2517–2528. https://doi.org/10.1098/rstb.2012.0054

Taylor, S. S., & Kornev, A. P. (2011). Protein kinases: Evolution of dynamic regulatory proteins. *Trends in Biochemical Sciences*, *36*(2), 65–77. https://doi.org/10.1016/j.tibs.2010.09.006

Tobiume, K., Matsuzawa, A., Takahashi, T., Nishitoh, H., Morita, K., Takeda, K., Minowa, O., Miyazono, K., Noda, T., & Ichijo, H. (2001). ASK1 is required for sustained activations of JNK/p38 MAP kinases and apoptosis. *EMBO Reports*, *2*(3), 222–228. https://doi.org/10.1093/embo-reports/kve046

Tobiume, K., Saitoh, M., & Ichijo, H. (2002). Activation of apoptosis signal-regulating kinase 1 by the stress-induced activating phosphorylation of pre-formed oligomer. *Journal of Cellular Physiology*, *191*(1), 95–104. https://doi.org/10.1002/jcp.10080

Tokumitsu, H., Iwabu, M., Ishikawa, Y., & Kobayashi, R. (2001). Differential regulatory mechanism of Ca2+/calmodulin-dependent protein kinase kinase isoforms. *Biochemistry*, *40*(46), 13925–13932. https://doi.org/10.1021/bi010863k

Tokumitsu, H., & Sakagami, H. (2022). Molecular Mechanisms Underlying Ca2+/Calmodulin-Dependent Protein Kinase Kinase Signal Transduction. *International Journal of Molecular Sciences*, *23*(19), 11025. https://doi.org/10.3390/ijms231911025

Tokumitsu, H., Takahashi, N., Eto, K., Yano, S., Soderling, T. R., & Muramatsu, M. (1999). Substrate recognition by Ca2+/Calmodulin-dependent protein kinase kinase. Role of the arg-pro-rich insert domain. *The Journal of Biological Chemistry*, *274*(22), 15803–15810. https://doi.org/10.1074/jbc.274.22.15803

Tokumitsu, H., Wayman, G. A., Muramatsu, M., & Soderling, T. R. (1997). Calcium/calmodulin-dependent protein kinase kinase: Identification of regulatory domains. *Biochemistry*, *36*(42), 12823–12827. https://doi.org/10.1021/bi971348i

Trabjerg, E., Nazari, Z. E., & Rand, K. D. (2018). Conformational analysis of complex protein states by hydrogen/deuterium exchange mass spectrometry (HDX-MS): Challenges and emerging solutions. *TrAC Trends in Analytical Chemistry*, *106*, 125–138. https://doi.org/10.1016/j.trac.2018.06.008

Trachootham, D., Lu, W., Ogasawara, M. A., Nilsa, R.-D. V., & Huang, P. (2008). Redox regulation of cell survival. *Antioxidants & Redox Signaling*, *10*(8), 1343–1374. https://doi.org/10.1089/ars.2007.1957

Traphagen, N. A., Hosford, S. R., Jiang, A., Marotti, J. D., Brauer, B. L., Demidenko, E., & Miller, T. W. (2021). High estrogen receptor alpha activation confers resistance to estrogen deprivation and is required for therapeutic response to estrogen in breast cancer. *Oncogene*, *40*(19), 3408–3421. https://doi.org/10.1038/s41388-021-01782-w

Trevelyan, S. J., Brewster, J. L., Burgess, A. E., Crowther, J. M., Cadell, A. L., Parker, B. L., Croucher, D. R., Dobson, R. C. J., Murphy, J. M., & Mace, P. D. (2020). Structure-based mechanism of preferential complex formation by apoptosis signal-regulating kinases. *Science Signaling*, *13*(622), eaay6318. https://doi.org/10.1126/scisignal.aay6318

Ubersax, J. A., & Ferrell, J. E. (2007). Mechanisms of specificity in protein phosphorylation. *Nature Reviews. Molecular Cell Biology*, *8*(7), 530–541. https://doi.org/10.1038/nrm2203

Vacratsis, P. O., & Gallo, K. A. (2000). Zipper-mediated oligomerization of the mixed lineage kinase SPRK/MLK-3 is not required for its activation by the GTPase cdc 42 but Is necessary for its activation of the JNK pathway. Monomeric SPRK L410P does not catalyze the activating phosphorylation of Thr258 of murine MITOGEN-ACTIVATED protein kinase kinase 4. *The Journal of Biological Chemistry*, *275*(36), 27893–27900. https://doi.org/10.1074/jbc.M002858200

Varadi, M., Anyango, S., Deshpande, M., Nair, S., Natassia, C., Yordanova, G., Yuan, D., Stroe, O., Wood, G., Laydon, A., Žídek, A., Green, T., Tunyasuvunakool, K., Petersen, S., Jumper, J., Clancy, E., Green, R., Vora, A., Lutfi, M., … Velankar, S. (2022). AlphaFold Protein Structure Database: Massively expanding the structural coverage of protein-sequence space with high-accuracy models. *Nucleic Acids Research*, *50*(D1), D439–D444. https://doi.org/10.1093/nar/gkab1061

Verdoodt, B., Benzinger, A., Popowicz, G. M., Holak, T. A., & Hermeking, H. (2006). Characterization of 14-3-3sigma dimerization determinants: Requirement of homodimerization for inhibition of cell proliferation. *Cell Cycle (Georgetown, Tex.)*, *5*(24), 2920–2926. https://doi.org/10.4161/cc.5.24.3571

Vidal, M. (2005). Interactome modeling. *FEBS Letters*, *579*(8), 1834–1838. https://doi.org/10.1016/j.febslet.2005.02.030

Vlastaridis, P., Kyriakidou, P., Chaliotis, A., Van de Peer, Y., Oliver, S. G., & Amoutzias, G. D. (2017). Estimating the total number of phosphoproteins and phosphorylation sites in eukaryotic proteomes. *GigaScience*, *6*(2), 1–11. https://doi.org/10.1093/gigascience/giw015

Vo, T. V., Das, J., Meyer, M. J., Cordero, N. A., Akturk, N., Wei, X., Fair, B. J., Degatano, A. G., Fragoza, R., Liu, L. G., Matsuyama, A., Trickey, M., Horibata, S., Grimson, A., Yamano, H., Yoshida, M., Roth, F. P., Pleiss, J. A., Xia, Y., & Yu, H. (2016). A Proteome-wide Fission Yeast Interactome Reveals Network Evolution Principles from Yeasts to Human. *Cell*, *164*(1–2), 310–323. https://doi.org/10.1016/j.cell.2015.11.037

Volkov, V. V., & Svergun, D. I. (2003). Uniqueness of ab initio shape determination in small-angle scattering. *Journal of Applied Crystallography*, *36*(3–1), 860–864. https://doi.org/10.1107/S0021889803000268

Wales, T. E., & Engen, J. R. (2006). Hydrogen exchange mass spectrometry for the analysis of protein dynamics. *Mass Spectrometry Reviews*, *25*(1), 158–170. https://doi.org/10.1002/mas.20064

Wang, B., Yang, H., Liu, Y. C., Jelinek, T., Zhang, L., Ruoslahti, E., & Fu, H. (1999). Isolation of high-affinity peptide antagonists of 14-3-3 proteins by phage display. *Biochemistry*, *38*(38), 12499–12504. https://doi.org/10.1021/bi991353h

Wang, X. S., Diener, K., Tan, T. H., & Yao, Z. (1998). MAPKKK6, a novel mitogen-activated protein kinase kinase kinase, that associates with MAPKKK5. *Biochemical and Biophysical Research Communications*, *253*(1), 33–37. https://doi.org/10.1006/bbrc.1998.9749

Wayman, G. A., Kaech, S., Grant, W. F., Davare, M., Impey, S., Tokumitsu, H., Nozaki, N., Banker, G., & Soderling, T. R. (2004). Regulation of axonal extension and growth cone motility by calmodulin-dependent protein kinase I. *The Journal of Neuroscience: The Official Journal of the Society for Neuroscience*, *24*(15), 3786–3794. https://doi.org/10.1523/JNEUROSCI.3294-03.2004

Wayman, G. A., Tokumitsu, H., & Soderling, T. R. (1997). Inhibitory cross-talk by cAMP kinase on the calmodulin-dependent protein kinase cascade. *The Journal of Biological Chemistry*, *272*(26), 16073–16076. https://doi.org/10.1074/jbc.272.26.16073

Wei, F., Qiu, C.-S., Liauw, J., Robinson, D. A., Ho, N., Chatila, T., & Zhuo, M. (2002). Calcium calmodulin-dependent protein kinase IV is required for fear memory. *Nature Neuroscience*, *5*(6), 573–579. https://doi.org/10.1038/nn0602-855

Weichsel, A., Gasdaska, J. R., Powis, G., & Montfort, W. R. (1996). Crystal structures of reduced, oxidized, and mutated human thioredoxins: Evidence for a regulatory homodimer. *Structure (London, England: 1993)*, *4*(6), 735–751. https://doi.org/10.1016/s0969-2126(96)00079-2

Weijman, J. F., Kumar, A., Jamieson, S. A., King, C. M., Caradoc-Davies, T. T., Ledgerwood, E. C., Murphy, J. M., & Mace, P. D. (2017). Structural basis of autoregulatory scaffolding by apoptosis signal-regulating kinase 1. *Proceedings of the National Academy of Sciences of the United States of America*, *114*(11), E2096–E2105. https://doi.org/10.1073/pnas.1620813114

Widmann, C., Gibson, S., Jarpe, M. B., & Johnson, G. L. (1999). Mitogen-activated protein kinase: Conservation of a three-kinase module from yeast to human. *Physiological Reviews*, *79*(1), 143–180. https://doi.org/10.1152/physrev.1999.79.1.143

Williams, C. J., Headd, J. J., Moriarty, N. W., Prisant, M. G., Videau, L. L., Deis, L. N., Verma, V., Keedy, D. A., Hintze, B. J., Chen, V. B., Jain, S., Lewis, S. M., Arendall, W. B., Snoeyink, J., Adams, P. D., Lovell, S. C., Richardson, J. S., & Richardson, D. C. (2018). MolProbity: More and better reference data for improved all-atom structure validation. *Protein Science: A Publication of the Protein Society*, *27*(1), 293–315. https://doi.org/10.1002/pro.3330

Xiang, W., & Wang, S. (2022). Therapeutic Strategies to Target the Androgen Receptor. *Journal of Medicinal Chemistry*, *65*(13), 8772–8797. https://doi.org/10.1021/acs.jmedchem.2c00716

Xiao, B., Smerdon, S. J., Jones, D. H., Dodson, G. G., Soneji, Y., Aitken, A., & Gamblin, S. J. (1995). Structure of a 14-3-3 protein and implications for coordination of multiple signalling pathways. *Nature*, *376*(6536), 188–191. https://doi.org/10.1038/376188a0

Yaffe, M. B. (2002). How do 14-3-3 proteins work?—Gatekeeper phosphorylation and the molecular anvil hypothesis. *FEBS Letters*, *513*(1), 53–57. https://doi.org/10.1016/s0014-5793(01)03288-4

Yaffe, M. B., Rittinger, K., Volinia, S., Caron, P. R., Aitken, A., Leffers, H., Gamblin, S. J., Smerdon, S. J., & Cantley, L. C. (1997). The structural basis for 14-3-3:phosphopeptide binding specificity. *Cell*, *91*(7), 961–971. https://doi.org/10.1016/s0092-8674(00)80487-0

Yang, C.-F., & Tsai, W.-C. (2022). Calmodulin: The switch button of calcium signaling. *Tzu Chi Medical Journal*, *34*(1), 15–22. https://doi.org/10.4103/tcmj.tcmj_285_20

Yang, X., Lee, W. H., Sobott, F., Papagrigoriou, E., Robinson, C. V., Grossmann, J. G., Sundström, M., Doyle, D. A., & Elkins, J. M. (2006). Structural basis for protein-protein interactions in the 14-

3-3 protein family. *Proceedings of the National Academy of Sciences of the United States of America*, *103*(46), 17237–17242. https://doi.org/10.1073/pnas.0605779103

Yano, S., Tokumitsu, H., & Soderling, T. R. (1998). Calcium promotes cell survival through CaM-K kinase activation of the protein-kinase-B pathway. *Nature*, *396*(6711), 584–587. https://doi.org/10.1038/25147

Yehia, G., Schlotter, F., Razavi, R., Alessandrini, A., & Molina, C. A. (2001). Mitogen-activated protein kinase phosphorylates and targets inducible cAMP early repressor to ubiquitin-mediated destruction. *The Journal of Biological Chemistry*, *276*(38), 35272–35279. https://doi.org/10.1074/jbc.M105404200

Yoshikawa, M., Iriyama, T., Suzuki, K., Sayama, S., Tsuruga, T., Kumasawa, K., Nagamatsu, T., Homma, K., Naguro, I., Osuga, Y., Ichijo, H., & Fujii, T. (2020). ASK1 promotes uterine inflammation leading to pathological preterm birth. *Scientific Reports*, *10*(1), 1887. https://doi.org/10.1038/s41598-020-58653-9

Yu, L., Min, W., He, Y., Qin, L., Zhang, H., Bennett, A. M., & Chen, H. (2009). JAK2 and SHP2 reciprocally regulate tyrosine phosphorylation and stability of proapoptotic protein ASK1. *The Journal of Biological Chemistry*, *284*(20), 13481–13488. https://doi.org/10.1074/jbc.M809740200

Zhang, H., Cao, X., Tang, M., Zhong, G., Si, Y., Li, H., Zhu, F., Liao, Q., Li, L., Zhao, J., Feng, J., Li, S., Wang, C., Kaulich, M., Wang, F., Chen, L., Li, L., Xia, Z., Liang, T., … Zhao, B. (2021). A subcellular map of the human kinome. *eLife*, *10*, e64943. https://doi.org/10.7554/eLife.64943

Zhang, L., Chen, J., & Fu, H. (1999). Suppression of apoptosis signal-regulating kinase 1-induced cell death by 14-3-3 proteins. *Proceedings of the National Academy of Sciences of the United States of America*, *96*(15), 8511–8515. https://doi.org/10.1073/pnas.96.15.8511

Zhao, Y., Conze, D. B., Hanover, J. A., & Ashwell, J. D. (2007). Tumor necrosis factor receptor 2 signaling induces selective c-IAP1-dependent ASK1 ubiquitination and terminates mitogen-activated protein kinase signaling. *The Journal of Biological Chemistry*, *282*(11), 7777–7782. https://doi.org/10.1074/jbc.M609146200

Supplements